The Institute of Paper Chemistry

Appleton, Wisconsin

Doctor's Dissertation

Investigation of the Role of Sulfate Ions
In the Reaction Between
Tetrahydroabietic Acid Monolayers and Aluminum Ions

Say Kyoun Ow

June, 1974

INVESTIGATION OF THE ROLE OF SULFATE IONS IN THE REACTION BETWEEN TETRAHYDROABIETIC ACID MONOLAYERS AND ALUMINUM IONS

A thesis submitted by

Say Kyoun Ow

B.S. 1963, Seoul National University

M.S. 1971, Lawrence University

in partial fulfillment of the requirements
of The Institute of Paper Chemistry
for the degree of Doctor of Philosophy
from Lawrence University,
Appleton, Wisconsin

Publication Rights Reserved by
The Institute of Paper Chemistry

June, 1974

TABLE OF CONTENTS

SUMMARY

It was hypothesized that the reported detrimental effect of excess sulfate on the internal sizing of paper in the closed white water system could be ascribed to possible influence of sulfate ions on the interfacial reaction between colloidal rosin acid particles and aluminum ions. The interfacial reaction forms aluminum resinate salt which is the active species in the rosin-alum sizing system. The primary purpose of this work was to characterize the role of sulfate ion in the reaction between resin acid monolayers and aluminum ions by investigating how and why excess sulfate affects the aluminum resinate formation in a surface chemical model system.

A tetrahydroabietic acid (TABSH) monolayer was spread on the liquid-air interface of aluminum nitrate substrate with and without sulfate at the acidic pH range (4.0-5.0). The interfacial reaction was monitored by measuring changes in physical and chemical properties of the monolayer when changes were made in the concentration of sulfate and pH of the substrate. The composition of the monolayer in terms of the free acid mole fraction was determined with multiple internal reflection spectroscopic technique using the multilayer sample built-up on a germanium plate. The physical properties were also measured from monolayer surface pressure-molecular area isotherms determined with an automatic recording surface balance of the Langmuir type.

The increase in the free acid mole fraction in the monolayer with increase in the $[SO_4]$ at pH 4.0 shows that excess sulfate can prevent the resin acid from reacting completely with aluminum ions. However, as pH is increased above 4.0, the inhibiting action of sulfate diminishes rapidly; at pH > 4.5 the sulfate has a little or no effect on the aluminum resinate formation at the interface. The changes in the π-$\underline{A}$ isotherm with increase in the $[SO_4]$ and in the pH corroborated these findings.

The well-established complex chemistry of aluminum and sulfate ions can explain that the inhibiting action of sulfate at pH 4.0 is due to the formation of $AlSO_4^+$ from unhydrolyzed aluminum ions [$Al(6H_2O)^{+3}$] which, otherwise, react with the resin acid forming aluminum triresinate. The diminishing effect of sulfate with increasing pH can be attributed primarily to the change in the distribution of hydrolyzed Al ions [$Al(OH)(5H_2O)^{+2}$]; the $Al(OH)(5H_2O)^{+2}$ ion increases in concentration relative to the $Al(6H_2O)^{+3}$ with increasing pH from 4.0 to 5.0. Apparently, the sulfate has no effect on the monolayer reaction with hydrolyzed Al ions forming the monobasic diresinate. This can be accounted for by the incapability of sulfate to form a stable basic sulfato-complex with the hydrolyzed ion and by the higher adsorbability of the hydrolyzed ion on the spread monolayer than the unhydrolyzed ion.

The contact angles of water, methylene iodide and formamide on the monolayers cast on the CMC film were measured to calculate the components of the free-surface energy of the monolayer. Thus, the changes in these components caused by the result of the sulfate effect on the monolayer reaction were observed. The inhibiting action of sulfate at pH 4.0 results in lowering the contact angle of water which corresponds to increasing the free acid mole fraction of the monolayer. The lowering of the contact angle of water was explained by the increase in the polar force component of the total surface energy caused by the fraction of free acid molecules which can overturn readily when brought into contact with liquid water.

INTRODUCTION

Many paper mills have had internal sizing troubles which appear to have been related to recirculation of the white water systems. Wilson and Duston (1) and others (2-4) have suggested that sulfate build-up in the white water system is related to deterioration of rosin-alum sizing. Sulfate ion accumulates in such systems whereas aluminum ion is largely absorbed by fibers and fillers and retained in the sheet. Aldrich and Janes (5) confirmed the fact that rosin sizing decreases as the sulfate level in a closed white water system is increased; however, they observed that the sizing could be improved by increasing the pH of the white water or by changing the point of rosin addition.

Several investigators have studied the effects of sulfate ions on rosin sizing with the view of their possible role in the retention mechanism of alum-rosin complexes, that is, size precipitates on cellulose fiber surfaces. Collins, et al. (6) found that sulfate ions reduce the electrophoretic mobility of aluminum flocs formed from aluminum chloride. Gorham and Thode (7) and later Guide (8) showed that excess sulfate decreases the net surface potential of size precipitates with a corresponding decrease in retention and deposition of the precipitates onto the fiber surface.

Strazdins (9) investigated the possible role of sulfate ions in rosin sizing by measuring electrokinetic charges of size precipitates, sized fibers (fines), and aluminum flocs. He said that sulfate ions can be beneficial to sizing under certain conditions when the sulfate ion can reduce or moderate the excessive positive charge accumulated on the fiber surface.

Strazdins speculates that the detrimental effect of excess sulfate may be due to an acceleration of premature agglomeration of size precipitates. This

agglomeration may be caused by an excessive reduction of the surface charge of complex aluminum ion flocs or by depletion of the positive charge of the aluminum owing to its coordination to the sulfate ion.

The coordination of sulfate ion and other inorganic anions by aluminum had been suggested earlier by Cobb and Lowe (10) on the basis of Thomas' theory (60, 68) of aluminum complex ions in aqueous solutions. They suggest the possibility that excess sulfate can decrease coordination of rosin and fiber by aluminum ions.

Major (11) studied the effect of oxalate ions on the reaction between resin acid monolayers and aluminum ions. He verified the hypothesis of Cobb and Lowe, in which a strongly coordinating anion like oxalate can prevent the reaction of rosin with aluminum ions by sequestering the aluminum ions.

It is apparent from the previous studies that excess sulfate has an effect on the retention of size precipitates formed in the colloidal rosin-alum sizing system because of an important role in changing the electrokinetic charges of size precipitates and fiber surfaces. However, it is not clear why the sulfate affects the electrokinetic charges. Moreover, neither Strazdins (9) nor Guide (8) and others (6,7) could give an unequivocal reason why their observed high retention of size precipitates does not always conform to the actual condition of better sizing development.

In view of the surface chemistry of internal sizing (12) the detrimental effect of excess sulfate can be ascribed also to its effect on the reaction of resin acids with aluminum ions besides its electrokinetic charge effect. The reaction of resin acids with aluminum ions and their reaction products is viewed as the most important factor in sizing development, since it produces low free-surface energy materials for better sizing (12).

Strazdins (9) excluded in his study on the role of sulfate the possibility that the sulfate can affect the reaction between resin acids and aluminum ions. No one has ever investigated the effect of sulfate on the aluminum resinate formation and its role in the formation reaction. Also, no evidence has been presented in the literature to confirm or deny the direct effect of sulfate on the reaction between colloidal resin acid aggregations and aluminum ions.

This thesis study was initiated, therefore, on the assumption that the sulfate can affect the reaction of aluminum resinate formation. The purpose of this thesis is to elucidate possible roles of sulfate ions in the reaction between resin acids and aluminum ions by investigating how and why excess sulfate affects the aluminum resinate formation. This study is expected to delineate how excess sulfate prevents the reaction, and how sulfate ions affect the nature of reaction products (i.e., structure and composition), depending upon its concentration in the aqueous aluminum salt solution. This study is also concerned with relating the results of the sulfate effects on the monolayer reaction to actual sizing development. Furthermore, this study is designed to provide a new insight into the nature of the reaction products between resin acids and aluminum ions possibly formed in the rosin-alum sizing system.

BACKGROUND TO THE THESIS PROBLEM (REVIEW OF THE LITERATURE)

SURFACE CHEMISTRY OF PAPER SIZING

THE THEORY OF INTERNAL SIZING (12)

Often the resistance of paper or paperboard to the penetration of water and various aqueous liquids must be increased for the material to fit its end-use requirements. One process by which the paper product is modified to give it the desired resistance is termed internal sizing. The nature of this modification can best be understood by analyzing the penetration of a liquid into a capillary tube. The extent of such penetration is given by Equation (1)

$$L^2 = (\gamma_{LV} r t \cos\theta)/(2\eta) \qquad (1)$$

where

L = depth of penetration

r = capillary radius

γ_{LV} = specific free-surface energy of the liquid-vapor interface

θ = contact angle between liquid and solid

t = time of penetration

η = coefficient of viscosity of the liquid

Differentiation of Equation (1) with respect to time yields Equation (2) which describes the rate of penetration of a liquid into a capillary tube. This is the Washburn equation (13) and it is valid

$$dL/dt = (\gamma_{LV} r \cos\theta)/(4L\eta) \qquad (2)$$

under the following conditions:

1. The driving pressure is limited to the capillary pressure;
2. The contact angle is acute;

3. The flow is laminar;

4. The air resistance and gravitational and inertial effects may be excluded or neglected.

These equations apply strictly for a single, uniform, cylindrical capillary. The structure of paper is not comprised of uniform capillaries. However, examination of Equation (2) for a single capillary can provide order of magnitude information about the factors involved in penetration.

For a given liquid and a given paper sample, this analysis suggests that one way to decrease the rate of penetration is to increase the contact angle. The surface chemical factors which determine the contact angle on a smooth solid surface are related to the Young-Dupre equation [Equation (3)] (14)

$$\cos\theta_A = (\gamma_{SV} - \gamma_{SL})/(\gamma_{LV}) \qquad (3)$$

where

θ_A = advancing contact angle between liquid and solid

γ_{SV} = specific free-surface energy (erg cm^{-2}) of the solid-vapor interface

γ_{SL} = specific free-surface energy of the solid-liquid interface

γ_{LV} = specific free-surface energy of the liquid-vapor interface.

According to Equation (3), θ_A may be increased by increasing γ_{LV} and/or by decreasing the difference between γ_{SV} and γ_{SL}.

Moreover, if the difference between γ_{SV} and γ_{SL} is made negative, θ_A will be $> 90°$ ($\cos\theta_A$ will be negative) and the liquid will not spontaneously penetrate the paper structure. In practice, γ_{LV} and γ_{SL} are difficult to increase and the objective of internal sizing is to lower the value of γ_{SV} (the specific free-surface energy of the solid-vapor interface).

MODIFICATION OF THE CELLULOSIC FIBER SURFACE

The specific free-surface energy of the solid-vapor interface can be changed significantly by altering the molecular species in the first layer of the solid. This layer may be modified by a number of factors. Among these are the following as summarized by Swanson (12):

1. The chemical composition of the molecule;
2. The structure of the molecule;
3. The orientation of the molecule on the solid surface;
4. The degree of packing of the molecules on the solid surface;
5. The strength of anchorage of amphipathic (polar-nonpolar) molecules in an oriented position;
6. The nature of the underlying solid molecules;
7. Possible electrical charge effects.

Langmuir (15) was the first to show that solid surfaces with high free-surface energies may be modified by depositing a fatty acid monolayer on the surface. This makes the wettable surface become hydrophobic. He observed that the contact angle between water and the modified, new surfaces depended upon the character of the underlying solid, i.e., the strength of anchorage of the amphipathic fatty acid molecules to the solid surfaces.

The hydrocarbon end of the fatty acid molecules has a low free-surface energy and tends to promote a high contact angle with water. The carboxyl group on the opposite end of the molecule has a high intrinsic free-surface energy and tends to promote wetting or a low contact angle with water. The attraction between the carboxyl groups and the polar solid surfaces is probably sufficient to orient the hydrocarbon portion of the molecules away from the solid surface initially.

However, a drop of polar liquid, water, possesses strong attraction for other polar groups, the carboxyl groups, and it competes with the solid surface for these groups. Consequently, the contact angle between water and the monolayer deposited on the solid surface depends on the strength of anchorage of monolayer molecules to the solid surface. It also depends on the proportion of amphipathic molecules in the monolayer which can be overturned upon contact with water.

Rideal and Tadayon (16,17) showed that the contact angle between water and solid crystalline stearic acid decreases with time because of the mobility of stearic acid molecules in the solid state and the orientation of the carboxyl groups into the interface between the solid acid and water.

Later Gaines (18) also showed evidence for the mobility of stearic acid molecules; the carboxylic acid molecules deposited on a nonreactive metal substrate can be reoriented from their "normal position" (polar head toward the substrate) to the overturned position when another reactive surface is brought into contact or a liquid water drop is placed on the surface.

Yiannos (19) studied the nature of molecular reorientation and demonstrated that the reduction in contact angle upon interfacial aging in the presence of water is related to the mobile fraction of the monolayer. The overturning of the movable carboxylic acid molecules at the interface which were not anchored on the solid surface by a chemical reaction appeared to be responsible for the lower contact angle.

The basic concepts of surface chemistry described above indicate that the problem of improving sizing reduces to one of decreasing the free-surface energy of the cellulosic fiber surface. This reduction can be achieved by covering a significant proportion of the surface with properly oriented and stably anchored,

bulky amphipathic molecules. The advantage of using the amphipathic molecules is that they have a better chance of being retained on the fiber surface through chemical and physical interactions than nonpolar molecules.

INTERNAL SIZING WITH THE ROSIN-ALUM SYSTEM

GENERAL CONCEPTS

The penetration of aqueous liquids into paper products can be retarded or prevented by achieving and maintaining a sufficiently low free-surface energy upon the exposed fiber surfaces of the dried sheet.

In a paper mill this is commonly done by reacting a sizing agent such as a partially saponified rosin or fortified rosin with aluminum sulfate [papermaker's alum, $Al_2(SO_4)_3$ *ca.* $14H_2O$] in the presence of the papermaking pulp (12,20).

The usual procedure is to add the rosin size to the pulp and after thorough mixing, follow this with sufficient aluminum sulfate to lower the paper stock pH to about 4.5.

The reaction product of size and alum is commonly called "size precipitate" in which the amphipathic molecule, basic aluminum resinate is the active sizing species (8,12,21-23). This material and/or charged aluminum resinate are believed to form in the pH range between 4 and 7 by the reaction of resin acids with aluminum ions (8,9,12,21-25). These aluminum resinates exist with free acid in colloidal aggregations which are retained on the fibers during the sheet formation (8,12,23-25). During the drying process these aggregates develop resistance to being wetted by water, and sizing is thereby achieved.

The basic aluminum resinate molecules in the aggregates are generally believed to be oriented and anchored with their hydrocarbon position pointing away

from the fiber surface (8,12,23). The position and orientation of the free acid molecules are not clear. Vandenberg and Spurlin believe that they are on the interior of the precipitate particle after drying (24). Guide (8) and Watkins (23) have pictured them as randomly spaced and oriented molecules with some of the carboxyls exposed on the fiber surface; the acid molecules were found to detract from sizing.

Rosin is composed of a mixture of 80 to 90% resin acids and 10 to 20% of neutral materials (26). The resin acids are diterpenoid monocarboxylic derivatives of alkylated hydrophenanthrenes. They are generally classified into two groups, the abietic type and the pimaric type. Commercial rosin (gum, wood, and tall oil rosin) contains 59 to 79% abietic acid type resin acids; the exact amount depends on the source and the method of isolation (27-29).

MECHANISM OF ROSIN SIZING

In spite of the numerous studies, an exact mechanism of rosin sizing has not yet been defined that explains the results obtained for all sizing conditions. The difficulty in formulating an iron-clad mechanism probably arises because the system possesses both colloidal and ionic characteristics (30). The mechanism of the rosin-alum sizing process has been investigated chiefly in terms of the physical and chemical properties of the size precipitates and the cellulose fiber.

Many proposed theories take for granted the chemical composition of the size precipitate and a mechanism of retention is the principal consideration. In other theories, the opposite viewpoint is taken; that is, retention is assumed and chemical composition of the size precipitate is believed to be the controlling factor.

Apparently, in order to describe the complicated sizing process, both the factors should be interrelated. Guide (8) and Swanson (12) have proposed that any rosin sizing mechanism must consider at least three factors:

1. formation of potentially low free-surface energy precipitates;
2. retention of the size precipitate upon the fiber surface;
3. conversion of the wet sizing compounds on the solid surface to a stable low free-energy which remains fixed even though aqueous fluids are brought into contact with it.

Swanson (12,20) has discussed in detail the importance of the composition of the size precipitate, the possible factors involved in the retention mechanism, and the importance of the stable anchorage of the size precipitate on the fiber surface.

Among those three factors, the composition and nature of the size precipitate appear to be the most important factors because the retention and the anchorage of the formed size precipitate are influenced directly or indirectly by the composition of the colloidal precipitates; the electrokinetic and/or surface charge of a colloidal particle in aqueous solution may depend upon the chemical nature of the surface of the colloidal particles in the environment of adsorbable ions (31).

THE CHEMICAL NATURE OF THE SIZE PRECIPITATE

It is believed (8,12,21-25) that the reaction products of resin acid with aluminum ion are basic aluminum resinates. Whether this is the dibasic aluminum monoresinate or the monobasic aluminum diresinate or a mixture of the two, or the aluminum triresinate is still subject to debate.

The analysis of the composition of the size precipitate had been restricted to chemical analysis and selective solvent extraction techniques until 1964 (25).

In the late 1940's, chemical analysis and solvent extraction work by Price (32) seemed to demonstrate that size precipitate formed in distilled water by the addition of alum to completely saponified rosin size (i.e., neutral sodium resinate) consists of an equimolar mixture of aluminum diresinate and free resin acids. This conclusion was supported by Back and Steenberg (21), who carried out similar studies using sodium abietate. All three authors explained their results by assuming an ionic mechanism for the reaction of sodium resinate with aluminum sulfate.

However, in 1955, Jayme and Seidel (33) claimed that the precipitate consists of aluminum triresinate, and that this trisalt could be decomposed by traces of water in certain organic solvents to form the disalt plus free resin acids. After further research they agreed that both aluminum mono- and diresinates, as well as free acids, are present in the size precipitate (34), but they still maintained that the trisalt is also present as a distinct compound.

Guide (8) also used solvent extraction and chemical analysis techniques to determine the composition of precipitates formed when perchloric acid was added to alkaline sodium aluminate-sodium abietate systems. He concluded that the size precipitates were not stoichiometric compounds and that they consisted of co-precipitates of aluminum abietates, abietic acid, and aluminum hydroxide. Guide considered the precipitation reaction to be ionic. In 1964, Davison (25) employed for the first time the infrared spectroscopic technique with the analytical pyrolysis and chemical analysis techniques to determine the composition of the precipitates formed by adding alum or alum and sulfuric acid to alkaline rosin size solutions. He found that the precipitate formed near pH 4.5 was approximately an equimolar mixture of monobasic aluminum diresinate and free resin acid. Very recently, Major (11) confirmed again the mixed composition of monobasic diresinate and free resin acid by infrared and chemical analysis.

Contrary to the work cited above, Watkins (23) and Strazdins (9) reported that rosin is colloidal within the normal pH range used in commercial rosin-alum sizing. Watkins postulated that the aluminum ion reacts with carboxyl groups available on the surface of the colloidal particle to give dibasic aluminum monoresinate and monobasic aluminum diresinate; the monoresinate is formed by the reaction of the carboxylic acid with $Al(OH)_2^{+1}$ ions, and the diresinate with $Al(OH)^{+2}$ ions.

Vandenberg and Spurlin (24) proposed from an electrophoretic study that under usual sizing conditions with slight excess alum, the alum interacts with sodium resinate, free rosin, and calcium resinate to form a positive colloid with a surface consisting of equimolar amounts of a positive aluminum diresinate species and free resin acids. The positive charge of the aluminum resinate results from the ionization of the initially formed basic aluminum diresinate at pH below about 7.5.

Ekwall and Bruun (22,37) analyzed by the chemical method the reaction product between resin acid monolayers and aluminum ions and found that the reaction product was composed of aluminum monoresinate and unreacted resin acid, when the formation of aluminum monoresinate was not completed.

Later Friberg and Bruun (38) studied the structure of the aluminum resinate formed in the monolayer reaction by employing IR spectroscopic and x-ray diffraction methods. They stated that the aluminum resinate was dibasic monoresinate even though the IR spectrum for their collected monolayer sample revealed the existence of unreacted free acid molecules in the monolayer.

In conclusion, there is disagreement in the literature concerning the structure of aluminum resinate as to whether mono-, di-, and triresinate all exist as distinct compounds.

The discrepancy among the reported analytical results of the composition of the size precipitate may be caused by the following factors:

1. Different reaction conditions for the formation of the size precipitate; pH, aluminum ion concentration relative to the concentration of rosin, and the counter-anion concentration, if these affect the aluminum resinate formation.
2. Possible decomposition of an initially formed aluminum resinate during the solvent extraction, washing, and drying stages, as Jayme and Seidel pointed out (34).
3. Some contamination (or occlusion) of aluminum hydroxide in their collected size precipitate as Guide (8) suggested.

Finally, it is felt that it is necessary to investigate further the exact nature of aluminum resinate formed in the reaction between resin acids and aluminum ions with consideration of the above factors.

STUDIES OF THE STRUCTURE OF ALUMINUM SOAP

In contrast to the unsettled nature of the size precipitate, the structure of aluminum soaps of fatty acids appears to be established in the literature.

Much more intensive investigations have been directed toward elucidating the structure and the existence of a specific aluminum soap with the chemical analysis and IR spectroscopic techniques, and with synthesizing the aluminum soap.

In the early 1930's, attempts to synthesize the trisoap failed (39) but McGee and McBain (40) reported that the monosoap could be synthesized by reacting lauric acid with aluminum hydroxide in the absence of water; however, the monosoap was converted by reacting lauric acid into the disoap. Gray and Alexander (41) proposed the di-soap formation in the presence of water.

In 1952, Harple, et al. (42) presented the IR spectroscopic and chemical analysis evidence for monobasic disoaps whose spectra contain a free hydroxyl band at 2.7 μm (3710 cm^{-1}). Scott, et al (43) confirmed the presence of a free OH band at 2.7 μm (3710 cm^{-1}) in the spectrum of the monobasic disoap by a deuteration experiment and studied the possible presence of the hydrogen-bonded OH band at 3.0 μm for the dibasic monosoap. Bauer, et al (44) clarified further the structure of the disoap with x-ray diffraction and rejected the existence of the monosoap.

In 1957, Leger, et al. (45) gave IR spectroscopic evidence for the trisoap formed by a stoichiometric reaction of trimethyl aluminum and lauric acids in the absence of water; they also found that the trisoap decomposed into the disoap and free acids on hydrolysis in the presence of water. In 1964, Ellis and Pauley (46) reported the formation of the trisoap in the reaction of stearic acid monolayers because they found no free OH band at 2.7 μm (3710 cm^{-1}) for the aluminum soap multilayer built-up on the calcium fluoride plate; they were able to calculate the formation constant of the tristearate which appeared to be reasonably constant in the acidic pH range (3.5-3.9).

Several authors (47-50) reported that the trisoap could be synthesized, but the trisoap formed in the bulk phase was found to decompose into the disoap in the presence of water.

In summary, it appears to be established that the aluminum trisoap is formed as a distinct compound but this soap in the bulk phase appears to be liable to hydrolytic decomposition in the presence of water. The monobasic disoap is generally believed to be formed by the reaction of fatty acid with aluminum ions in the presence of water. The monosoap claimed by early authors has not yet been confirmed convincingly by later investigators as a primary reaction product of fatty acids.

MECHANISM OF THE REACTION OF RESIN ACIDS WITH ALUMINUM IONS

The mechanism of aluminum resinate formation in the rosin-alum sizing system is not yet settled. Guide (8) and Davison (25) and others (21,32) explained their results on the assumption that the reaction between sodium resinate and alum is ionic.

On the contrary, Watkins (23), Strazdins (9), Vandenberg and Spurlin (24) reported that rosin is colloidal within the normal pH range used in commercial rosin alum sizing. Thode, et al (35) and Ninck Block (51) reported also earlier that rosin is colloidal within the normal pH range used in sizing.

Consequently, it seems to be reasonable to postulate that in the actual sizing system the aluminum resinates and/or charged aluminum resinates are formed by the reaction between the resin acid molecules on the surface of the colloidal particle and aluminum ions surrounding the particle. This interfacial reaction is not believed to be ionic because the resin acids are not believed to be ionized significantly in the acidic sizing pH (4.0-5.0). Abietic acid, the main component of rosin, has an ionization constant value (pKa) of 6.4 (52).

Recently, Major (11) reported that the reaction mechanism between nonionized resin acid monolayers and aluminum ions is consistent with an ion-exchange mechanism in which cation exchange occurs between the monolayer carboxyl groups and aluminum cations of the substrate solution depending upon the concentration of aluminum ions.

The ion-exchange reactions between polyacrylic acids and polyvalent metal ions have been studied by evaluating the stability constants of metal ion complexes (53-56).

Chmutov and his coworkers in Russia (57) have reported that the sorption of metal ions on carboxylic acid cation-exchange resins involves the following

mechanism:

$$M^{n+} + nRCOOH \rightleftharpoons M(RCOO)_n + nH^+$$

i.e., the number of carboxyl groups reacting is equal to the charge of the metal ion, in the formation of complexes of metal ions with various resins.

Langmuir and Schaefer (58) and Davis and Rideal (59) suggested that the rate of the interfacial reaction between a fatty acid monolayer and metal ions present in water depends upon adsorption kinetics of individual metal ions.

In summary, the reaction between the resin acid monolayer on the surface of the colloidal particle and aluminum ion present in water is believed to be an ion-exchange reaction like the formation of complexes of metal ions with carboxylic acid cation-exchange resins; the monolayer reaction at the water interface may be dependent upon the charge of metal ions present in the water and their adsorption kinetics onto the spread monolayer.

CHEMISTRY OF ALUMINUM SALTS IN WATER

ALUMINUM SPECIES IN THE ABSENCE OF SULFATE IONS

It is now well recognized (10,60-63) that the aluminum ion forms a hydrate in aqueous solution, surrounding itself with six coordinated water molecules being octahedrally spaced about the Al^{+3} ion.

Because of the high charge and the small ionic radius of the hydrated aluminum ion, the hydrated aluminum is highly susceptible to hydrolysis upon dissolution. It is well known that the hydrate aluminum ion is acid in the Bronsted sense and undergoes hydrolysis according to the following reactions:

$$[Al(H_2O)_6]^{+3} + YH_2O \xrightleftharpoons{H_2O} [Al(OH)_Y(H_2O)_{6-Y}]^{+(3-Y)} + YH_3O^+ .$$

Upon hydrolysis, the $Al(OH)^{+2}$ ion species, and the $Al(OH)_2^{+1}$ ion species (64, 67) and the $Al(OH)_3$ precipitate (in all cases, water molecules in the first coordination sphere will be omitted) can exist in an aluminum salt solution such as aluminum chloride and aluminum nitrate.

Although many workers (61-63,65,70-74) do not believe the formation of $Al(OH)_2^{+1}$ ions upon hydrolysis, some workers (64,67) were able to calculate the second stage hydrolysis constant of aluminum ion and found that the concentration of $Al(OH)_2^{+1}$ ion is small compared to the concentration of $Al(OH)_1^{+2}$ ions in the pH range 4.0-5.0 (67). The formation constant for $Al(OH)_1^{+2}$ in the first-stage hydrolysis was reported to have a value of $10^{-5.02}$ (64); other reported values varied in the range of $10^{-4.61}$ to $10^{-5.74}$ depending upon the method of determination, the measuring temperature, and the total aluminum ion concentration (66). The value for the formation constant of $Al(OH)_2^{+1}$ in the second-stage hydrolysis was approximated to be 10^{-6} (64,67).

From the known values of the formation constants for the hydrolyzed Al ions, at low pH (pH <4) the predominant species appears to be the hydrated tripositive ion $[Al(H_2O)_6^{+3}]$. As the pH is raised from 4.0 to 5.0, the hydrolyzed Al ion, particularly the divalent hydroxoaluminum ion $[Al(OH)(H_2O)_5^{+2}]$ is believed to increase in concentration (67). When the pH is raised by the addition of base, it is possible to add ca. 2.5 equivalents of base per mole of Al ion, either as OH^- or HCO_3^-, to dilute solutions of aluminum nitrate or chloride or perchlorate in water at room temperature without obtaining a permanent precipitate.

As the dissolved solution of aluminum salt is aged, the hydrolysis is followed by slow polymerization. The hydrolyzed aluminum ions are linked to each other by the hydroxyl bridging process called olation (60,68). The simplest polymerization product between monomeric hydrolyzed species would result in the formation of a

dimer, which is believed to have the following structure (69):

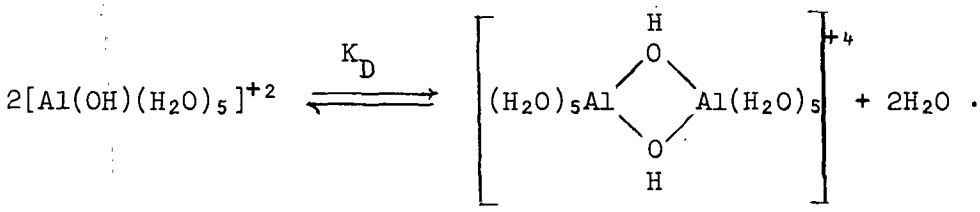

Evidence for this dimerization has been given by calculating the equilibrium constant of the dimerization; the reported value (K_D) varied from 60 (70) to 6000 (71) [pK_{22} from Al^{+3} ions: ca. 7.5 (70), 6.23 (71)].

Beyond the dimer, further polymerization of the hydrolyzed species is possible, resulting in the formation of polynuclear complexes (trimer, tetramers, etc.) which may exhibit various charges, depending upon the structure of the ion finally produced.

However, there is much less agreement as to what polymerized ion species exist in the solution which is increased in pH by adding base ions ([OH]/[Al] > 1.0) and aged. Perhaps the most important reason is the slow kinetics of the complexing reactions of the hydrolyzed ion species when the average number of hydroxide ions bound per aluminum atom ([OH]/[Al]) is in the range from 1 to 2.5, in sharp contrast with the hydrolytic reaction producing the $Al(OH)^{+2}$ species (65,66).

Matijevic, et al. (72) proposed $Al_8(OH)_{20}^{+4}$ at pH > 5.2 from a coagulation effects technique; similarly the species, $Al_7(OH)_{17}^{+4}$ was proposed by Beidermann (73) from potentiometric data. Recently Aveston (74) suggested the existence of the species $Al_{13}(OH)_{32}^{7+}$ in his two weeks aged solution from an ultracentrifugation and acidity measurement. The formation of the heptavalent polymerized species with the monomeric species, $Al(OH)_1^{+2}$, is supported by Akitt and his coworkers (62) from their Al^{27} NMR study. Other proposed species were reviewed by Patterson

and Tyree (66) who also supported from a light-scattering study the size of the polynuclear hydroxocomplex proposed by Aveston (74).

However, it is generally believed (62,75-77) that those polymerized hydroxocomplex species do not exist in the freshly prepared aluminum salt solution with pH < 5.2 because the formation is only possible at high pH, high temperature and longer reaction time (73); longer times of the order of 10 to 30 hours would be required at 20°C (77). The fraction of polynuclear complex ions in a solution appears to be decreased on dilution (85).

In a recent study of hydrolysis of dilute aluminum solutions, Frink and Peech (64) found only the species $Al(OH)^{+2}$, and no evidence for dimers or polymers in the pH range of 3.7 to 5.2 at the Al concentration range of 10^{-5} to 10^{-2}M of $AlCl_3$ and $Al(ClO_4)_3$. The study by Eyring, et al. (65) of the kinetics of proton transfer supports the species $Al(OH)^{2+}$, but is totally inconsistent with a dimerization. However, Akitt, et al. (62) and Kubota (71) suggested the possibility that the dimer of $Al(OH)^{+2}$ and $Al_2(OH)_2{}^{+4}$, can exist even in the freshly prepared solution of aluminum salt (0.2-0.3M).

In summary, the most probable aluminum ion species existing in the freshly prepared, dilute aluminum salt solution are believed to be Al^{+3}, $Al(OH)^{+2}$ and/or the dimer of $Al(OH)^{+2}$, $Al_2(OH)_2{}^{+4}$ at the concentration of total aluminum ions near 10^{-3}M in the pH range of 4.0 to 5.0.

ALUMINUM SULFATE COMPLEX IN THE PRESENCE OF SULFATE

It has been known since the work of Thomas (60) that certain anions possess a strong tendency to complex with the aluminum ion by replacing the coordinated aquo groups:

$$[Al(H_2O)_6]^{+3} + ZL^{-p} \rightleftharpoons [AlL_Z(H_2O)_{6-Z_p}]^{+(3-Z_p)} + ZpH_2O \ .$$

Thomas (60) gave the order of ascending coordinative affinity of the common anions for aluminum as:

> Nitrate (least coordinated), chloride, sulfate, acetate, tartrate, citrate = oxalate, hydroxyl (most), which is an order of complex formation or coordination common to many metal ions.

The sulfate ion in the acidic aluminum sulfate solution is generally believed to complex with an unhydrolyzed, hydrated aluminum ion forming the $AlSO_4^{+1}$ ion species. The existence of $AlSO_4^{+1}$ in the freshly prepared acidic aluminum solution was suggested by Behr and Wendt (76a), Nanda and Aditya (76b) and Nichide and Tsuchiya (76c) in the early 1960's. Recently, Stryker and Matijevic (76) calculated a stability constant (K_{AlSO_4}) of the $AlSO_4^{+1}$ with the value of 3.7×10^{-2} l/mol. from a study of coagulation effects of aluminum sulfate in acidic solution:

$$K_{AlSO_4} = \frac{[AlSO_4^{+}]}{[Al^{+3}][SO_4^{2-}]} = 3.7 \times 10^{-2} \text{ l/mol.}$$

Other reported values of the formation constant (K_{AlSO_4}) are: 110 (76), 1590 (75), and 5400 (77). Miceli and Steuhr (75) measured the kinetics of the sulfate ion complexing with Al^{+3} ion. Very recently, Akitt, et al. (78) gave unequivocal evidence for the formation of $AlSO_4^{+1}$ ions by means of Al^{27} NMR spectroscopy. They also reported that the $AlSO_4^{+1}$ is probably formed from the SO_4^{-2} rather than the HSO_4^{-} ion. No evidence was obtained of the formation of $Al(SO_4)_2^{-1}$.

Over the higher pH range (pH > 4), the sulfate ions may act as "penetrators" replacing some hydroxyl groups in the hydrolyzed aluminum complex ion, as Thomas and Vartanian (79) assumed, forming aluminum sulfate complex ions having the composition $[Al_8(OH)_{10}(SO_4)_5]^{4+}$ (61). However, it is not known whether the

sulfate ion can complex with hydrolyzed Al ion, $Al(OH)^{+2}$, forming a basic sulfato complex [$Al(OH)SO_4$].

Several investigators have suggested formulations for the basic aluminum sulfate complexes and these are reviewed by Matijevic and Stryker (61). All these species are supposedly of low positive charge, neutral, or even negatively charged, such as $Al(OH)SO_4$, $Al_2(OH)_4SO_4$, $Al(OH)SO_4$, or $Al(OH)_2SO_4^-$. The formation constants of these complex ions are not available in the literature.

In conclusion, in an aqueous dilute, acidic aluminum salt solution containing sulfate ion, the following aluminum ion species may exist:

Al^{+3}, $AlSO_4^{+1}$, $Al(OH)^{+2}$, $Al_2(OH)_2^{+4}$ or $Al(OH)SO_4$ or its dimeric or polymeric complex ions.

The concentration of each ionic species is expected to vary depending upon the pH, concentration of SO_4^{-2}, Al^{+3} or OH^- and ionic strength of the freshly prepared, dilute aluminum salt solution. However, it is possible to predict the behavior of each ionic species existing in the fresh solution because the formation constants or stability constants of some of the complex aluminum ions are available in the literature.

ADSORBABILITY OF HYDROLYZED ALUMINUM IONS

Langmuir and Schaefer (58) suggested that the adsorption of metal ions on the undersurface of the monolayer spread on the water should be considered an important factor in the interfacial reaction of the monolayers with metal ions present in water. The adsorption of such metal ions on the monolayer should depend chiefly upon the concentration of the adsorbable ion species and their rate of diffusion to the monolayer.

It is now a well-established fact (80-85) that hydrolyzed aluminum ion species have enhanced adsorbability on lyophobic surfaces as compared with the unhydrolyzed species. This tendency to be adsorbed is especially pronounced for polymeric hydrolyzed species, i.e., $Al_8(OH)_{20}^{+4}$ (80,81). No adequate theory for this enhanced adsorption by hydrolysis is available, but a few qualitative reasons have been suggested by Stumm and his coworker (82):

(1) The effective charge density of the Al ion is reduced with increasing degree of hydroxidation and multimerization. Hydrolyzed species are large and less hydrated than nonhydrolyzed species. The hydroxo-aluminum complexes are less "hydrophilic" as compared with the strongly hydrated, nonhydrolyzed aluminum ion. Correspondingly, these isopolycations will accumulate at the solid-liquid interface.

(2) The enhancement of adsorption is apparently due to the presence of a coordinated OH^- group. Simple OH^- ions are bound at many solid surfaces and are frequently potential determining ions; hydroxo metal complexes may similarly or to an even larger extent be adsorbed to the solid surface (84-85).

Alternatively, the replacement of an aquo group by a hydroxo group in the coordination sheath of a metal atom may render the complex more hydrophobic by reducing the interaction between the central metal atom and the remaining aquo groups. This reduction in solvent-hydroxo complex interaction might then in turn enhance the formation of (covalent) bonds between the metal atom and specific sites (i.e., COOH groups) on the solid surface by reducing the energy necessary to displace water molecules from the coordination sheath.

Adsorption of hydrolysis species of aluminum must be assumed to occur on most interfaces including the resin acid monolayers in contact with aqueous aluminum solutions, and is thus of considerable significance in the reaction of the monolayers forming basic aluminum resinate complexes.

WETTABILITY AND MEASURE OF SOLID SURFACE ENERGY

The contact angle formed by a sessile drop of liquid resting on a solid surface has long been used as an inverse measure of the wettability of the solid. In the paper industry the measurement of contact angles between a drop of water or other aqueous liquid and the surface of a paper sample has been used for testing the paper for sizing (TAPPI Standard T 458).

The changes in surface free energy ΔF^S, accompanying a small displacement of the liquid such that the change in area of solid covered ΔA, may be expressed according to Adamson (87) as

$$\Delta F^S = \Delta A(\gamma_{sl} - \gamma_{sv}) + \Delta A - \gamma_{lv} \cos(\theta - \Delta\theta) \qquad (4)$$

where γ_{sl} is the specific free energy in ergs/cm^2 of the solid-liquid interface, γ_{sv} is the specific surface free energy of the solid in equilibrium with vapor, γ_{lv} is the specific free energy of the free liquid surface in equilibrium with its vapor, and θ is the solid-liquid contact angle as measured through the liquid between the solid surface and a tangent to the liquid surface at the three-phase boundary. At equilibrium

$$\lim_{\Delta A \to 0} \Delta F^S/\Delta A = 0$$

and

$$\gamma_{sl} - \gamma_{sv} + \gamma_{lv} \cos\theta = 0$$

or

$$\gamma_{lv} \cdot \cos\theta = \gamma_{sv} - \gamma_{sl}. \qquad (5)$$

Alternatively, in combination with the definition of work of adhesion, W_A,

$$W_A = \gamma_{sv} + \gamma_{lv} - \gamma_{sl} :$$

$$W_A = \gamma_{lv} (1 + \cos\theta) \qquad (6)$$

where W_A is the reversible work of adhesion to the solid.

Equation (5) was stated in qualitative form by Young in 1805 (86), and the equivalent equation, Equation (6), was stated in more definite form by Dupre in 1869 (89) along with the definition of work of adhesion. Equation (5) is the more common form, and is generally called the Young equation.

It is important to keep in mind that phases are supposed to be mutually in equilibrium and, in particular, the designation γ_{sv} is a reminder that the solid surface near the liquid should have an equilibrium adsorbed film of vapor having a film pressure, π_e. Thus,

$$\gamma_{lv} \cos\theta = \gamma_s - \gamma_{sl} - \pi_e. \qquad (7)$$

This distinction between γ_s (the surface free energy of the solid in a vacuum) and γ_{sv} seems to have been first made clear by Bangham and Razouk (90). The value of π_e at equilibrium conditions can be calculated from an integration of the liquid-vapor-solid adsorption isotherm. This term has been frequently neglected, and a critical review of such an assumption has been recently presented by Fowkes (91).

The contact angles are known to be affected by the surface roughness on a microscopic scale. Wenzel developed a relationship between the surface roughness and the contact angle (92) and discussed the roughness factor, r (defined as the ratio of the true area of the solid to the apparent area or envelope). The apparent or measured contact angle, θ', was related to the true contact angle by the well-known expression, $r = \cos\theta'/\cos\theta$, obtained by combining Young's equation

and the definition of r. The consequences of Wenzel's equation have been discussed by Zisman (88). Recently, Tamai and Aratani (93) verified experimentally Wenzel's relation using a model of a rough surface.

Quantitative application of contact-angle measurement to the determination of the solid surface free energy has been limited by the difficulty in evaluating the interfacial-energy term γ_{sl} in the Young equation.

The determination of the surface energy of a solid is of interest in fields of adhesion and adsorption where intermolecular forces operate across an interface. As yet, no general method of measuring solid surface energy has been found.

Zisman (88) has introduced the concept of critical surface tension γ_c as an empirical method of determining the wettability of solid surfaces by plotting the cosine of the contact angle vs. the surface tensions of a series of homologous liquids. The point at which the resulting line intercepts the line $\cos\theta = 1$ is called the critical surface tension γ_c. The actual meaning of γ_c has been the subject of much discussion and has led to various interpretations (94-100).

Girifalco and Good (95,100-103) and Fowkes (91,98,104-106) have brought much order to the system of combined forces at and across an interface. These theories have been extended to cover particular situations by several authors, including Owens and Wendt (99), Dann (97), Chan (96), and Wu (107).

THEORY OF INTERFACIAL FREE ENERGY

The concepts of interfacial free energy can be expressed according to Good and Elbing (103)

$$\gamma_{12} = \gamma_1 + \gamma_2 + 2\,\phi_{12}\sqrt{\gamma_1\gamma_2}\,. \qquad (8)$$

Where γ_{12} is the interfacial free energy at the interface between Phase 1 and Phase 2 and γ_1 and γ_2 are the surface free energies of Phase 1 or Phase 2, respectively. ϕ_{12} is defined as the ratio of the free energy of adhesion between Phases 1 and 2 to the geometric mean of the free energies of cohesion of the separate phases.

Expressions for the free energies of adhesion and cohesion in terms of molecular properties were derived by integration of a Lannard-Jones potential energy function from equilibrium intermolecular distance to infinite separation (103). The resulting expressions for ϕ_{12} are of the form,

$$\phi_{12} = (A_{12}/\sqrt{A_{11} \cdot A_{12}})(\gamma_1\gamma_2/\gamma_{12}^2) = \phi_A \cdot \phi_r \qquad (9)$$

where the $\underline{A}$'s are the attractive constants in the potential energy function between the phases designated as subscripts and the $\underline{r}$'s represent equilibrium intermolecular distances. The term $\phi_{\underline{r}}$ is generally very close to unity, provided that the molecular sizes of the two substances are not drastically different (103). The other component of ϕ,

$$\phi_A = A_{12}/\sqrt{A_{11}\ A_{22}} \qquad (10)$$

where $\underline{A}_{12} = \underline{A}^d_{12} + \underline{A}^o_{12}$,

is evaluated from the parameters that determine intermolecular potential functions. For the general case, the secondary intermolecular interacting forces are contributed by the orientation effect forces ($\underline{A}^o_{12}$), dispersion forces ($\underline{A}^d_{12}$), and induction forces. However, the induction effect is negligible (103).

Under these conditions, the components of $\underline{A}_{12}$ can be expressed as geometric means of the components of $\underline{A}_{11}$ and $\underline{A}_{22}$:

$$A^d_{12} \simeq \sqrt{A^d_{11}\ A^d_{22}} \qquad (11)$$

$$A_{12}^{\circ} = \sqrt{A_{11}^{\circ} A_{22}^{\circ}}. \qquad (12)$$

Assuming the approximation of Equation (11) to be valid, Equation (10) may be combined with Equations (11) and (12), to give

$$\phi_A = \sqrt{(A_{11}^{d}/A_{11})(A_{22}^{d}/A_{22})} + \sqrt{(A_{11}^{\circ}/A_{11})(A_{22}^{\circ}/A_{22})} \cdot \cdot \qquad (13)$$

It is useful to define a quantity, p, which may be termed the "fractional polarity" for each surface:

$$p_1 = A_{11}^{\circ}/A_{11} \qquad (14)$$

$$p_2 = A_{22}^{\circ}/A_{22}. \qquad (15)$$

The complements, d, of these quantities represent the relative significance of dispersion forces at each surface:

$$d_1 = A_{11}^{d}/A_{11}, \qquad (16)$$

$$d_1 + p_1 = 1, \quad i=1,2. \qquad (17)$$

Equation (13) then becomes:

$$\phi_A = \sqrt{d_1 d_2} + \sqrt{p_1 p_2}. \qquad (18)$$

The fractional quantities corresponding to p and d were defined in terms of polar and nonpolar components of surface free energy:

$$d_1 = \gamma_1^{d}/\gamma_1, \qquad (19)$$

$$p_1 = \gamma_1^{p}/\gamma_1. \qquad (20)$$

If these quantities are substituted into Equation (18), Equation (8) then becomes (with $\phi_r = 1$):

$$\gamma_{12} = \gamma_1 + \gamma_2 - 2\sqrt{\gamma_1^d \gamma_2^d} - 2\sqrt{\gamma_1^p \gamma_2^p} \quad . \tag{21}$$

This relationship is the same equation which was recently proposed by Owens and Wendt (99).

If one of the substances is nonpolar, and capable of interaction by dispersion forces only, then Equation (21) reduces to that proposed by Fowkes (98):

$$\gamma_{12} = \gamma_1 + \gamma_2 - 2\sqrt{\gamma_1^d \gamma^d}, \text{ for } \gamma_2^p \text{ or } \gamma_1^p = 0. \tag{22}$$

EVALUATION OF SURFACE-FREE ENERGY

On the assumption that the solid surface is so smooth that the effect of roughness on contact angle can be neglected, and that $\pi_e = 0$, Fowkes has derived by combining Equation (7) and Equation (22) an expression for the contact angle of a liquid on solid in terms of the dispersion force contributions of each:

$$1 + \cos\theta = 2\sqrt{\gamma_s^d}\left(\sqrt{\gamma_l^d}/\gamma_{lv}\right). \tag{23}$$

Since values of γ_l^d have been published for many liquids (98), it is possible to approximate γ_s^d from a simple measurement of θ by the use of Equation (23) in cases where only dispersion forces operate (i.e., the liquid or solid is nonpolar).

For cases when both forces operate, a more useful form of Equation (23) was obtained by combining (21) with the Young equation by Owens and Wendt (99)

$$\cos\theta = -1 + 2\sqrt{\gamma_s^d}\,(\gamma_l^d/\gamma_{lv}) + 2\sqrt{\gamma_s^p}\left(\sqrt{\gamma_l^p}/\gamma_{lv}\right) \quad . \tag{24}$$

They used this equation to calculate the components of surface energy for several solid polymers. Brown (124) used this technique to calculate the components of surface energy of corona treated cellophane.

In the present study the Owen-Wendt technique will be used to determine changes in components of surface free energy of monolayers cast on the carboxymethyl cellulose film as the composition of the reacted monolayer is varied by the influence of excess sulfate.

CONTACT ANGLES OF WATER ON THE ROSIN ACID MONOLAYERS

The works of Back and Steenberg (21), Ekwall and Bruun (37), Guide (8) and Major (11) show that considerably higher contact angles (90 to 105°) occur between water and aluminum rosinate than between water and rosin acid (60 to 70°). However, no one has yet evaluated quantitatively the surface free energy of the rosin and aluminum rosinate, and the difference in components of surface free energy between two solid surfaces.

Furthermore, the reason for the contact angle of water being lower on the rosin acid than on aluminum rosinate has not been fully delineated. A probable reason for the lower contact angle for the rosin-acid-water system, however, has been postulated by Swanson (12,20). It is suggested that the lowering of contact angles of water on rosin acid is due to overturning of the amphipathic molecules when a strongly polar liquid such as water is placed on the surface. On the other hand, aluminum resinate molecules somehow cannot overturn readily when in contact with water.

Consequently, it would be interesting to investigate in this study how and why the surface free energy of the monolayer is changed when the free acid fraction in the monolayer is increased, in order to verify Swanson's hypothesis.

SURFACE CHEMICAL MODEL OF ROSIN-ALUM SYSTEM

The formation of (basic) aluminum resinate in the rosin-alum sizing system is believed to occur at the interfaces between colloidal resin acid particles and the surrounding aqueous solution containing hydrated aluminum ions (9,11,21-24,35,36,51). It is also assumed that the aluminum resinate can form at the surface of cellulosic fibers; the fiber surface first adsorbs aluminum ions from the solution due to its base exchange capacity, and then the adsorbed aluminum reacts with colloidal resin acid particles on the fiber surface. Wherever the reaction location occurs in the rosin-alum-fiber system, the success of the rosin sizing operation depends upon this surface reaction. Both the retention and stabilization of the size precipitate on the fiber surface are functions of the (basic) aluminum resinate content of the precipitate (11).

Ekwall (108) noted that the behavior of substances in monolayers is directly connected with their behavior in colloidal aggregations. The packing of molecules in the surface of a colloidal particle can be no closer than in a condensed monolayer of the same substance on an aqueous substrate. This correlation has been proven for the alkali salts of n-long paraffin chain fatty acids by x-ray investigation (109). The molecular packing area is the average cross-sectional area of the molecules (A_K, A^2, $mole^{-1}$) at the point of film collapse for a monolayer under lateral compression.

Ekwall and Bruun (109,110,37) first used the surface chemical model for the reaction between hydrated aluminum ions and colloidal resin acid.

These workers found that π_K (surface pressure of the monolayer at the point of film collapse for a monolayer under lateral compression) and A_K values can be used to follow the reaction between resin acid monolayer molecules and aluminum ions in the substrate.

Strazdins (36) also used a surface model system to determine the aluminum counterion shielding effect on the colloidal surface. He reported that sulfate ions and especially citrate ions appeared to show strong film contraction effects which could be related to reduction in the electrokinetic charge of the underlying aluminum ion lattice. He suggested that the sulfate ion could moderate the high positive charge density of aluminum complex flocs to improve the retention and uniformity of rosin deposition on fibers. Strazdins did not take into consideration the possibility that sulfate ion could also be involved in the reaction between resin acid and aluminum directly or indirectly, in ways other than the effect on the electrokinetic charge on the surface of colloidal particles.

Recently, Major (11) also used a surface chemical model to determine the effect of oxalate on the reaction between tetrahydroabietic acid monolayer and aluminum ions. He verified Cobb and Lowe's hypothesis that oxalate ions inhibit the reaction by sequestering the aluminum ions.

It is generally believed (111) that carboxylic acid molecules in a monolayer on an aqueous substrate are oriented so that the polar carboxyl groups are in the substrate.

PRESENTATION OF THE THESIS PROBLEM

It is hypothesized that the reported detrimental effect of excess sulfate on rosin sizing can be attributed to an inhibiting effect of sulfate on the reaction between resin acids and aluminum ions forming aluminum rosinates at pH 4.0-5.0. This hypothesis is based on the probability that the sulfate ion can coordinate with hydrated aluminum ions forming the sulfate complexes in preference to the formation of aluminum resinates.

The well-established complex chemistry of aluminum ions also leads to the hypothesis that the structure of aluminum resinate formed in the reaction may be different depending upon the pH and, accordingly, the effect of sulfate on the reaction may vary with changing pH. In this hypothesis, the aluminum resinate formation is considered to be an ion-exchange reaction in which the cations are exchanged between hydrated Al ions and nonionized carboxyl groups of colloidal resin acid particles.

From the above basic hypotheses on the reaction between resin acid and aluminum ions, and possible effects of excess sulfate on the reaction, the purpose of this thesis is to answer the following questions:

(1) Does excess sulfate in the rosin-alum sizing system inhibit (prevent) the reaction between resin acids and aluminum ions at the pH range of 4.0 to 5.0?

(2) If the excess sulfate does prevent the reaction of resin acids with aluminum ions, what is the mechanism involved?

(3) If the sulfate does not prevent the reaction, why is the reaction not influenced by sulfate ions, and then what is responsible for the known detrimental effect of excess sulfate on rosin sizing?

(4) When sulfate affects the reaction, how will the free-surface energy of the reaction product be changed in connection with the effect on the actual sizing development?

EXPERIMENTAL APPROACH TO THESIS PROBLEM

The effect of excess sulfate on the reaction between colloidal resin acid agglomerates and aluminum ions will be investigated with the surface chemical model using the resin acid monolayer. The resin acid monolayer is pictured as similar to the surface of a colloidal resin acid particle with an infinite radius. The effect of sulfate on the interfacial reaction will be quantitatively determined from changes in the physical and chemical properties of the monolayer when the sulfate concentration in the aluminum salt substrate solution is increased while holding the pH at 4.0.

The effect of pH on the sulfate effect will be examined also by the same method when the pH of the substrate solution is changed at a constant concentration of aluminum and sulfate.

The multiple internal reflectance (MIR) spectroscopic technique will be applied to analyze the composition of the monolayer, and to study the structure of aluminum resinate formed in the monolayer and the role of sulfate ions in the formation of the aluminum resinate complex.

MIR spectroscopy (112) has several advantages over conventional transmittance spectroscopy for the study of monolayers (113-117):

1. It allows use of uncollapsed monolayer samples which are transferred directly onto a prism plate from the surface of the substrate solution. This eliminates the possibility of structural changes of the reacted monolayer caused by the monolayer collapsing. Transmittance spectroscopy must use the "collapsed" monolayer sample collected by the skimming technique (11).

2. MIR spectroscopy does not require extensive drying of the cast monolayer samples collected on the plate because MIR spectra are less affected by contamination of water. This technique also avoids possible decomposition of the reaction products formed initially in the monolayer during drying (38).

Consequently, the MIR spectrum for the uncollapsed monolayer samples should reveal the exact composition of the reacted monolayer and help clarify the structure of aluminum resinate formed in situ in the interfacial reaction.

The changes of free-surface energy and its components for the monolayer will be determined by contact-angle measurement using the Owens-Wendt equation. This should permit correlation of the effect of sulfate on the reaction between resin acid monolayers and aluminum ions with sizing development as experienced in actual rosin-alum sizing practice.

The contact angle data and calculated components of free-surface energy for the monolayer will also provide corroboratory information regarding the chemical composition and structure of the monolayer under investigation.

EXPERIMENTAL

EXPERIMENTAL DESIGN OF SURFACE CHEMICAL MODEL

The surface chemical model consists of a monolayer of tetrahydroabietic acid spread on an aqueous substrate at pH range of 4.0 to 5.0. This is the common pH range for free resin acid sizing at most paper mills (12) without precipitating the aluminum hydroxide complex (37).

The basic substrate used was aqueous $Al(NO_3)_3 \cdot 9H_2O$ solution containing potassium sulfate. The concentration of sulfate in the substrate solution was increased by adding the desired amount of sulfate to newly prepared aluminum nitrate solution. The Al concentration was held at $[Al] = 3.16 \times 10^{-3}$M in the pH range 4.0 to 4.5. For the monolayer reactions at pH's above 4.50, the Al concentration was decreased to 3.16×10^{-4}M to avoid precipitating $Al(OH)_3$. The Al concentrations of 3.16×10^{-3}M and 3.16×10^{-4}M in the substrate solution were selected for the monolayer reaction at pH 4.0-4.5, and at pH 4.5-5.0, respectively, because Bruun (37,110) reported that the maximum interactions occurred between the resin acid monolayers and aluminum ions under those substrate conditions without significant precipitation of aluminum hydroxide. Major (11) also selected the Al concentration of 3.16×10^{-3}M for the reaction at pH 4.0.

In all cases the substrate solution was freshly prepared and used as soon as possible (within 2 hours) to avoid any complication in the interfacial reaction caused by possible polymerization of hydrolyzed Al ions in the substrate.

Although the abietic acid is the predominant acid in commercial rosin, the monolayers of this material were not used because they oxidize rapidly at the water-air interface (109,110). Instead tetrahydroabietic acid (the fully saturated abietic acid-type resin) monolayers were used because they give the

same type of π-A isotherm as unoxidized abietic acid monolayers and they are not subject to rapid oxidation (109,110). The tetrahydroabietic acid will be referred to as TABSH as Major did (11), in all cases. It is also well recognized (109,110, 52,11) that TABSH acid monolayers are not significantly ionized in aqueous solutions with a pH range 4.0 to 5.0.

PREPARATION OF TETRAHYDROABIETIC ACID SPREADING SOLUTIONS

The sample of tetrahydroabietic acid (TABSH) was obtained from Hercules, Incorporated. The sample was further purified by recrystallization from methanol to remove a small fraction of n-hexane insoluble material. The recrystallized sample was analyzed by gas chromatography (as given in Appendix I) in order to determine its isomeric composition and the contamination of other types of resin acids. The analysis indicated the absence of other resin acids and essentially the same isomeric composition as the acid used by Major (11).

n-Hexane was used to prepare the TABSH spreading solution in a volumetric ground-glass stoppered flask whose volume was calibrated by the double weighing method. The concentration of the TABSH spreading solution for monolayers was 4.92×10^{17} molecules ml^{-1} (0.251 $mg \cdot ml^{-1}$) of solution.

The concentration used for monolayers to be built-up on the germanium plate for their MIR spectra was 5.27×10^{17} molecules ml^{-1} (0.268 $mg \cdot ml^{-1}$) of solution. The spreading solutions were stored in a clean desiccator over calcium chloride and pure hexane solvent in order to minimize solvent evaporation from the volumetric flasks.

The n-hexane solvent for the preparation of the spreading solution was twice distilled from pyrex glass, and the middle cut was slowly percolated through an adsorption column of alumina and silica gel.

PREPARATION OF SUBSTRATE SOLUTIONS

The water used for the substrate solution was deionized and triply distilled, the second distillation from alkaline permanganate. Laboratory distilled water for cleaning the trough of the surface film balance was obtained from a commercial pyrex still using feed water deionized through a mixed-bed ion-exchange resin column. The redistilled water was obtained from a two-stage pyrex still using the laboratory distilled water as feed. The detailed procedure for obtaining the redistilled water is described in Neuman's thesis (118). The purity of water was checked for inorganic contaminant by measuring the specific conductance, and for organic contaminant by the surface chemical technique as described by Major (11) (detecting film pressure due to spreadable contaminant). Only water with a specific conductance less than 1.2×10^{-6} ohm^{-1} cm^{-1} was used for the substrate.

The aluminum nitrate (or aluminum sulfate) plus potassium sulfate substrate solution was prepared by dissolving the desired amount of the aluminum salt with the desired volume of the sulfate stock solution. The stock solution of potassium sulfate was prepared at the concentration of 0.5M. Since the stock solution sometimes showed slight turbidity due to insoluble dust particles, the solution was filtered through Millipore (pore size 0.22 μm) to obtain a clear solution before adding the aluminum nitrate. No significant change in the sulfate concentration after the filtration was observed by an emission spectroscopy technique.

The pH of the substrate solution was adjusted approximately 30 minutes, after additions of aluminum nitrate and the sulfate stock solution, with 0.1N or 0.5N hydrochloric acid, and 0.2N potassium hydroxide or 1N sodium hydroxide solutions. The acid and base solutions of high concentration (i.e., 0.5N HCl, 1N NaOH) were used in case a considerable amount of the acid or base was required to adjust pH;

this was done to minimize the decrease in the aluminum concentration caused by the addition of the acid or base solution.

When the base solution was added to the aluminum nitrate solution, the solution was thoroughly agitated to reduce localized aluminum hydroxide precipitation while adding the base very slowly in a dropwise manner.

The volume of the acid or base solution added usually was too small to affect significantly the desired concentration of aluminum ions in the substrate with excess sulfate.

When a considerable amount of the base was required to raise the pH of the aluminum nitrate solution without excess sulfate, the predetermined volume of the base solution was first diluted before adding to the aluminum solution to minimize the localized precipitation of aluminum hydroxide.

Less than 1.0 equivalent of OH ion per mole of Al ion was added to all the aluminum nitrate substrate solutions containing potassium sulfate and to the aluminum nitrate solutions with pH < 4.5 (without sulfate ion). However, it was necessary to add ca. 2.0 equivalents of OH^- ion per mole of Al to the aluminum nitrate solutions with the $[Al] = 3.16 \times 10^{-4}$ M and $[SO_4] = 0$ for the pH adjustment above 4.8.

All the substrate solutions were transferred to the trough in less than 2 hours after the preparation, and then the monolayer was spread on the substrate.

The final stabilized, adjusted pH of the prepared substrate was recorded just prior to transferring to the trough (approximately 30 minutes later after the pH adjustment). The adjusted pH was not changed significantly during the times of the experiment. All the prepared substrate solutions were entirely

free of visible precipitate after preparation except those of the substrates with the [Al] = 3.16×10^{-3}M, the [SO_4] = 0.2M, and the pH > 4.4.

DETERMINATION OF SURFACE PRESSURE-AREA ISOTHERMS

APPARATUS

The π-A isotherms for the determination of A_{10}, $A_{K,EX}$ and $\pi_{K,EX}$ were obtained with the automatic recording Langmuir-Adam film balance which was used by Major (11). This instrument had been modified by Neuman (118) to include constant surface pressure operation. It was necessary to maintain a constant surface pressure for the Langmuir-Blodgett multilayer deposition on the germanium plate used for the MIR spectroscopy and for casting the monolayer on the carboxylic methyl cellulose (CMC) film used for the contact angle measurements.

The automatic film balance consisted of a Lucite trough (34 by 5.8 by 0.5 inch) which was rigidly mounted to an aluminum support and contained a well (3¼-in. long, 2.0-in. wide, and 3-in. deep) centered about 4 inches from the mica float. The well accommodated the teflon holder with the germanium plate for the multilayer deposition and the glass slide coated with the CMC film. The trough edges were covered with teflon tape (3M Co. Scotch Brand, 3-mil thickness). Purified white paraffin wax (melting range 63-69°C) was applied while molten to cover the tape seams and remaining parts of the trough. The surface pressure was measured with a Cenco du Nouy torsion head equipped with a monel torsion wire (torsion constant 0.374 dyne/cm/degree), a slightly paraffined mica float, thin teflon foil and loops (0.002-in. thickness) and a magnetic damper.

The operational sensitivity of the surface pressure measurements and of the constant pressure operation was ± 0.2 dyne cm^{-1} mm^{-1}. The operational sensitivity is the reciprocal of the slope of the surface pressure calibration curve (119).

The compression barrier speed was 1.97 cm/min which corresponded to an average compression rate of 2.51 A^2 $molecule^{-1}$, $minute^{-1}$ for the surface pressure-area isotherms. This was the maximum rate for the balance but it was lower than used by Bruun (110), and Major (11). The design used the null-deflection balance to detect a change in the surface pressure, and the compression barrier was automatically activated to correspondingly return the balance to null position. Detailed descriptions of the instrument and other related equipment for the automatic surface balance are given by Major (11) and Neuman (118).

TECHNIQUE

The substrate solution which was added to the trough by a graduated cylinder was allowed to condition for about half an hour. The test and film-free reference surfaces of the substrate solution were cleaned by sweeping them with movable barriers. A micropipet was used to deposit 9.84×10^{16} molecules on the test area from 4.92×10^{17} molecule ml^{-1} n-hexane solution of TABSH. This spreading solution was placed on the center of the test surface in a dropwise manner. The time allowed for the reaction before the monolayer was compressed was about 10 minutes which is sufficient time for n-hexane to evaporate, and for the reaction of monolayer with aluminum ions to reach an equilibrium state (58,11).

The average area available to the monolayer molecules was reduced at the constant compressing rate. The π-A isotherm for the monolayer was recorded continuously over the range of 58 A^2 to 36 A^2 per molecule.

In practice, the displacement of the recorder pen along the Y-axis of the chart on the X-Y recorder provided a measure of the surface pressure. The displacement of the chart along the time axis provided a measure of the position of the compression barrier.

The correlation of the surface pressure and the displacement of the chart recorder pen was determined by the same calibration method which Major (11) and Neuman (118) employed for their studies. The surface pressure is calculated from the relation (119),

$$\pi = (wg\ell_c)/(\ell_f L), \tag{25}$$

where

π = surface pressure, dynes/cm

w = calibration weight, grams

g = gravitational constant

ℓ_c = lever arm for the calibration weights, cm

ℓ_f = lever arm for the float, cm

L = effective length of the float, cm

The effective float length, L, is generally taken as the length of the float plus half the width of the gaps occupied by the teflon end loops.

The surface pressure, π, is generally considered to be equal to the reduction of the pure liquid-surface tension by the film:

$$\pi = \gamma_o - \gamma \tag{26}$$

where γ_o is the surface tension of the pure liquid, in dynes cm^{-1} and γ is the surface tension of the film-covered surface, in dynes cm^{-1}.

The calibration curve for correlating π to the pen displacement was essentially linear in the range of surface pressure measured in this study (0-40 dynes cm^{-1}). The pressure sensing device, the torsion balance head, was calibrated daily during the π-A isotherm determinations.

The average cross-sectional area of the monolayer molecules $\underline{A}$, was measured by dividing the total area occupied by the monolayer molecules by the known number of the monolayer molecules (9.84×10^{16} molecules). The total area occupied by the monolayer molecules $\underline{A_t}$ is equal to

$$A_t = (BW) + C \qquad (27)$$

where $\underline{B}$ = the test area length, the distance between the edge of the mica float and the leading edge of the compressing barrier in cm; $\underline{W}$ = the test area width, the width of the substrate solution surface in cm; and $\underline{C}$ = area occupied by the teflon end loops in cm^2. The length of the test area was experimentally measured with a metric scale attached to the trough.

After each π-$\underline{A}$ isotherm determination, the compression barrier was returned to its initial position. The film material was skimmed from the trough, and then the trough was flooded with distilled water. The remaining liquid was removed from the trough by suction. The trough edges were cleaned with $\underline{n}$-hexane. The trough was then filled and flooded with distilled water and emptied by suction.

The π-$\underline{A}$ isotherms were generally reproducible and were similar to the isotherms determined by Major under the same substrate condition. Reproducibility of π-$\underline{A}$ measurement was checked with TABSH monolayer on hydrochloric acid substrates as shown in Appendix II.

The standard error for the $\pi_{\underline{K},\underline{EX}}$ values of the TABSH monolayer was less than 0.1. The standard errors for the $\underline{A}_{\underline{K},\underline{EX}}$ and $\underline{A}_{10}$ values were, however, greater than 0.1, but less than 0.21.

The π-$\underline{A}$ measurement was carried out to obtain corroborative information about the sulfate effect on the monolayer reaction after the changes in the chemical composition of the monolayer were obtained as a function of the $[SO_4]$

with the MIR spectroscopic technique. Major (11) found that the effect of anion (oxalate) on the monolayer reaction can be monitored by the determination of changes in π-A isotherms or by analyzing the composition of the monolayer; either of these two methods gives identical results regarding the effect of anion on the monolayer reaction forming aluminum resinate.

SPECTROSCOPIC ANALYSIS OF THE MONOLAYER

MULTILAYER DEPOSITION ON THE GERMANIUM PLATE

Langmuir-Blodgett multilayers were deposited on the germanium prism plate (purchased from Wilks Scientific Co.) to obtain IR spectra with the MIR spectroscopic technique for the composition analysis of the monolayer.

Cleaning of the Germanium Plate

The germanium plate (52.5 by 10 by 1 mm thick, 45° face angle) was selected because the germanium has the highest refractive index of the available crystals for the internal reflection spectroscopy, is insoluble in acidic aqueous solution, and is chemically inert (112).

The most important experimental requirement for reproducible results is cleanliness of the germanium plate. After some experiments, the following cleaning procedure was adopted. The plate was thoroughly washed with a detergent solution (Tide), rinsed with distilled water, rubbed with cotton swab soaked in redistilled methyl alcohol, and in redistilled methyl ethyl ketone (MEK). In the final stage of rubbing and rinsing, the plate was transferred to a teflon plate holder and again the whole thing was rinsed with MEK and dried in a vacuum oven at 80°C to remove the solvent. This was followed by an electrostatic cleaning with Plasma cleaner (an electrodeless radio frequency gas discharge

apparatus, purchased from Harrick Scientific Corporation). The cleanness of the plate could be checked either by observing drainage of solvent from the plate or examining the internal reflection spectrum of the surface of the plate.

The cleaned plate was then immediately immersed in the Langmuir trough. If the cleaned plate was not used immediately, the plate was stored for less than 30 minutes in an aluminum desiccator over aluminum shot which had been ignited previously at 500°C. Storage in the aluminum desiccator prevented the surface from being contaminated with organic materials from air while waiting for immersion (122).

Technique of Multilayer Deposition

The monolayers to be deposited were spread on the substrate solutions prepared by the method described previously. The volume of the TABSH spreading solution (5.27×10^{17} molecules ml^{-1}) was adjusted to furnish enough molecules for the multilayer deposition. This avoided the necessity of spreading a second monolayer on the used substrate surface.

The spread TABSH molecules (approximately 1.57×10^{17} molecules) were allowed to react for 30 minutes. The monolayer was compressed, usually to a surface pressure of 18 dynes cm^{-1}, and the automatic film balance controls were set for the constant pressure operation. The Ge plate was immersed through the compressed monolayer. The monolayer was not transferred onto the Ge plate during the first immersion stage unless the surface of the plate was not cleaned enough (this is another way of checking the cleanness of the Ge plate). The first monolayer was deposited on the first withdrawal operation. The first deposited monolayer was usually wet, so that it was necessary to dry the prism completely in air or in the vacuum oven at 70-80°C for approximately one minute. The second monolayer was readily deposited by the immersion operation only on the dried initial monolayer.

The drying procedure after the deposition process was necessary until at least the first five layers were built up. In the later deposition process, the Y-type multilayer (119) could be built-up continuously without the drying process after every withdrawal operation. However, when the multilayers were built up with free TABSH monolayer from the hydrochloric substrate or with the monolayer from aluminum nitrate substrate with excess sulfate, the drying process was necessary for every two or three dipping operations. This was due to their slowness in the drying of the wet deposited monolayer.

When the substrate contained a high concentration of potassium sulfate (> 0.1M), it was found that some potassium sulfate salt was crystallized on the deposited monolayers. Since this crystallized potassium sulfate was found to interfere with the next monolayer deposition during the next immersing stage, the salt had to be rinsed out by immersing the dried deposited monolayer in distilled water for about 30 seconds. This rinsing process was repeated whenever the plate was taken out of the substrate solution. It was confirmed that this rinsing action on the deposited monolayers did not deplete the molecules transferred on the Ge plate; the rinsing action did not cause a significant decrease in intensities of the C-H and the COOH absorption bands for the deposited multilayer sample after being rinsed. Without the rinsing, Y-type multilayers could not be built-up on the Ge plate. The rinsing action is also believed to reduce a possible interference of K_2SO_4 absorption peaks with the absorption peaks under investigation.

The aluminum nitrate plus potassium sulfate substrate solution used in this experiment was aged on the average 2 hours to give sufficient time for an equilibrium of the inorganic reactions between aluminum ions and sulfate ions.

However, it was found as shown in Appendix III that the increase in the aging time from 80 minutes to 25 hours did not significantly affect the degree of reaction between TABSH monolayers and aluminum ions on the aged substrate.

The number of layers in the built-up multilayer varied from 33 layers to more than 50 layers, in order to get equally strong absorption bands in the MIR spectra. The number needed depends upon the chemical nature of the monolayer. For the monolayer spread on the substrate with excess sulfate (e.g., the $[SO_4] = 0.3\underline{M}$), a greater number of layers had to be deposited on the Ge plate to obtain the same strong intensities of the absorption bands under investigation as those for the monolayer spread on the substrate with no excess sulfate. This is due to the fact that free TABSH molecules have a larger average molecular area than aluminum resinate molecules (11,37). The building-up of the multilayers normally required two or three hours.

During the multilayer deposition periods, it was discovered that some spread molecules leaked under the compression barrier. The leakage problem was serious for monolayers consisting mainly of free TABSH molecules, but for monolayers of mainly aluminum resinate, the leakage was stopped. The leakage problem could be remedied by spreading a counterbalancing TABSH monolayer on the other side [cleaned (left) side] of the barrier. This counterbalancing monolayer stopped the compressed monolayer from leaking, possibly by means of counterbalancing osmotic pressure developed under the compressing barrier and near small edge gaps. The leakage appeared to cause an experimental error in determining the composition of the monolayer, possibly due to some loss of chiefly free acid molecules in the compressed monolayer.

The apparatus for the Langmuir-Blodgett monolayer and multilayer depositions used in this study is shown in Fig. 1. A detailed description of the apparatus is given in Neuman's thesis (118).

TECHNIQUE OF MIR SPECTROSCOPY

The infrared MIR spectra of the built-up multilayer samples were observed with the aid of a Perkin-Elmer model 621 prism grating spectrophotometer equipped with a Wilk's double beam internal reflection attachment. The attenuated total reflection attachment has been designed so that the radiation can be reflected between the plate faces 50 times at a well-defined angle of incidence of 45° (120,121). An exact duplicate set of optics, including a reference germanium plate, in the reference beam compensated for atmospheric absorption.

Water or carbon dioxide in the atmosphere was found to cause the double beam spectrophotometer to record inaccurately by reducing the pen response for a given change in transmittance at the adsorption frequencies of these materials. To overcome this problem, the interior of the instrument including the ATR attachment compartment was purged with clean, dry air by using a Perkin-Elmer air drier accessory.

Observed absorbance ratios for spectral bands depend upon the choice of base lines in the spectra for quantitative analysis. This choice, in turn, depends upon details of the experimental set-up.

For this reason, the germanium prism-plate in the same orientation in the same holder was always used, and the arrangement was disturbed as little as possible. The P.E. 621 spectrophotometer controls were set as follows:

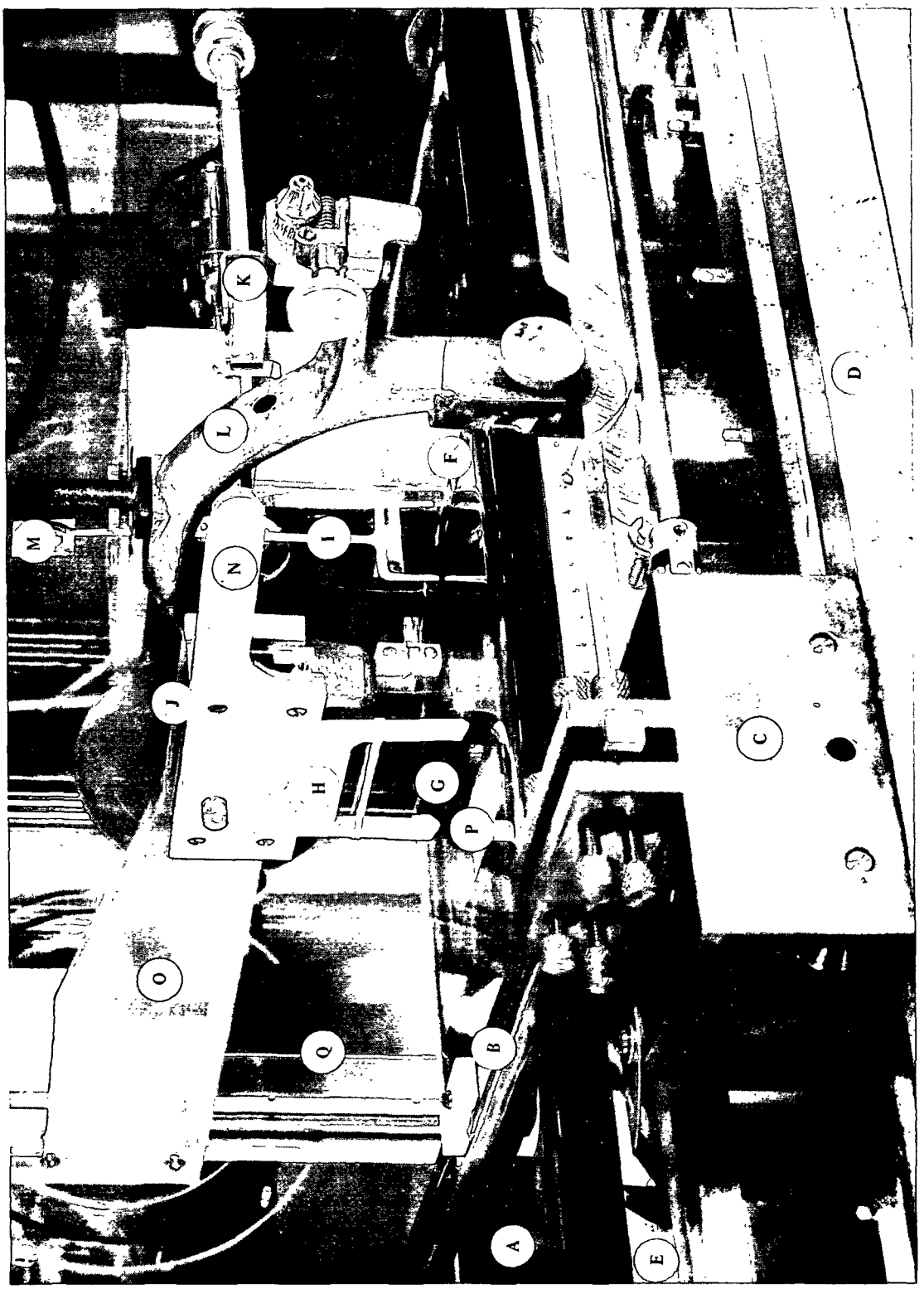

Figure 1. A View of the Automatic Langmuir Film Balance and Apparatus for Langmuir-Blodgett Multilayer Deposition. A. Lucite Trough; B. Bronze Compression Barrier Covered with Teflon; C. Compression Barrier Carriage; D. Aluminum Guide Rail; E. Trough Scale; F. Mica Float; G. Germanium Prism Plate; H. Teflon Holder for Germanium Plate; I. Float Arm and Pointer Assembly; J. Unislide Assembly; K. Magnetic Damper; L. Torsion Head; M. Mirror; N. Teflon Slide Holder; O. Extension Arm; P. Dipping Well; Q. Unislide Assembly with Slide and Venier

slit program:	1000
slit (scale change):	2X
gain:	5.0 for 1X, and 4.6 for 5X expansion
attenuator speed:	1100 (1X) and 750 (5X)
suppression:	6.0 (1X) and 0 (5X)
scan time:	20 (1X) and 32 (5X)

The spectrum for the multilayer sample was determined between 2.6 μm (3850 cm^{-1}) and 11.0 μm (900 cm^{-1}).

For replicate samples of TABSH film (multilayer or spread layer) on a germanium plate, the standard error was less than ± 0.01 for the absorbance of the multilayer sample at 1695 cm^{-1} (nonionized COOH groups), relative to the absorbance of the multilayer at 2930 cm^{-1} showing the total amount of molecules deposited on the Ge plate (Appendix IV).

MEASUREMENT OF CONTACT ANGLES ON THE MONOLAYERS CAST ON THE CMC FILM

PREPARATION OF INSOLUBLE CMC FILMS

Hercules's Cellulose Gum (7LF Grade), sodium carboxymethyl cellulose (Na-CMC), was dissolved in distilled water. The properties of 7LF Cellulose Gum are: DP = 400, mol. weight = 80,000, substitution range (DS): 0.65-0.85. In order to reduce lumps or agglomerates in the dissolved solution of cellulose, the powder was wet with redistilled methanol which does not cause Na-CMC to swell, prior to the addition to cold water. Three or five parts of methanol per part of Na-CMC were added. The solution was prepared with a laboratory agitator at the concentration of 3.5%. Since the dissolved solution of cellulose gum, however, contained lots of undissolved agglomerates or lumps, the solution was ultracentrifuged and

filtered through a fritted glass filter to reduce the lumps. However, small amounts of tiny lumps could not be removed with the centrifuging and filtering process.

In order to make CMC film on a glass slide, the microscope glass slide (3 by 1 inch) was cleaned first with detergent and in chromic acid cleaning solution. Just prior to dipping the slide into the Na-CMC solution, the slide was cleaned once more in the Plasma cleaner. The Na-CMC solution completely wet and spread on the cleaned slide.

The film thickness could be controlled by the number of dippings into the cellulose solution. In the thicker film, however, more lumps appeared and made the surface rough. Thus, a thin film (0.015-mm thick) was cast on the glass slide by dipping it once in the cellulose solution.

The wet film was dried slowly in the clean air. The Na-CMC film dried on the glass slide was immersed in 0.5M HCl solution for about one hour (this is sufficiently long for insolubilization) to insolubilize the cellulose film by exchanging the sodium ion with hydrogen in the carboxyl groups of Na-CMC. The insolubilized film was immersed in distilled water to rinse off impurities such as soluble cellulose particles and sodium salts of the cellulose gum.

DEPOSITION OF MONOLAYERS ON CMC FILM-GLASS SLIDES

The monolayer spread on the aqueous surface was transferred onto the CMC film by the Langmuir-Blodgett method described previously. Prior to the monolayer transfer the π-A isotherm was determined for the monolayer on the substrate under investigation, and then the compressed monolayer was expanded to a surface pressure of zero. The expanded monolayer was then recompressed to a desired film pressure (18 dynes cm^{-1}) for the monolayer transfer. The CMC film-glass slide was dipped through the compressed monolayer and withdrawn at a constant speed

of 7.5 mm/minute. The monolayer was transferred onto the CMC film during the withdrawing stage. The CMC film cast with the monolayer was stored in the desiccator over phosphorus pentoxide powder for the contact angle measurement.

The smoothness of the surface of the pure CMC film, and of surfaces covered with pure TABSH monolayer and with aluminum resinate monolayers were examined with transmission electron-microscopy as shown in Appendix V.

MEASUREMENT OF CONTACT ANGLES

Contacting Liquids

In order to calculate the surface-free energy and its components from contact angle data, the measurement of finite contact angles between each surface and at least two different liquids are required according to the theory previously outlined. It was further required that the liquids differ significantly with respect to the polar component of their surface tension.

Three suitable liquids were selected to give reasonably stable, finite contact angles on the TABSH monolayers; water, methylene iodide and formamide. Water represents a liquid having a high polar component to its surface tension and could be paired with the methylene iodide, which has very weak polar forces. Formamide was also used as an alternative polar liquid because it has weaker polar force than water (98). However, the contact angle measurement with formamide gave poor reproducibility as compared to water and methylene iodide, partly because of poor stability of the contact angle on the cast monolayer.

The water was triply distilled as previously described. The two organic liquids were obtained as reagent grade from a commercial supplier and were purified by passing through an activated aluminum-silica gel column. The surface tensions of purified methylene iodide and formamide were 50.5 and 57.4 dynes cm^{-1},

respectively, at 22.5°C by the measurement with a Cenco-duNouy tensiometer. The surface tension of triply distilled water was 72.4 dynes cm^{-1} at 22.5°C. The appropriate corrections to these data for the meniscus shape for water, and other organic liquids were made using the published data of Harkins and Jordan (123) and with the correction procedure used by Brown (124).

Apparatus and Procedure

Contact-angle measurements were made at room temperature (21°C) and 48% RH with the apparatus used by Brown (124) and modified recently by Ferris (125) with a high speed camera. The detailed description of this apparatus is given in Ferris' thesis.

The sample slide (the CMC film-glass slide on which the monolayer was deposited) was placed on a horizontal platform inside the Lucite contact-angle chamber. The liquid drops were dispensed from a Gilmont microburet.

The advancing contact angle of each droplet was photographed in three frames in one second using Kodak high contrast copy film. The pictures were developed and the angles were determined by the use of an approximate formula suggested by Back and Steenberg (21), and used by Yiannos (19). The formula relates the contact angles with the base and the height of the droplet

$$\tan(\theta/2) = 2h/b \qquad (28)$$

where

θ = contact angle

h = height of the droplet

b = base of the droplet

The actual values of h and b of the contact angles on the negative film were read with the microcomparator which reads automatically three coordinate points of a droplet. The actual calculations of contact angles in Equation (28) were carried out with the computer. Since the contact angles of water on the monolayer decreased so rapidly upon contacting the monolayer, instead of an equilibrium contact angle, an arbitrary initial advancing contact angle was obtained by linearly extrapolating three angles measured in one second. For example, the contact angle of water on pure TABSH monolayer decreased from 51 to 43° during one second. The decrease in the contact angle on the reacted monolayer was not significant (89.0 → 88.5).

EXPERIMENTAL RESULTS

EFFECT OF EXCESS SULFATE ON THE REACTION BETWEEN TETRAHYDRO-ABIETIC ACID MONOLAYERS AND ALUMINUM IONS AT pH 4.0

CHANGES IN MIR SPECTRUM WITH INCREASING SULFATE CONCENTRATION

The top ten IR-MIR spectra shown in Fig. 2 are for multilayer samples of monolayer reacted on aluminum nitrate plus potassium sulfate substrate at pH 4.0. The Al concentration was held at 3.16×10^{-3}M and the sulfate concentration was increased from 0 to 4.5M. The top spectrum is for the monolayer reacted in the absence of sulfate ions at pH 4.0. The bottom spectrum for pure TABSH monolayer transferred from hydrochloric acid substrate with pH 4.0 is also given in the figure for comparison.

As the $[SO_4]$ is increased, the following absorption bands attributed to the acid fraction increase in intensity relative to the hydrocarbon band at 2930 cm^{-1} (126):

1. The sharp, strong band at 1695 cm^{-1} (5.9 μm) for the C=O stretching vibration.
2. The broad band at 1275 cm^{-1} (7.85 μm) for the coupled C-O stretching and OH bending vibration.
3. The very broad band in the region of 3300-2500 cm^{-1} (3.03-4.00 μm) for the hydrogen bonded O-H stretching.

The following absorption bands that are usually ascribed to carboxylate anion forming a salt (127) decrease as the $[SO_4]$ in the substrate is raised:

1. The band at 1590 cm^{-1} (6.3 μm) for the asymmetrical stretching vibration of the ionized carboxyl group.

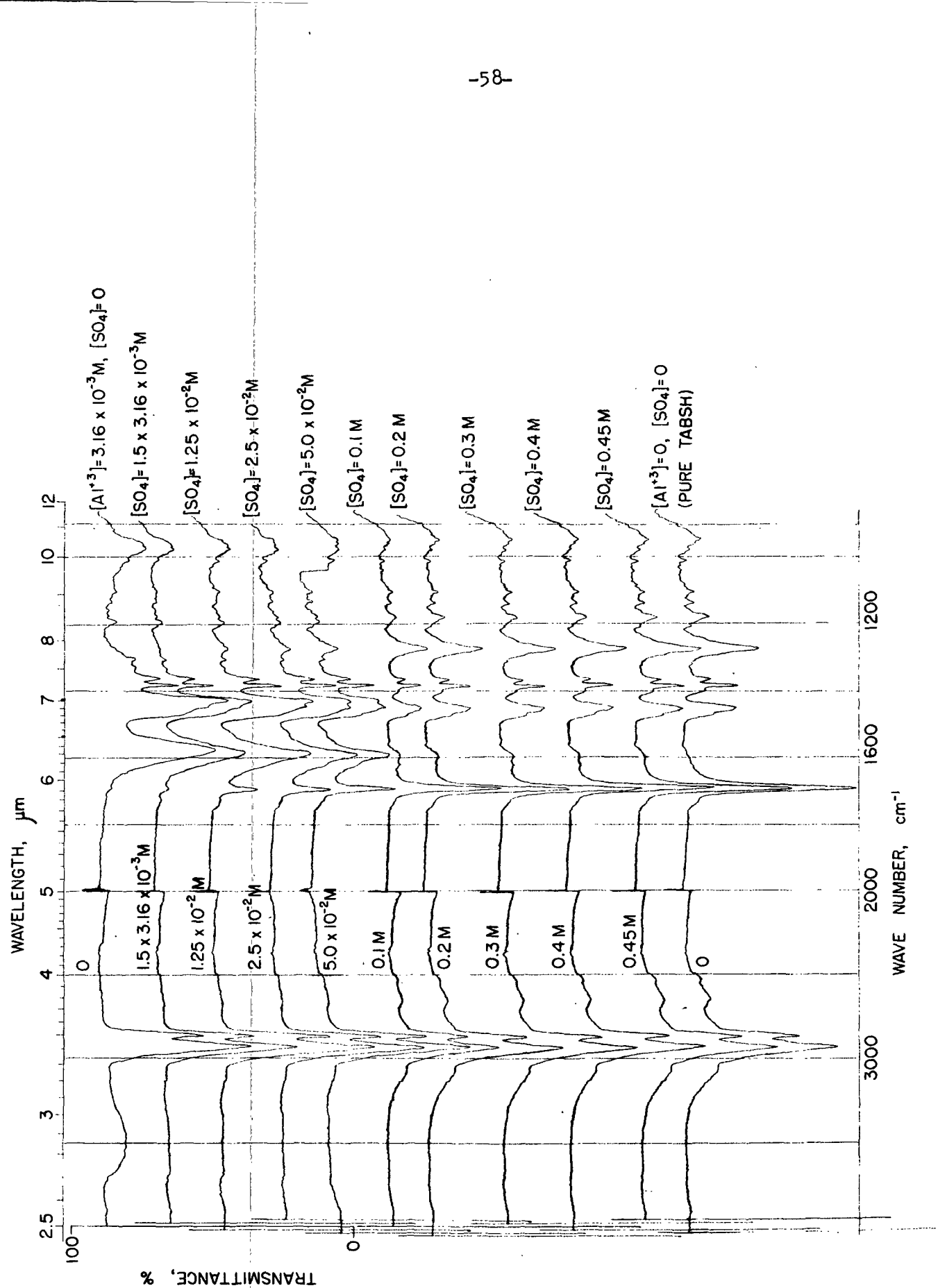

Figure 2. MIR-IR Spectra of Pure TABSH Monolayer and the Monolayers Reacted on Aluminum Nitrate plus Potassium Sulfate Substrates in Which the Sulfate Concentration is Changed at pH 4.0, the $[Al^{+3}] = 3.16 \times 10^{-3}$ M

2. The band at 1430 cm^{-1} (6.98 μm) for the symmetrical vibration of the ionized carboxyl group.

The absorption bands for the hydrocarbon portion of the materials are as follows:

1. The band at 2930 cm^{-1} (3.42 μm) for the stretching of the methyl groups.
2. The band at 1450 cm^{-1} (6.90 μm) for the antisymmetrical bending vibration of the C-H bond in the methyl groups.
3. The band at 1385 cm^{-1} (9.22 μm) for the symmetrical C-H bending vibration of the methyl groups.

The top spectrum for the monolayer reacted on the substrate free of sulfate ions shows that only ionized carboxyl groups exist in the monolayer; at least the number of nonionized COOH groups appears to be negligible. This indicates that all the TABSH molecules spread on the substrate react with aluminum ions to form aluminum resinate salt in the absence of sulfate ions.

As the $[SO_4]$ is increased, the primary changes in the spectrum are attributed to the presence of increasing proportions of free acid in the monolayer. The acid absorption bands at 1695 and 1275 cm^{-1} increase in intensity relative to the hydrocarbon at 2930 cm^{-1}. Likewise, the salt absorption bands at 1590 cm^{-1} and 1435 cm^{-1} decrease in relative intensity. As the $[SO_4]$ is increased to 0.1M ($[SO_4]/[Al]$ = 31.6), the salt bands decrease substantially.

When the $[SO_4]$ = 0.4M ($[SO_4]/[Al]$ = 126), the spectrum for the monolayer on the substrate is almost the same as that for the pure TABSH monolayer. However, at this high concentration of $[SO_4]$ and at even higher concentrations of $[SO_4]$, i.e., 0.45M, the spectra for the multilayer samples transferred from the substrates appear to contain the weak broad band of ionized carboxyl groups. This

behavior may indicate that a trace of the TABSH molecules on the substrate with excess sulfate still react to form the salt, aluminum resinate.

It should be noted in Fig. 2 that all the spectra for the monolayers consisting mostly of the salt molecules do not reveal the presence of hydroxyl groups coordinated to aluminum ions; none of the spectra shows either a weak sharp band near 2.7 μm for the free OH group (42-45), or a strong broad band near 3 μm for the hydrogen-bonded OH groups, as other investigators reported (11,38,43,45). The spectra expanded at the 5 times ordinate scale also do not show any O-H absorption in the range of 2.6 to 3 μm. However, the spectrum for the monolayer reacted in the absence of sulfate ions shows the broad weak absorption bands near 3500 cm^{-1}, ranging from 3700 to 3300 cm^{-1}. The cause of the broad band near 3500 cm^{-1} was investigated and will be discussed later.

The spectra for the reacted monolayers on the substrates with low sulfate (i.e., the $[SO_4] < 0.1M$) show the absorption at 975 cm^{-1} (10.14 μm) and the band intensity decreases with increasing the $[SO_4]$. The absorption at 975 cm^{-1} is ascribed to the aluminum-oxygen linkage in the aluminum resinate complex formed in the reacted monolayer. However, this band is not associated with the presence of OH groups as Scott, et al. reported (43) from an isotope-exchange experiment.

The absence of a distinctive strong absorption band between 1038 and 1170 cm^{-1} and between 970 and 995 cm^{-1} (128,129) (S-O stretching vibration) indicates that the sulfate ion is not directly involved in the monolayer reaction forming aluminum resinate.

CHANGES IN COMPOSITION OF THE MONOLAYER

Composition Analysis

The chemical composition of the monolayers transferred from aluminum nitrate plus potassium sulfate substrates was determined in terms of the mole fraction of free acid ($\underline{X}_{TABSH}$). The free acid mole fractions of the samples of multilayer built-up on the Ge plate were ascertained from a quantitative treatment of the infrared spectra obtained by the internal reflectance spectroscopy. An absorbance ratio method was employed to calculate the free acid mole fraction from the measured relative heights of absorption peaks (130).

The quantitative analysis of the multilayer samples was carried out as follows. For any given sample on the Ge plate (11,131):

$$K_{CH} A_{CH} = N_{CH} \tag{28}$$

$$K_{COOH} A_{COOH} = N_{COOH} \tag{29}$$

$$K_{COO^-} A_{COO^-} = N_{COO^-} \tag{30}$$

where the A values are the absorbance of the C-H reference band at 2930 cm^{-1}, the COOH free acid band at 1695 cm^{-1}, and the COO^- salt band at 1590 cm^{-1}, respectively, and where N refers to the corresponding number of moles of the species.

The absorbance values depend upon the absorptivity and the thickness of the sample according to Beer's law. The K values do not depend to a great extent upon the thickness of the sample in the multiple internal reflectance spectroscopy (112). Rather the K values depend chiefly upon the absorptivity. It is assumed that the absorptivities of the COOH of TABSH at 1695 cm^{-1} and of the COO^- of ionized TABSH ($TABS^-$) at 1590 cm^{-1} are constant for various mixtures of TABSH and $TABS^-$ on an

identical Ge plate. The absorptivity of the C-H at 2930 cm^{-1} is also assumed the same for TABSH and $TABS^-$.

The mole fraction of TABSH on the Ge plate may be represented by Equation (31)

$$X_{TABSH} = N_{COOH}/(N_{COOH} + N_{COO^-}). \qquad (31)$$

The total concentration of TABSH acid (nonionized and ionized) on the Ge plate can be related to the absorbance of hydrocarbon at 2930 cm^{-1}. Thus

$$N_{COOH} + N_{COO^-} = N_{CH} \qquad (32)$$

and then combining the above equations

$$X_{TABSH} = N_{COOH}/N_{CH} = (K_{CH}/K_{COOH})(A_{COOH}/A_{CH}). \qquad (33)$$

Likewise the salt mole fraction, X_{TABS^-} can be obtained as follows

$$X_{TABS^-} = (K_{CH}/K_{COO^-})(A_{COO^-}/A_{CH}). \qquad (34)$$

For each spectrum, base lines were drawn between 3800 and 2200 cm^{-1}, and between 1800 cm^{-1} and 1500 cm^{-1}.

Peak heights at 2930, and 1695 or 1590 cm^{-1} were measured for use in Equation (33) and (34) (130). With the base lines selected, the value of K_{CH}/K_{COOH} was obtained from the spectra for multilayer samples of pure TABSH monolayer. The value of K_{CH}/K_{COO^-} was also obtained from the spectra for multilayer samples of aluminum resinate monolayer formed at pH 4.0.

The reproducibility of the infrared absorbance ratio values, K_{COOH}/K_{CH}, was examined on a germanium plate (Appendix IV) with pure TABSH. The absorbance ratio values appeared to be reproducible when the sample concentration (the number

of monolayers) on an identical Ge plate was increased to obtain the absorbance value of the C-H band between 3.0 and 0.4.

With the assumption that the absorbance ratio values do not vary with composition and that Beer's law is obeyed, Equation (33) was used to calculate $\underline{X}_{TABSH}$ values. However, when the intensity of the COOH band for the sample under investigation is too weak to be measured accurately in the presence of atmospheric noise bands, Equation (34) was also used to calculate $\underline{X}_{TABS^-}$ values first, by measuring the $\underline{A}_{COO^-}/\underline{A}_{CH}$ values, instead of the $\underline{A}_{COOH}/\underline{A}_{CH}$. The $\underline{X}_{TABSH}$, in turn, can be also obtained from the relationship

$$X_{TABSH} = 1 - X_{TABS^-} \cdot \qquad (35)$$

The values of $\underline{X}_{TABSH}$ are about the same regardless whether they are obtained from Equation (33) or from Equation (34) and (35), when both the intensities of the COOH and the COO^- band are strong enough.

The assumption concerning the absorptivity ratio was also used by Bagg, et al. (131) for calcium stearate plus stearic acid monolayer materials (multilayer built-up on silver chloride plate or skimmed films). Stearic acid or stearate monolayers built-up on calcium fluoride plates showed only slightly negative deviation from Beer's law at 2900 and 1716 cm^{-1} (46).

The reproducibility of this determination was investigated under a constant condition of aluminum sulfate substrate at pH 4.0. The values of $\underline{A}_{COOH}/\underline{A}_{CH}$ and $\underline{X}_{TABSH}$ for the TABSH multilayer samples reacted on the substrate are given in Appendix VI.

For these replicate samples, the standard error of the mole fraction value is less than ± 0.01. Thus, the composition analysis of the monolayer by the MIR

spectroscopic technique is believed to be very reproducible and reliable as long as conditions of the substrate, i.e. pH, the [Al] and the [SO_4], are held constant. However, an experimental error due to possible variation of the reference absorbance value may be ± 0.02 for a single measurement of $\underline{X}_{TABSH}$ value of the monolayer.

Changes in Free Acid Mole Fraction as a Function of Sulfate Concentrations

The $\underline{X}_{TABSH}$ values of the monolayers transferred from aluminum nitrate plus potassium sulfate substrates are given in Table I and shown in Fig. 3 (data points). These results were calculated with Equation (33), or (34) and (35) for data taken from the MIR spectra shown in Fig. 2. The dotted line is for pure TABSH.

At the [SO_4] = $1.5 \times 3.16 \times 10^{-3}$M, which is an equivalent concentration of sulfate for aluminum sulfate, the reacted monolayer already appears to contain about 10% of free TABSH. As the [SO_4] is increased to 0.05M, the free acid mole fraction increases gradually. However, when the [SO_4] is increased further, the increase ($\underline{X}_{TABSH}$) appears to be rapid but becomes slow when the [SO_4] is higher than 0.3M. Finally at the [SO_4] = 0.45M, the monolayer consists of essentially all free acid molecules.

These results of the compositional analysis of the monolayers clearly indicate that reaction of TABSH monolayers with aluminum ions forming the salt, aluminum resinate, is gradually inhibited by excess sulfate ions at pH 4.0. However, the inhibiting action of sulfate on the reaction is not as complete as for oxalate as observed by Major (11); for a complete inhibition of the salt formation reaction a high addition of sulfate appears to be required, i.e., the [SO_4]/[Al] $\simeq$ 140, while in the case of oxalate ions the [oxalate]/[Al] = 2.0 was required.

TABLE I

CHANGES IN FREE ACID MOLE FRACTIONS OF MONOLAYERS REACTED ON ALUMINUM NITRATE PLUS POTASSIUM SULFATE SUBSTRATES AS A FUNCTION OF SULFATE CONCENTRATION[a,b]

Concentration of Sulfate Ions		$\underline{A}_{COOH}/\underline{A}_{C-H}$			Spectrum
Mole/liter	$Log_{10}[SO_4]$	$(\underline{A}_{COO^-}/\underline{A}_{C-H})$	$\underline{X}_{TABSH}$	pH	No.
0	0	(0.227/0.383 = 0.594)	0	3.980	102
$1.5\times3.16\times10^{-3}$	-2.324	0.051/0.328 = 0.052 (0.17 /0.328 = 0.528)	0.04 (0.12)[d]	4.005	104
1.25×10^{-2}	-1.900	0.078/0.424 = 0.184 (0.201/0.424 = 0.474)	0.15 (0.20)	4.001	105
2.50×10^{-2}	-1.602	0.106/0.376 = 0.282 (0.163/0.376 = 0.433)	0.23 (0.27)	3.990	106
5.0×10^{-2}	-1.301	0.152/0.357 = 0.426 (0.137/0.357 = 0.384)	0.34 (0.35)	4.001	107
1.0×10^{-1}	-1.000	0.311/0.358 = 0.870 (0.057/0.358 = 0.159)	0.70 (0.73)	4.010	86
2.0×10^{-1}	-0.699	0.261/0.348 = 1.053	0.85	4.005	89
3.0×10^{-1}	-0.533	0.361/0.329 = 1.098	0.88	4.001	91
4.0×10^{-1}	-0.398	0.375/0.331 = 1.132	0.91	4.015	92
4.5×10^{-1}	-0.347	0.412/0.340 = 1.210	0.97	3.955	93
0[c]	0	0.493/0.396 = 1.245[c]	1.00	3.993	95-1

[a] Substrates were at 22.5°C with pH = 4.0, the [OH]/[Al] of all these substrates < 1.0.

[b] [Al] = 3.16×10^{-3} M in all substrates.

[c] Pure TABSH multilayer transferred from hydrochloric acid substrate with pH 4.0.

[d] $\underline{X}_{TABSH} = 1-\underline{X}_{TABS^-}$, $\underline{X}_{TABS^-}$ (the salt mole fraction) is calculated with Equation (34).

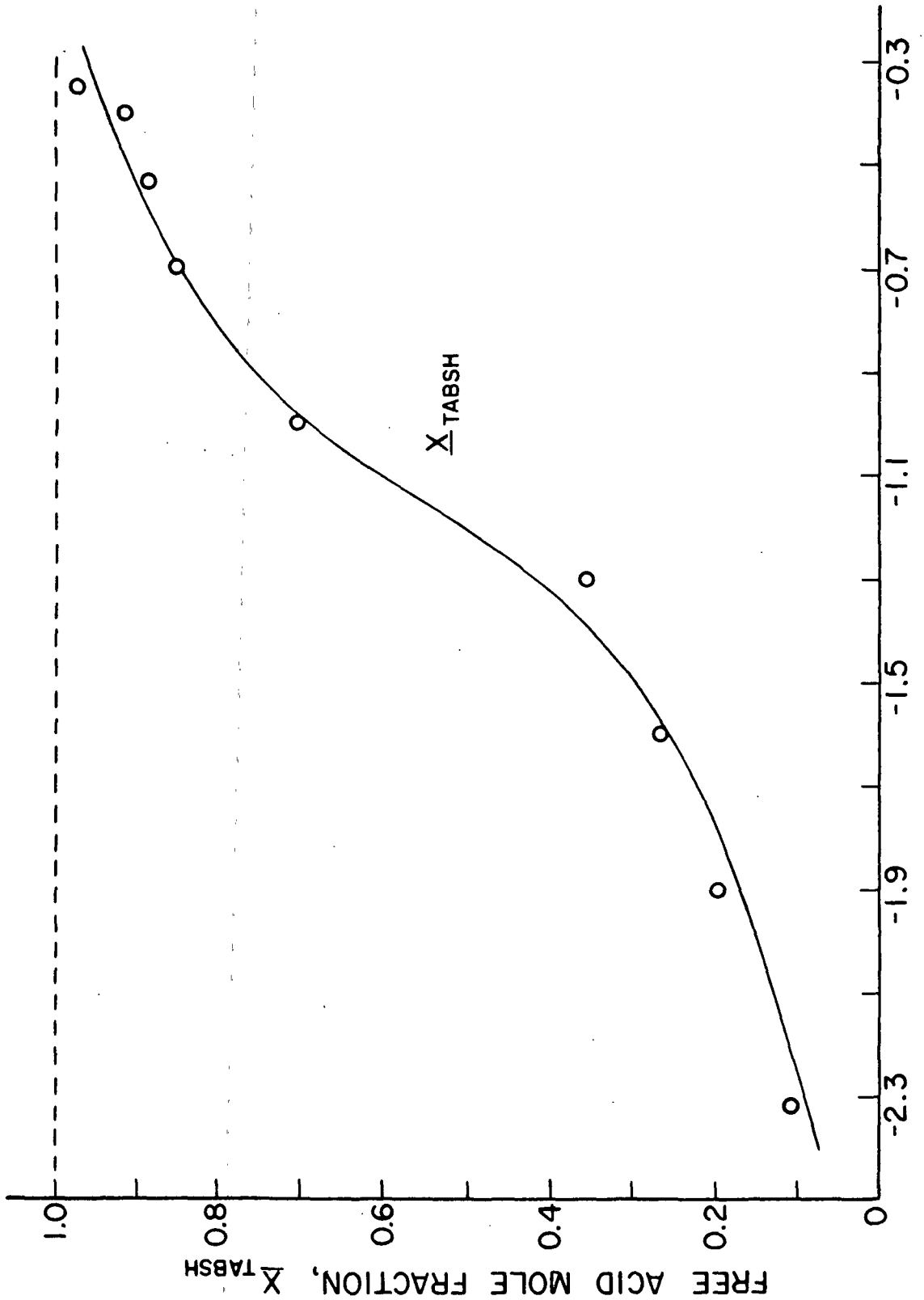

Figure 3. Changes in Free Acid Mole Fraction of TABSH Monolayers Reacted on Aluminum Nitrate plus Potassium Sulfate Substrates as a Function of Sulfate Concentration

CHANGES IN π-A ISOTHERMS AT pH 4.0

The π-A isotherms in Fig. 4 are for the monolayers formed when TABSH is spread on aluminum nitrate substrate at various potassium sulfate concentrations. The [Al] was held constant at 3.16×10^{-3}M and the [SO_4] was varied between $1.5 \times 3.16 \times 10^{-3}$M (= the [$SO_4$] in $Al_2(SO_4)_3 \cdot 18H_2O$) and 0.45M. The pH of the substrate was adjusted to 4.00 ± 0.03 with 0.2N KOH and 0.1N HCl solution. A small amount of 0.2N KOH solution was added only to the substrate with the [SO_4] = 0, and with the [SO_4] = $1.5 \times 3.16 \times 10^{-3}$M (the [OH]/[Al] < 0.1).

The bottom π-A isotherm in Fig. 4 is for the aluminum resinate monolayer on the substrate with no sulfate. The top π-A isotherm in the figure is for pure TABSH monolayer on hydrochloric acid substrate with pH 3.90. This isotherm is typical of a liquid condensed monolayer (110) which behaves as a highly oriented liquid (119). The bottom isotherm for an aluminum resinate monolayer appears to be a typical isotherm of solidlike liquid film whose average molecular area is smaller, and whose surface pressure at a given molecular area is higher as compared to those of the unreacted monolayer.

One of the characteristics of the isotherms of aluminum resinate monolayer as compared with other isotherms shown in Fig. 4 is a continuous secondary rise in surface-film pressure at the left of the transition region.

As the [SO_4] increases, the isotherm loses the characteristics associated with the presence of aluminum resinate in the monolayer. When the [SO_4] is increased beyond 0.2M, the π-A isotherm appears to be the same as the one for pure TABSH monolayer.

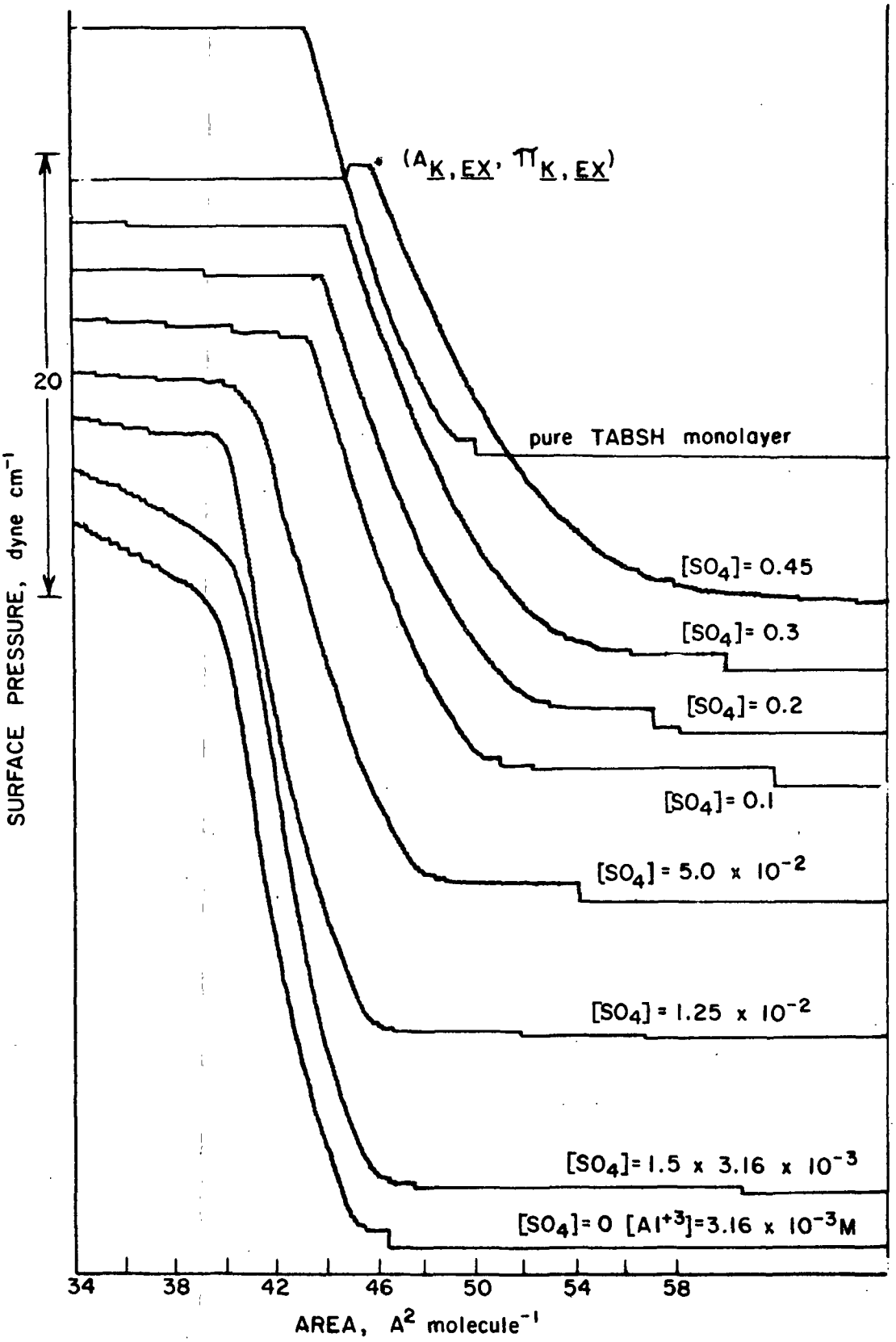

Figure 4. π-A Isotherms* for TABSH Monolayers Spread on Aluminum Nitrate plus Potassium Sulfate Substrates in Which the Sulfate Concentration is Changed at pH 4.0 ([Al] = 3.16 × 10^{-3}M)

*The base line of each curve has been shifted arbitrarily to avoid confusion.

These changes in values of the π-$\underline{A}$ isotherms are given in Table II and Fig. 5 (data points). The dotted lines in the figure represent the $\underline{A}_{10}$, $\underline{A}_{\underline{K},\underline{EX}}$ and $\pi_{\underline{K},\underline{EX}}$ values for the TABSH monolayer on hydrochloric acid.

TABLE II

$\pi_{\underline{K},\underline{EX}}$, $\underline{A}_{\underline{K},\underline{EX}}$, $\underline{A}_{10}$, AND $\underline{A}_{18}$ VALUES FOR THE TABSH MONOLAYER FORMED ON ALUMINUM NITRATE PLUS POTASSIUM SULFATE SUBSTRATES[a] WITH pH 4.0

Substrate Condition [SO_4]	Substrate Condition [Al]	pH	$\pi_{\underline{K},\underline{EX}}$	$\underline{A}^2_{\underline{K},\underline{EX}}$	$\underline{A}^2_{18}$	$\underline{A}^2_{10}$
0	0	3.950	19.6±0.2[b]	43.4±0.28[b]	43.8±0.39[b]	45.9±0.52[b]
0	3.16×10^{-3}	4.010	29.2	39.9	41.5	43.3
$1.5\times3.16\times10^{-3}$	"	4.015	29.2	40.4	42.0	43.3
1.25×10^{-2}	"	4.010	27.5	40.1	41.4	43.0
5.0×10^{-2}	"	4.001	24.5	41.1	42.2	43.3
1.0×10^{-1}	"	4.007	20.6	43.3	44.0	46.3
2.0×10^{-1}	"	3.970	20.5	43.9	44.5	47.1
3.0×10^{-1}	"	3.965	20.3	44.7	48.1	46.8
4.5×10^{-1}	"	3.970	19.9	45.7	46.3	49.6

[a] Substrates were at 22.5°C, reaction time = 10 minutes, and $d\underline{A}^2/d\underline{t}$ = 2.52 A^2 molecule^{-1} minute^{-1}.

[b] 95% Confidence limit.

The average molecular area of the monolayer molecule π = 10 dynes cm^{-1} is $\underline{A}_{10}$. This quantity was picked arbitrarily to use in comparing the isotherms. The $\underline{A}_{18}$ is the average molecular area of the compressed monolayer molecules at π = 18 dynes cm^{-1}, film compressing pressure for the monolayer transfer. The quantity, $\underline{A}_{\underline{K},\underline{EX}}$, is the average molecular area of the monolayer molecules in A^2 molecule^{-1} at the

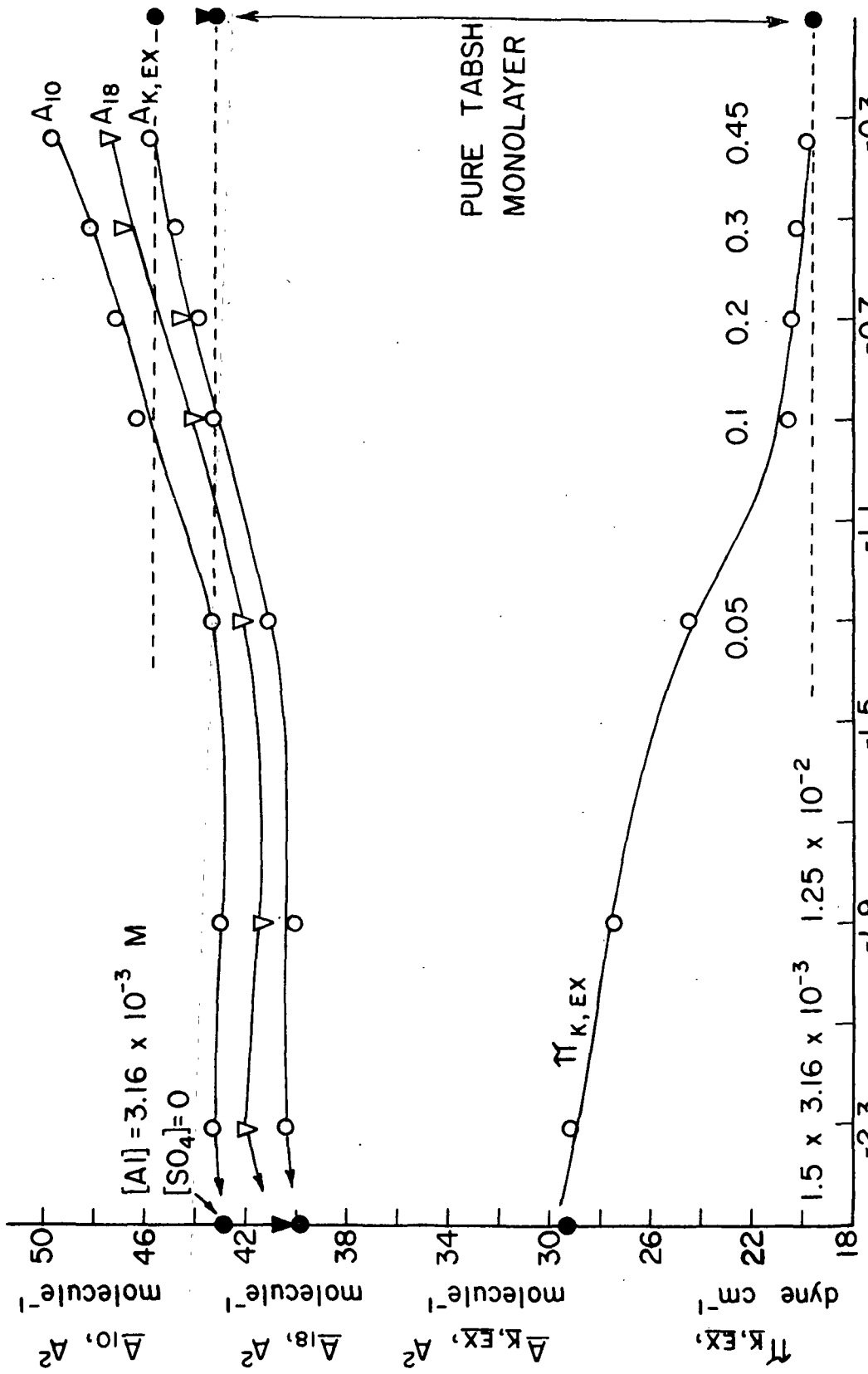

Figure 5. Changes in $\pi_{K,EX}$, $A_{K,EX}$, A_{10} and A_{18} Values for the TABSH Monolayer Formed on Aluminum Nitrate plus Potassium Sulfate Substrates as a Function of Sulfate Concentration at pH 4.0 ([Al] = 3.16 x 10^{-3}M)

extrapolated collapse point (see arrow in Fig. 4). The surface pressure of the monolayer at the collapse point is $\pi_{\underline{K},\underline{EX}}$.

The values of $\underline{A}_{10}$, $\underline{A}_{18}$ and $\underline{A}_{\underline{K},\underline{EX}}$, in general, increase gradually to the same values for pure TABSH monolayer on hydrochloric acid when the [SO_4] is increased from $1.5 \times 3.16 \times 10^{-3}\underline{M}$ to $0.1\underline{M}$, and then rise smoothly as the [SO_4] is increased beyond $0.1\underline{M}$.

As shown in Fig. 5, as the [SO_4] increases up to $0.45\underline{M}$, the $\pi_{\underline{K},\underline{EX}}$ value decreases to the same value as for pure TABSH monolayer. It should be noted in the figure that as the [SO_4] increases, the $\pi_{\underline{K},\underline{EX}}$ value decreases in the same manner as the increase in the $\underline{X}_{TABSH}$ as shown in Fig. 3. The surface pressure decreases in the manner corresponding to the increase in free acid mole fraction.

Apparently, the changes in the molecular area and the surface pressure values are attributed to the increase in the acid mole fraction in the monolayer as the [SO_4] in the substrate is increased.

Consequently, these data indicate that excess sulfate prevents the aluminum ion from reacting with the TABSH monolayer and forming an aluminum resinate at pH 4.0. When the [SO_4] is greater than $0.1\underline{M}$, a large portion of TABSH molecules in the spread monolayer does not react with aluminum ion and, when the [SO_4] = $0.45\underline{M}$, essentially no aluminum ion reacts with the TABSH monolayer.

As the [SO_4] is increased above $0.1\underline{M}$, the molecular area of the spread TABSH monolayer is increased more than the one for pure TABSH monolayer. The continuous increase in the molecular area may be due to a physically expanding effect by a high content of salt in the substrate solutions. The similar expanding effect by the high addition of salts has been also observed by previous workers such as Ekwall and Bruun (22), Bruun (110), and Schulman and Rideal (132). On the basis

of surface potential measurements Schulman and Rideal (132) explained the expansion due to increased interaction between the polar groups of the acid molecules in the monolayer and the inorganic anions near the surface of the substrate.

CHANGES IN CONTACT ANGLES ON THE CAST MONOLAYER FORMED AT pH 4.0

The contact angles of water, methylene iodide and formamide on the monolayer cast on the CMC film were measured for the determination of changes in surface free energy for the monolayer, and are tabulated in Table III.

TABLE III

CONTACT ANGLES ON TABSH MONOLAYERS[a] CAST ON THE CMC FILM FROM ALUMINUM NITRATE PLUS POTASSIUM SULFATE SUBSTRATES WITH pH 4.0

Substrate Condition			Initial Advancing Contact Angles,[b] degree		
$[SO_4]$, M	[Al], M	pH	Water (γ_ℓ=72.4)[c]	Methylene Iodide (γ_ℓ=50.5)[c]	Formamide (γ_ℓ=57.4)[c]
0 (pure TABSH monolayer)	0	4.0	41.5±1.5[d]	31.5±1.3[d]	16.3±3.7[d]
0	3.16×10^{-3}	4.01	90.0±3.2	49.0±1.4	70.5±2.3
0.00474	"	4.025	90.4±3.0	50.0±6.5	66.1±1.3
0.0125	"	4.010	86.4±2.0	49.4±1.3	55.0±5.9
0.05	"	4.001	87.3±5.0	49.4±1.0	53.8±10.7
0.1	"	4.007	62.9±3.6	48.5±2.8	54.4±7.5
0.2	"	3.970	56.6±8.2	49.7±2.3	50.7±12.4
0.3	"	3.965	49.3±16.0 (38.5±6.4)[e]	48.8±7.3 (28.2±0.8)[e]	35.9±3.9 (23.3±4.3)[e]
0.45	"	3.970	35.3±4.7 (34.4±1.6)	46.2±0.9 (28.9±9.0)	17.6 (11.8±1.9)

[a]The monolayer was reacted for 10 min at the interface and transferred onto the CMC film-glass slide at a constant compressed film pressure, π_{comp}=18 dynes/cm.

[b]The contact angles were determined by linear extrapolation to t (contact time)=0.

[c]Liquid surface tension in dynes/cm, measured at 22.5°C.

[d]95% Confidence limits.

[e]The cast monolayer was rinsed with triple-distilled water to remove contaminated potassium sulfate salt on the monolayer.

The monolayer used for contact angle measurement was transferred at a constant film pressure, π = 18 dynes cm^{-1}, from the substrate onto the CMC film. The $[SO_4]$ in the substrate was increased from 0 to 0.45M at pH 4.0.

Figure 6 shows a decrease in the contact angles of water and methylene iodide with increasing $[SO_4]$ in the substrate with pH 4.0. The decrease in the contact angles of nonpolar liquids, i.e., methylene iodide, is small, while the decrease in water contact angle is large, particularly when the $[SO_4]$ is higher than 0.05M.

It is of interest to note in Fig. 6 that the curve for the water contact-angles plotted against $\log_{10}[SO_4]$ appears to be similar to the curve for X_{TABSH} (see Fig. 3), and also to the curve for the $\pi_{K,EX}$ value (see Fig. 5).

The reproducibilities of formamide contact angles are poor largely because of instability of the contact angle on the cast monolayer.

When the $[SO_4]$ increased higher than 0.2M, the contact angles on the cast monolayer transferred from the substrate containing excess sulfate gave poor reproducibility. This was found to be caused by contamination of the monolayer with potassium sulfate salt during the monolayer transfer stage from the substrate to the CMC film. The contaminating K_2SO_4 could be rinsed off by immersing the cast monolayer into distilled water for a short period (in 60 sec). The rinsed monolayer was dried over $CaCl_2$ + $CaSO_4$ in a desiccator for more than 24 hours. However, the rinsed monolayer gave lower contact angles with improved reproducibility as compared with the contact angles on the unrinsed monolayer. In the preliminary experiment it was observed that the rinsing action on the cast monolayer did not cause a depletion of the molecules deposited on the germanium plate. Accordingly, the decrease in contact angles after the rinsing may be due not to a depletion of deposited molecules, but to overturning of free acid molecules which will be discussed later.

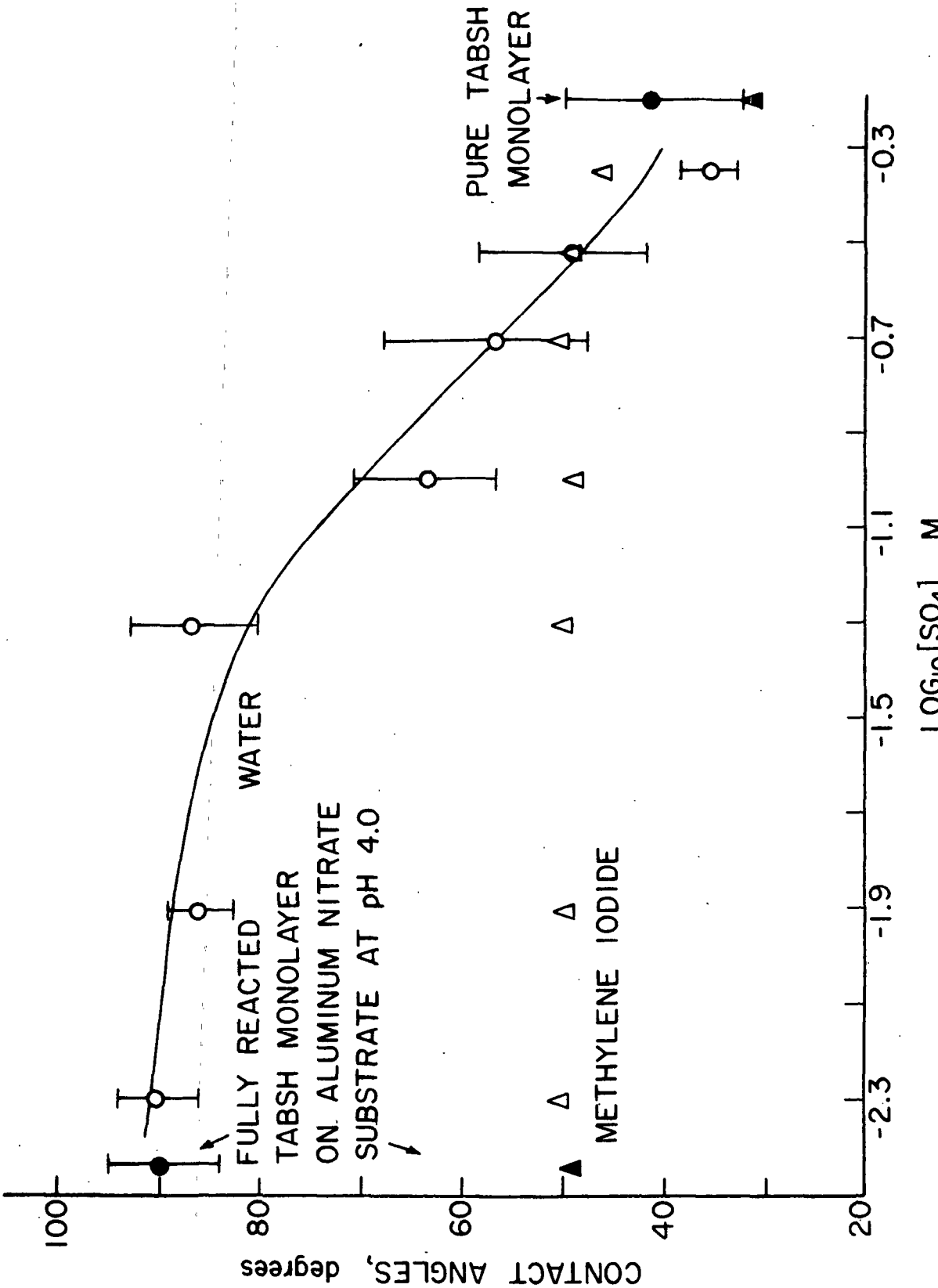

Figure 6. Changes in the Contact Angles of Water and Methylene Iodide on TABSH Monolayers Cast on the CMC Film as a Function of $[SO_4]$

EFFECT OF pH OF THE SUBSTRATE ON THE SULFATE EFFECT

CHANGES IN MIR SPECTRUM WITH INCREASING pH

In order to investigate the possible pH effect on the inhibiting effect of excess sulfate, monolayer samples were prepared by building up the multilayer on the Ge plate from aluminum nitrate plus potassium sulfate substrate while varying the pH. The [Al] and [SO_4] in the substrates were held constant at 3.16×10^{-3}M and 0.2M, respectively. The pH of the substrate was varied between 3.685 and 4.63 with 0.5N HCl and 0.1N NaOH solution. The base was added only to the substrates of which pH was adjusted to 4.51 and 4.63 (the [OH]/[Al] was less than 1.0). The substrate solution with pH 4.51 and 4.61 showed some turbidity upon the addition of OH ion, indicating slight precipitation of aluminum hydroxide, or that the solution might be supersaturated with respect to aluminum hydroxide (64).

The seven MIR spectra shown in Fig. 7 are for the monolayer samples. The top two spectra are for the monolayer samples transferred from the substrates of which pH was adjusted by adding the base.

As the pH of the substrate is increased, the acid absorption bands at 1700 cm^{-1} and 1275 cm^{-1} decrease in intensity relative to the hydrocarbon bands at 2930 cm^{-1}. Likewise, the salt absorption bands at 1590 cm^{-1} and 1435 cm^{-1} and the Al-O band at 975 cm^{-1} (10.14 μm) increase in relative intensity. When the pH is raised higher than 4.51, the spectrum for the multilayer sample does not show any of the acid band, indicating that the monolayer formed at that pH range consists of all aluminum resinate molecules.

These results indicate that the mole fraction of the salt, aluminum resinate, in the monolayer samples is steadily increased as pH is increased in the presence

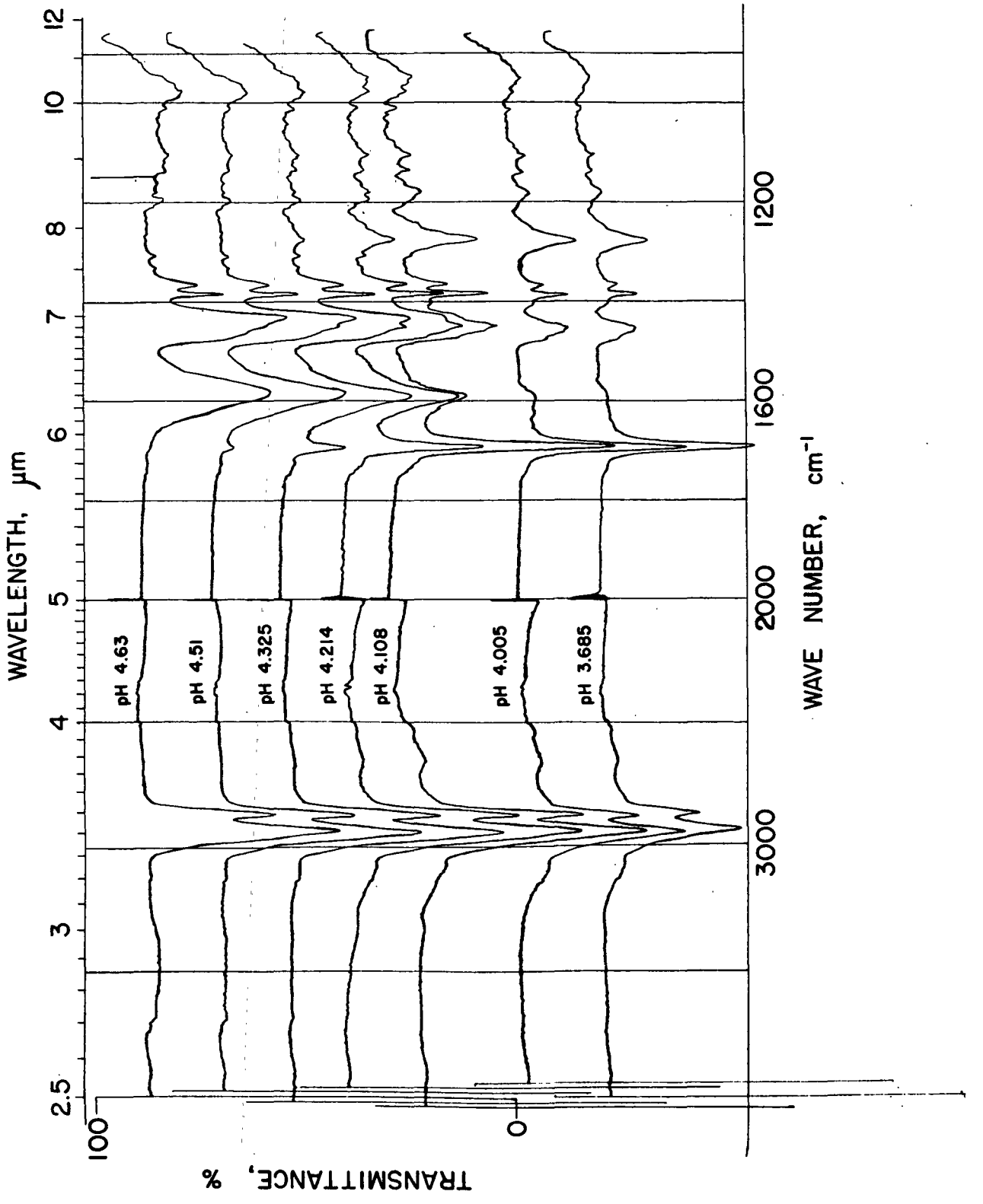

Figure 7. MIR-IR Spectra of TABSH Monolayers Reacted on Aluminum Sulfate plus Potassium Sulfate Substrate in Which pH is Changed at the $[SO_4] = 0.2\underline{M}$ ($[Al^{+3}] = 3.16 \times 10^{-3}\underline{M}$) (the $[OH]/[Al] < 1.0$)

of excess sulfate. This trend in the monolayer composition can account for the diminishing of the inhibiting effect of sulfate on the monolayer reaction with increasing the pH.

It should be noted in Fig. 7 that, as the pH of the substrate containing excess sulfate is increased, neither bonded OH absorption band, nor S-O absorption band appear in the frequency range 3600-3200 cm^{-1} (for bonded OH) and 1200-990 cm^{-1} (for SO_4) (126-128). This indicates again that the reacted monolayers at pH > 4.0 in the presence of sulfate contain neither inter- or intramolecular bonded OH groups nor SO_4 groups in the structure of aluminum resinate complexes formed in the monolayer. However, a free OH absorption band appears near 2.7 μm for the aluminum resinate monolayers formed at pH > 4.3, even though its intensity appears to be weak. The presence of this free OH group in the aluminum resinates formed at pH > 4.0 will be discussed later with the spectra obtained from aluminum resinate monolayers formed in the absence of sulfate.

CHANGES IN FREE ACID MOLE FRACTION WITH INCREASING pH

The $\underline{X}_{TABSH}$ values of the monolayer samples transferred from aluminum nitrate plus potassium sulfate substrates are given in Table IV and shown in Fig. 8. These were calculated with Equation (6) for data taken from the MIR spectra shown in Fig. 7.

The obtained value of $\underline{X}_{TABSH}$ decreases abruptly as the pH is increased from 4.0 to 4.4 in the presence of excess sulfate. These data indicate that the inhibiting action of sulfate ions on the reaction between TABSH monolayers and aluminum rapidly decreases as a result of a small increase in the pH. Thus, the salt formation of TABSH monolayer with aluminum ions appears to be increased with increasing pH; when the pH is higher than 4.4, the salt formation reaction appears not to be influenced by the presence of excess sulfate.

TABLE IV

CHANGES IN FREE ACID MOLE FRACTION OF THE MONOLAYERS REACTED ON ALUMINUM NITRATE PLUS POTASSIUM SULFATE SUBSTRATES[a] AS A FUNCTION OF pH[b]

Sample No.	pH[b]	A_{COOH}/A_{C-H}	Mole Fraction of Free Acid (X_{TABSH})	Spec. No.
TAB-Al-S-1-21	3.685	0.321/0.200=1.153	0.93	101
TAB-Al-S-1-11	3.985	0.356/0.325=1.095	0.88	89
TAB-Al-S-1-10	4.005	0.261/0.248=1.053	0.85	88
TAB-Al-S-1-20	4.108	0.249/0.416=0.840	0.68	100
TAB-Al-S-1-19	4.214	0.195/0.426=0.458	0.37	99
TAB-Al-S-1-16	4.325	0.072/0.366=0.197	0.16	96
TAB-Al-S-1-17	4.510[c]	0.017/0.339=0.05	0.04	97
TAB-Al-S-1-18	4.63[c]	∿0.0/0.323=0	0.0	98

[a]The $[Al^{+3}] = 3.16 \times 10^{-3}$M, the $[SO_4] = 0.2$M.

[b]pH was adjusted with 0.5N HCl and 1N NaOH (the [OH]/[Al] < 1.0).

[c]When the base was added to raise the pH, slight precipitation of $Al(OH)_3$ was visible (the [OH]/[Al] = 0.12 for pH 4.51; 0.37 for pH 4.63).

Consequently, excess sulfate has little or no effect on the reaction between TABSH monolayer and aluminum ions at a pH above 4.4 or 4.5.

CHANGES IN π-A ISOTHERM WITH INCREASING pH

The effect of excess sulfate on the monolayer reaction at different pH was examined again by determining changes in the π-A isotherm after an addition of excess sulfate in the aluminum nitrate substrate with pH 4.4 and 4.9. For the reaction at pH 4.4, the [Al] was held constant at 3.16×10^{-3}M and the $[SO_4]$ added to the aluminum nitrate solution was 0.2M. For the reaction at pH 4.9,

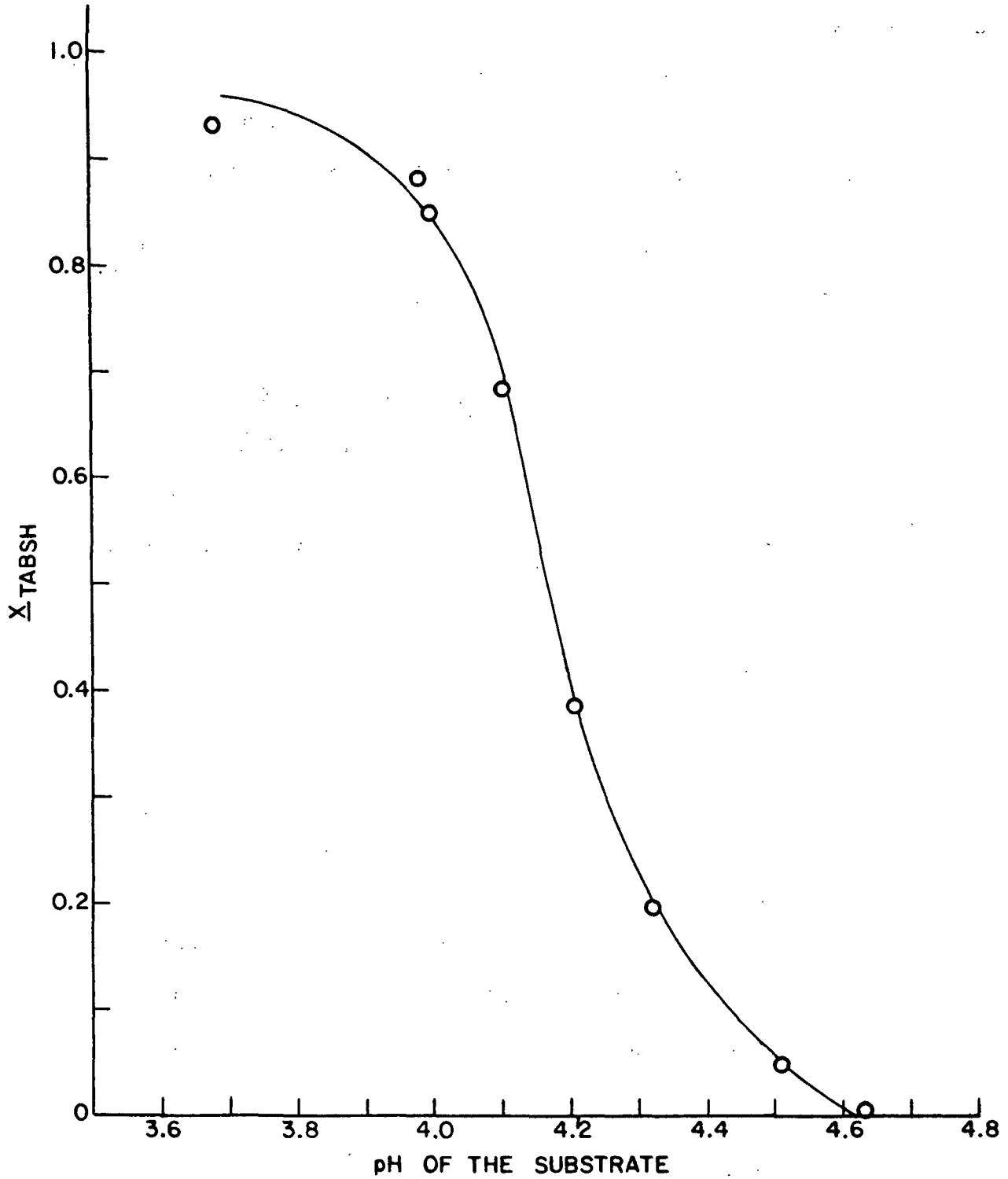

Figure 8. Changes in Free Acid Mole Fraction of the Monolayers Reacted on Aluminum Nitrate plus Potassium Sulfate Substrates as a Function of pH

the [Al] and the [SO_4] in the substrate were 3.16×10^{-4}M and 0.1M, respectively. Slight precipitation of aluminum hydroxide was observed upon the preparation of the substrate with the [SO_4] = 0, pH = 4.4, ([OH]/[Al] = 0.64), but the solution became clear upon aging for 30 min. In other substrate solutions, no precipitation of aluminum hydroxide could be observed upon the preparation.

The changes in the π-A isotherm for the monolayer formed on aluminum nitrate substrate free of sulfate with increasing pH from 4.0 to 4.95 are shown in the left side of Fig. 9. The right side of Fig. 9 shows the changes for the monolayer formed on the substrate with excess sulfate with increasing pH from 4.0 to 4.91. Comparison of the isotherms in the left side of the figure with those in the right side shows that the bottom π-A isotherm in the left side for the monolayer formed at pH 4.0 loses the characteristics of the aluminum resinate monolayer as shown in the right side of Fig. 9.

In contrast to the changes at pH 4.0, the middle and top isotherms formed at pH 4.4 and 4.9 do not lose their characteristics of compressed film behavior, even though they are changed to some degree by the addition of excess sulfate.

The changes are reflected in the $A_{K,EX}$ and $\pi_{K,EX}$ values of the π-A isotherms as given in Table V and shown in the bottom half of Fig. 10 (data points). The $\pi_{K,EX}$ value decreases to a great extent and the $A_{K,EX}$ value increases significantly by the addition of excess sulfate at pH 4.0. The addition of excess sulfate does not cause a significant change in molecular area values for the monolayer formed at pH 4.4 and 4.9, but the $\pi_{K,EX}$ values decrease to some degree. However, the decreased values of $\pi_{K,EX}$ are higher than the value for the aluminum resinate monolayer formed at pH 4.0.

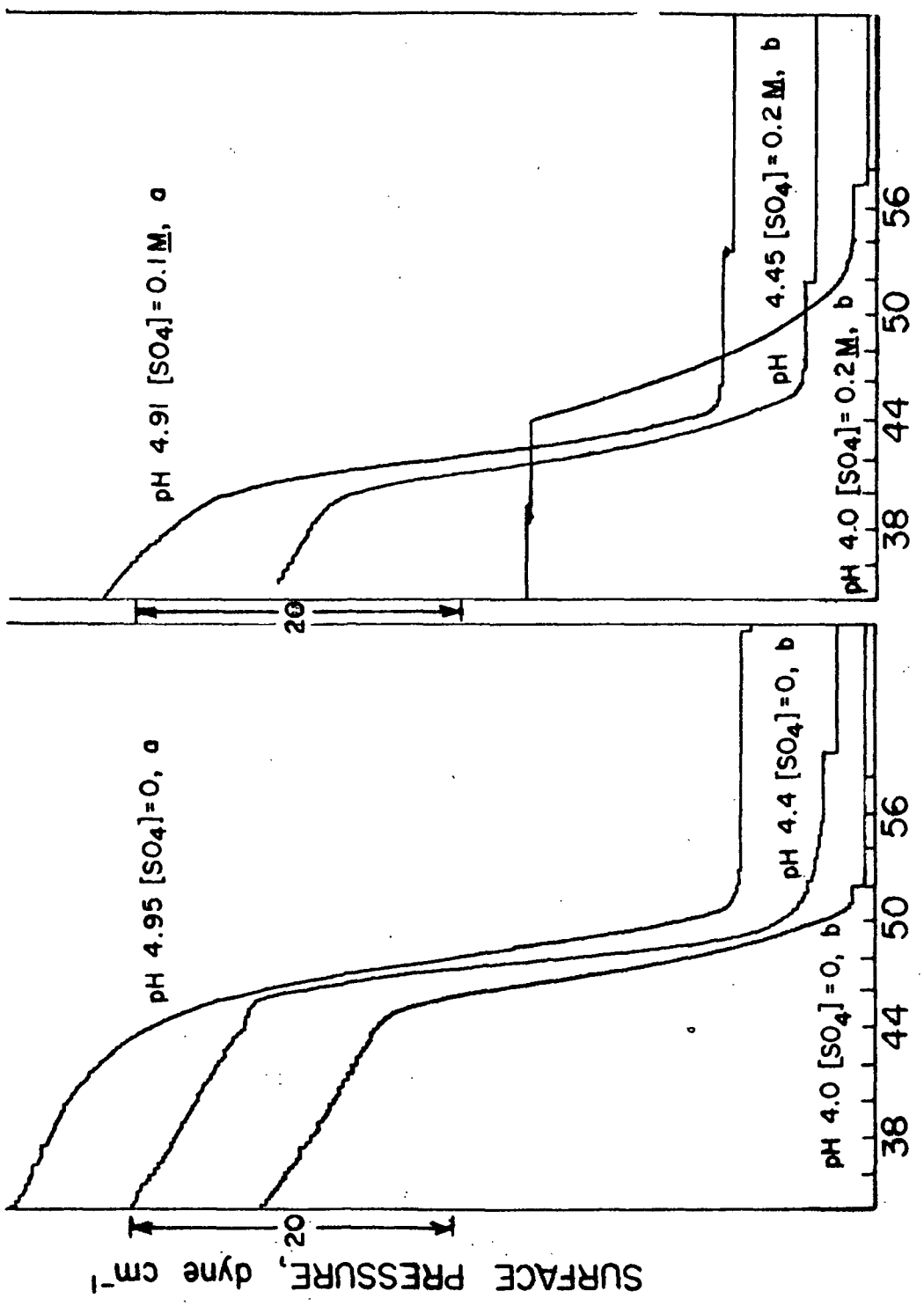

Figure 9. Changes in π-A Isotherms of TABSH Monolayers Reacted on Aluminum Nitrate of Substrates Without (Left) Sulfate with Increasing pH and with (Right) Excess Sulfate (0.2M) with Increasing pH

[a] [Al] = 3.16×10^{-4} M
[b] [Al] = 3.16×10^{-3} M

TABLE V

$\pi_{K,EX}$, $A_{K,EX}$, A_{10}, AND A_{18} VALUES FOR THE TABSH MONOLAYERS FORMED ON ALUMINUM NITRATE PLUS POTASSIUM SULFATE SUBSTRATES[a] WITH VARIED pH

Substrate Condition		pH	$\pi_{K,EX}$	$A^2_{K,EX}$	A^2_{18}	A^2_{10}
$[SO_4]$	[Al]					
0	3.16×10^{-3}	4.010	29.2	39.9	41.5	43.3
1.0×10^{-1}	"	4.007	20.6	43.3	44.0	46.3
2.0×10^{-1}	"	3.970	20.5	43.9	44.5	47.1
0	"	4.405	35.5	40.3	42.4	43.0
0.2M	"	4.455	29.9	39.7	41.4	42.8
0	3.16×10^{-4}	4.950	38.6	39.6	42.6	43.8
0.1M	"	4.905	33.5	40.0	41.7	42.7

[a] Substrates were at 22.5°C; reaction time = 10 minutes, and $dA^2/dt = 2.52$ A^2 molecule^{-1} minute^{-1}.

It should also be noted in the left side of Fig. 9 and in Fig. 10 that the surface pressure at the collapse point increases as the pH of the substrate is raised. The changes in the $\pi_{K,EX}$ value upon increasing the pH suggest possible changes in the chemical nature of the aluminum resinate monolayers with increasing the pH at which the aluminum resinate is formed.

These data are consistent with the results observed by the composition analysis and help to establish the fact that excess sulfate has little or no effect on the reaction between TABSH monolayers and aluminum ions at a pH above 4.4 or 4.5. These results also strongly suggest the possibility that the aluminum resinate formed at pH 4.0 is apparently different in its chemical nature from the salt formed at a pH above 4.4.

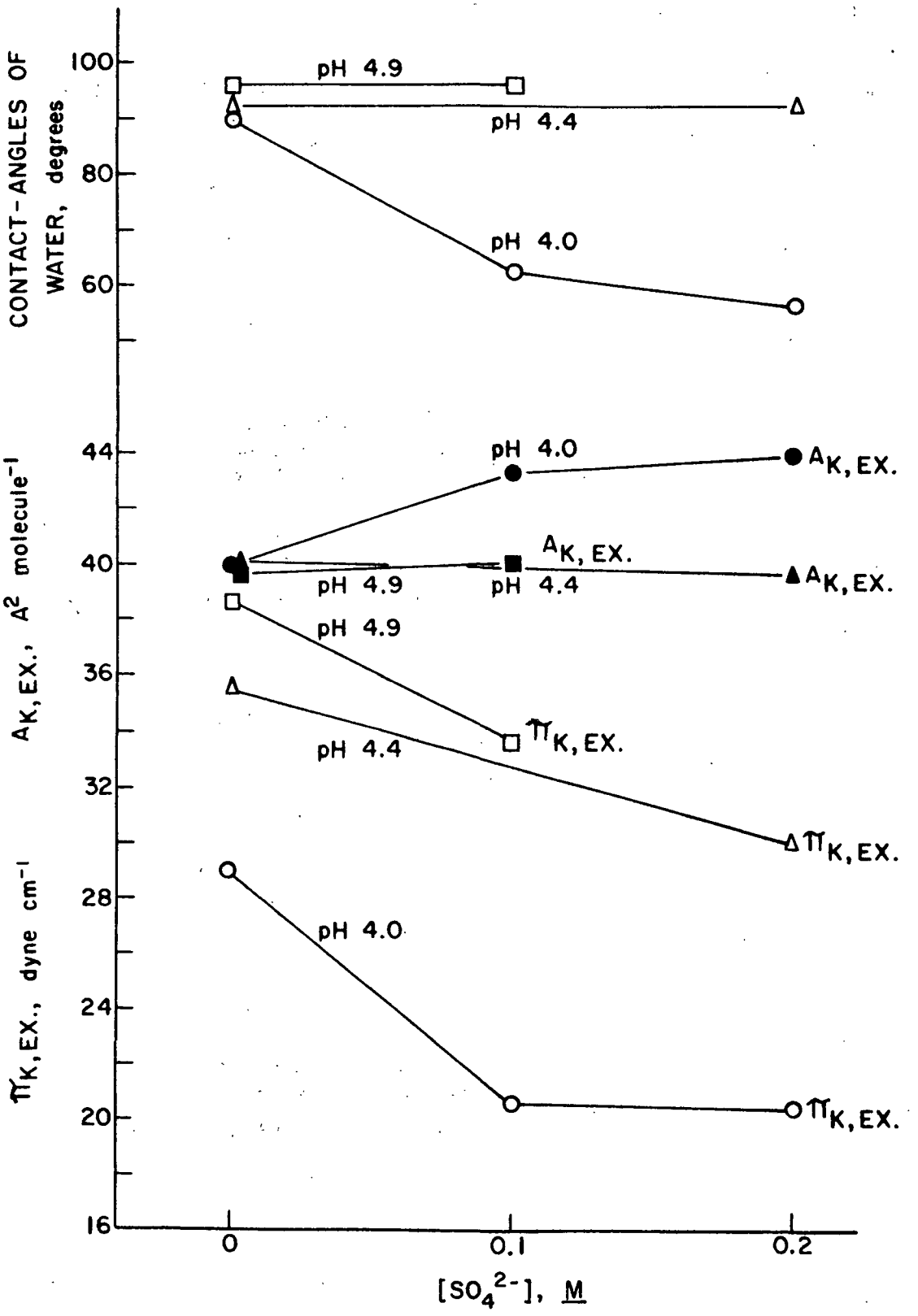

Figure 10. Comparison of Changes in Contact Angles of Water, $A_{K,EX}$ and $\pi_{K,EX}$ Values for Reacted TABSH Monolayers with Increasing the $[SO_4]$ at Different pH (4.0, 4.4 and 4.9)

CHANGES IN CONTACT ANGLES ON THE CAST MONOLAYER AT DIFFERENT pH

The monolayers used for the determination of π-A isotherms were cast on the CMC film and the contact angles of water, methylene iodide and formamide on the cast monolayer were measured. The contact angle data are tabulated in Table VI and the changes in the contact angle of water are compared with the changes for the monolayer formed at pH 4.0 in Fig. 10.

TABLE VI

CONTACT ANGLES ON TABSH MONOLAYERS[a] CAST ON THE CMC FILM FROM ALUMINUM NITRATE PLUS POTASSIUM SULFATE SUBSTRATES WITH DIFFERENT pH

Substrate Condition			Initial Advancing Contact Angles,[b] degree		
$[SO_4]$, M	[Al], M	pH	Water (γ_ℓ=72.4)[c]	Methylene Iodide (γ_ℓ=50.5)[c]	Formamide (γ_ℓ=57.4)[c]
0	3.16×10^{-3}	4.01	90.0 ± 3.2[d]	49.0 ± 1.4[d]	70.5 ± 2.3[d]
0.1	"	4.007	62.9 ± 3.6	48.5 ± 2.8	54.4 ± 7.5
0.2	"	3.970	56.6 ± 8.2	49.7 ± 2.3	50.7 ± 12.4
0	"	4.405	92.8 ± 1.2	51.8 ± 1.9	70.9 ± 4.9
0.2	"	4.455	92.8 ± 0.8	49.6 ± 1.9	70.9 ± 5.2
0	3.16×10^{-4}	4.950	95.4 ± 1.6	51.2 ± 0.9	74.2 ± 2.0
0.1	"	4.905	95.5 ± 1.7	51.8 ± 0.4	67.8 ± 2.0

[a]The monolayer was reacted for 10 min at the interface and transferred onto the CMC film-glass slide at a constant compressed film pressure, π_{comp}=18 dynes/cm.
[b]The contact angles were determined by linear extrapolation to t (contact time)=0.
[c]Liquid surface tension in dynes/cm, measured at 22.5°C.
[d]95% Confidence limits.

As shown in the figure, the contact angles of water on the cast monolayers formed at pH 4.4 and 4.9 are not decreased by the addition of excess sulfate in the substrate. These data indicate again that the chemical composition of the

monolayer formed in the absence of sulfate is not changed by the addition of excess sulfate in the aluminum nitrate substrate with pH > 4.4.

As illustrated in Table VI, the contact angle of water on the cast aluminum resinate monolayer appears to be increased when the pH of the substrate is increased.

The observed difference in the water contact angles on the cast monolayer formed at different pH again suggests that the chemical nature of aluminum resinate formed in the monolayer reaction may vary depending upon pH of the aluminum nitrate substrate. This result would be consistent with that of the π-A isotherm determinations at varied pH.

CHANGES IN MIR SPECTRA FOR ALUMINUM RESINATE MONOLAYERS WITH INCREASING pH

The results of the π-A isotherms determination and of the contact-angle measurements indicated the possibility that the chemical nature of aluminum resinate formed in the monolayer may vary depending upon the pH. Thus, the nature of the aluminum resinate monolayer formed in the absence of sulfate was investigated with MIR spectroscopy using the multilayer sample. The top three spectra shown in Fig. 11 are for the aluminum resinate monolayers formed in the absence of sulfate at pH 3.98, 4.4, and 4.86, respectively. The bottom spectrum is for the aluminum resinate monolayer formed in the presence of excess sulfate at pH 4.98. The [Al] was decreased from 3.16×10^{-3}M to 3.16×10^{-4}M when the pH was raised above 4.4 to avoid the precipitation of aluminum hydroxide.

As shown in Fig. 11, as the pH is increased above 4.0, the weak, sharp absorption band at 2.69 μm (3710 cm^{-1}) shows up and its intensity appears to increase with increasing pH. More apparent change of this band can be seen in Fig. 12, in which the spectra of Fig. 11 are expanded at 5 times the expanded ordinate scale in the wavelength range between 2.8 μm (3900 cm^{-1}) and 3.2 μm (3100 cm^{-1}).

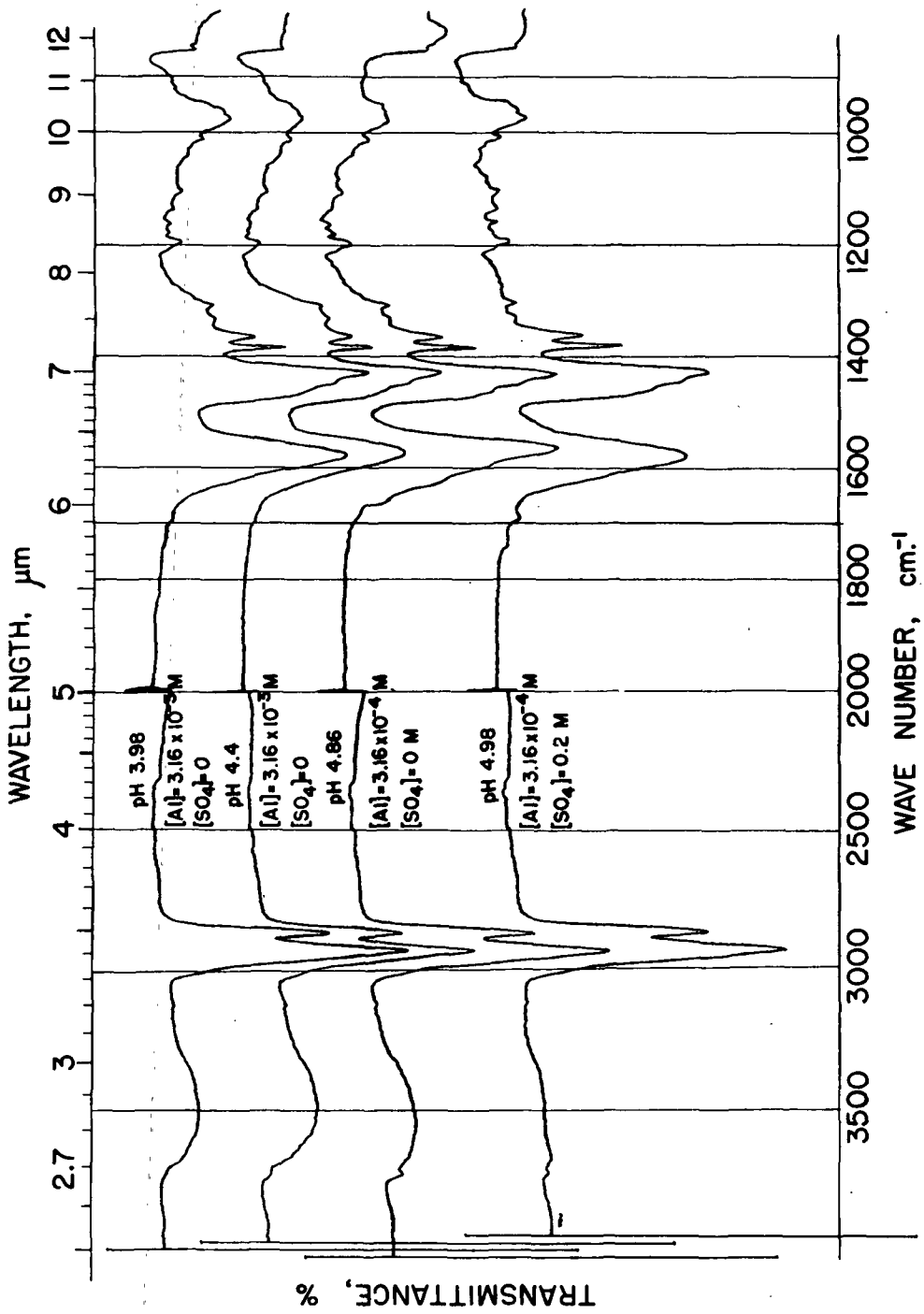

Figure 11. MIR-IR Spectra for Aluminum Resinate (TABS-Al) Monolayers Formed on Aluminum Nitrate Substrates Without Sulfate at pH 3.98, 4.4, and 4.86, and with an Excess Sulfate (0.2M) at pH 4.98

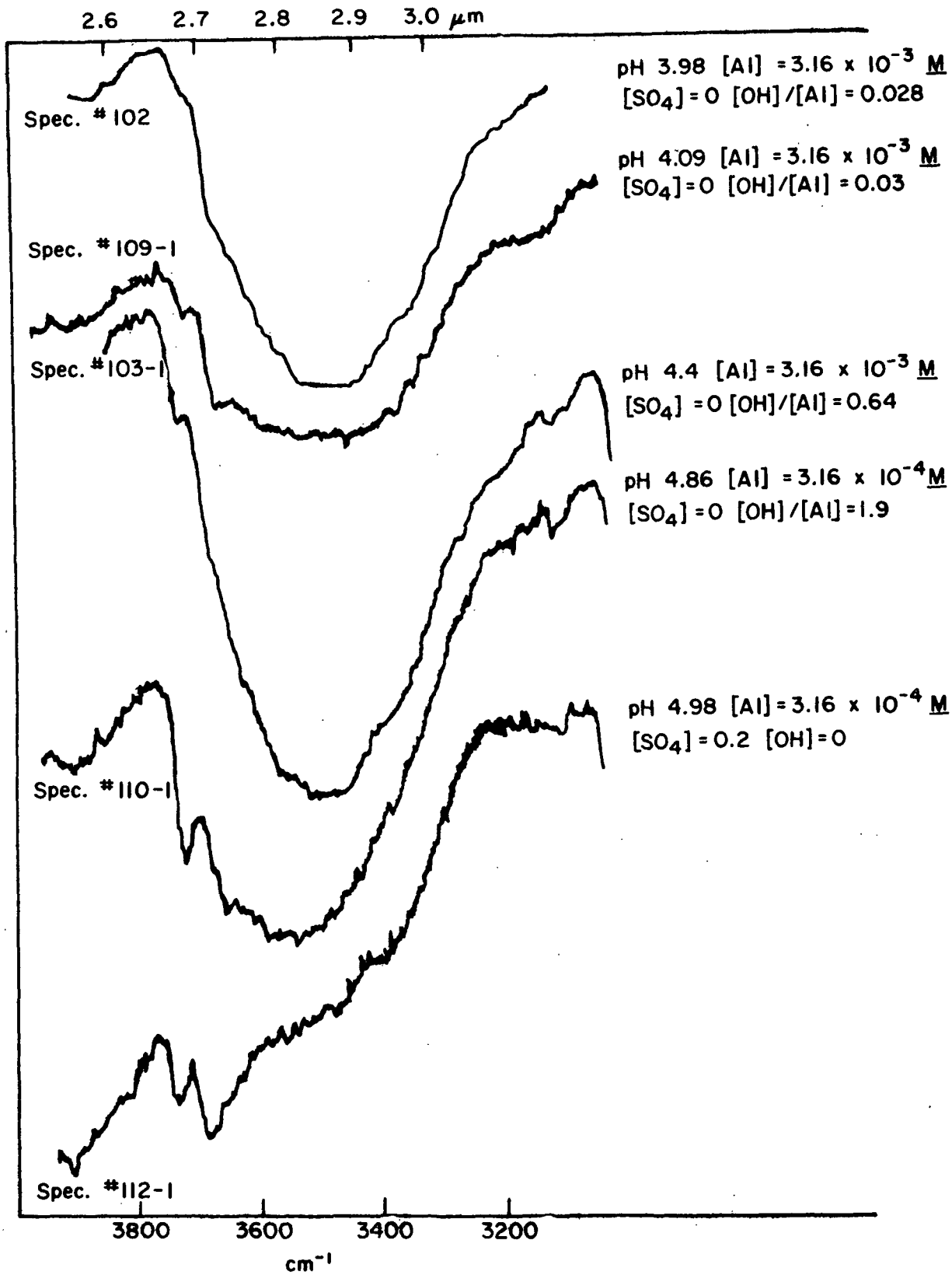

Figure 12. Expanded MIR-IR Spectra in the Frequency Range of 3800 cm^{-1} to 3200 cm^{-1} for the Spectra Shown in Fig. 11 at the 5X Ordinate Scale. The Spectrum for pH 4.09 was also Included

Figure 12 also includes the spectrum for the aluminum resinate monolayer formed near pH 4.1. In the case of the aluminum resinate formed at pH 4.4, the intensity at 2.69 μm (3710 cm^{-1}) still appears to be weak, possibly due to overlapping of the strong broad band near 3500 cm^{-1}.

The weak, sharp absorption band at 2.69 μm (3710 cm^{-1}) is attributed to the presence of free OH groups in the aluminum resinate monolayer, in agreement with all the previous investigators (42-46) who assigned this band to their basic aluminum soap. There is no reason to suspect a different assignment in this case. In this connection, it was found by an investigation that the strong broad band near 3500 cm^{-1} in the 3750-3300 cm^{-1} region cannot be assigned to bonded OH groups of aluminum resinate complexes, as one might suspect. (This investigation will be discussed in the next section.)

It should be noticed in Fig. 11 that the peak of the ionized carboxyl band near 1590 cm^{-1} appears to be slightly shifted to a longer wavelength as the pH is increased; this band also becomes broader as compared to the band for aluminum resinate formed at pH 4.0. The band shifting and broadening may be due to possible increase in the intra- and intermolecular interaction between ionized carboxyl groups and coordinated OH groups in the aluminum resinate monolayer formed at the raised pH.

Therefore, these spectroscopic results may be able to account for the observed changes in the π-A isotherms and in the contact angle data with increasing pH. The absence of the free OH band in the spectrum indicates that the aluminum resinate monolayer formed at pH 4.0 consists chiefly of triresinate complex which is free of OH groups.

In contrast to the aluminum resinate formed at pH 4.0, the aluminum resinate monolayers formed at the raised pH, i.e., 4.98 or 4.4, consist chiefly of a basic aluminum resinate complex containing a free OH group (not bonded OH group) in the structure. This result further suggests that aluminum resinate monolayers formed in the pH range between 4.0 to 5.0 may be composed of a mixture of triresinate and hydroxylated resinate (possibly monobasic diresinate).

IDENTIFICATION OF THE BROAD ABSORPTION BAND NEAR 3500 CM^{-1}

As shown in Fig. 2, 7, and 11, the broad absorption band near 3500 cm^{-1} in the 3750-3300 cm^{-1} region always appears for the monolayer samples spread on aluminum nitrate substrates free of sulfate.

The broad bands in this frequency region can be assigned to a stretching vibration of inter- and intramolecular bonded hydroxyl groups (126,127), but the source of the hydroxyl group is not known in this case. Three possible sources of the hydroxyl groups were hypothesized for multilayer samples cast on the Ge plate:

1. Presence of hydrated water molecules in the multilayer sample.
2. Presence of basic aluminum resinate complexes, specifically dibasic monoresinate in which inter- and intramolecular bondings are likely to occur among adjacent OH groups (8,42).
3. Contamination of aluminum hydroxide precipitates which are possibly adsorbed on the spread monolayers during the multilayer deposition.

Considering these possible sources, a series of experiments was carried out to identify the cause for the broad absorption and the following results were obtained.

1. THE EFFECT OF THE ADDITION OF SULFATE

The top spectrum shown in Fig. 13 is for the aluminum resinate monolayer sample transferred from the aluminum nitrate substrate with added hydroxyl ions ([OH]/[Al] = 1/31.6). The second spectrum from the top is for monolayers of aluminum resinate plus a small fraction of free acid (see Table I) transferred from the substrate containing aluminum nitrate plus potassium sulfate with added hydroxyl ions ([OH]/[Al] = 1.15/31.6).

As demonstrated with the top two spectra in the figure, the small addition of sulfate resulted in a substantial decrease in its intensity near 3500 cm^{-1}. The broad shape of the absorption band appeared to be diminished in the spectrum for the monolayer reacted in the presence of sulfate. The diminishing of the broad band by the addition of excess sulfate was also observed at any pH under investigation (pH 4.0-5.0).

This indicates that the broad absorption band appears only for the monolayer sample reacted on the aluminum nitrate substrate free of sulfate.

2. HYDROGEN-DEUTERIUM EXCHANGE EXPERIMENT AND THE EFFECT OF DRYING

If the broad band is caused by the presence of hydrated water molecules in the multilayer sample on the Ge plate, the band of hydrogen-bonded water would be shifted to a lower frequency, i.e., near 2500 cm^{-1} after a hydrogen-deuterium exchange (133).

A multilayer sample on the Ge plate was immersed in D_2O for 30 minutes at 60°C or for 2 hours at the room temperature; no band shift was observed for the multilayer sample.

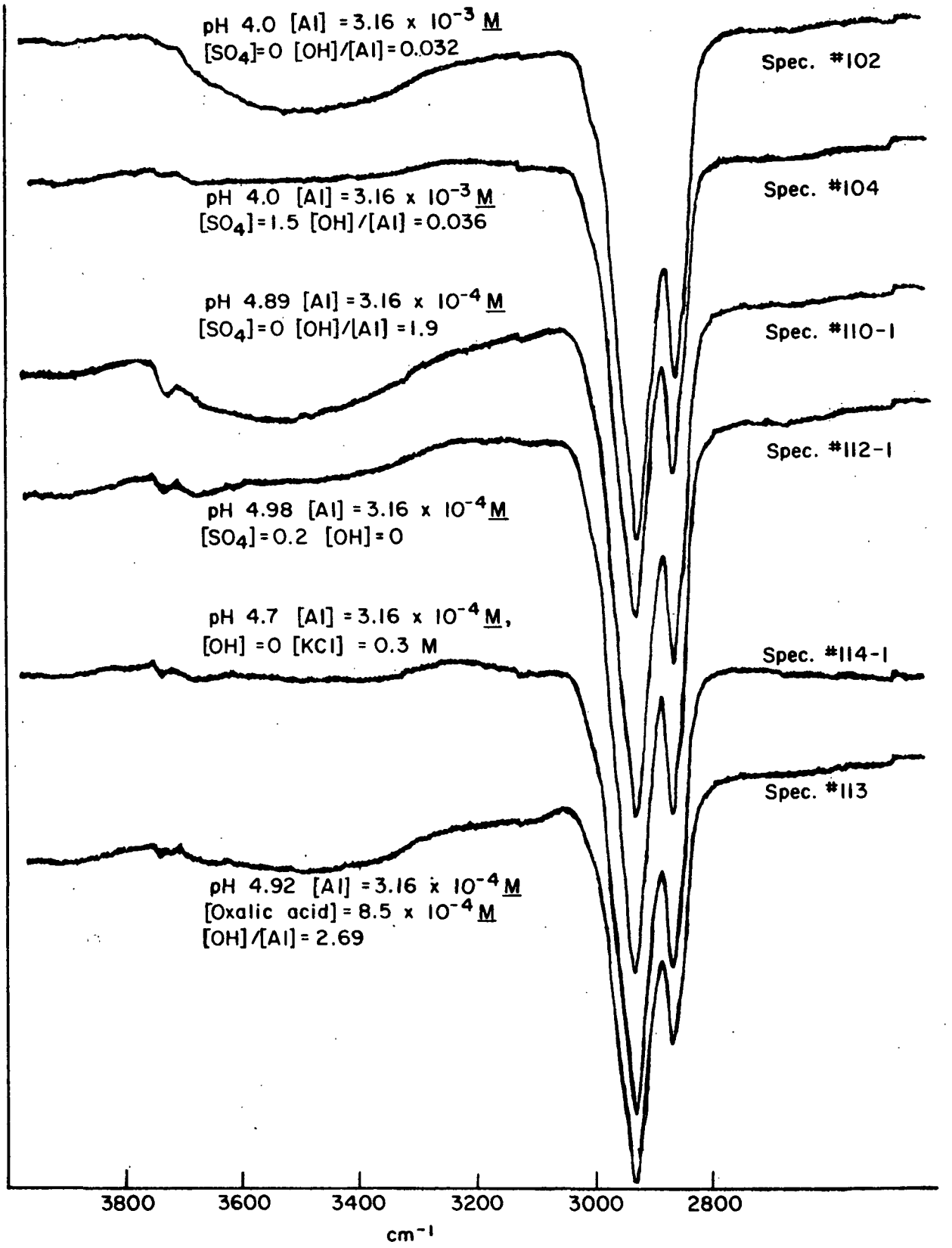

Figure 13. Changes in MIR-IR Spectra of TABSH Monolayer Formed at Aluminum Nitrate Substrates by the Addition of Potassium Sulfate, Potassium Chloride and Oxalic Acid Into the Substrate (the Frequency Range; 3800 cm^{-1}-2800 cm^{-1})

Although the hydrophobicity of the surface of the multilayer sample might hinder the penetration of D_2O into the multilayer, this result would not indicate the possibility that any hydrated water molecules are involved in the broad absorption in that frequency region.

The absence of water molecules appeared to be confirmed by the result of a drying experiment; an extensive drying of the cast multilayer sample (drying in the vacuum oven at 100°C for 5 hours) did not diminish the broad band.

3. THE EFFECTS OF THE ADDITION OF POTASSIUM CHLORIDE, AND OF OXALIC ACID

Analogous to the effect of potassium sulfate, the addition of potassium chloride in the aluminum nitrate substrate resulted in the diminishing of the broad band. However, it may be pointed out that the substrate with the [Cl]=0.3M did not require the addition of OH ions to adjust the pH.

The spectrum of the monolayer reacted on the aluminum nitrate plus potassium chloride substrate with pH 4.7 is shown in Fig. 13 (the second spectrum from the bottom). The excess chloride did not affect the salt formation in the monolayer reaction.

In contrast to the effect of chloride, the addition of oxalate ions having strong coordinating power to aluminum ions did not diminish the broad band near 3500 cm^{-1}. But oxalate decreased the intensity of the salt band at 1680 cm^{-1}. This indicates that the oxalate prevents aluminum ions from reacting with the TABSH monolayer even at pH 5.0 as it does at pH 4.0 (11). It may be interesting to point out that the pH of the aluminum nitrate plus oxalic acid had to be adjusted by adding a considerable amount of KOH ([OH]/[Al] = 2.7 at pH 4.92). Upon adding the base to the solution, slight precipitation of aluminum hydroxide could be seen, but after aging the solution it appeared to be free of any "visible" precipitation.

These results indicate that the broad band is caused by the addition of OH ions when the pH adjustment is required in the absence of sulfate or chloride ions. However, this absorption band cannot account for the formation of dibasic aluminum resinate complexes, because the addition of sulfate or chloride to the substrate with pH > 4.4 diminishes only the broad band near 3500 cm^{-1} without affecting the salt absorption band at 1680 cm^{-1}.

4. MIR SPECTRUM OF ALUMINUM HYDROXIDE PRECIPITATES

From the above experiment, it was speculated that the broad band might be caused by the adsorption of aluminum hydroxide (precipitate) on the spread monolayer during the multilayer deposition. It was often observed that a localized formation of aluminum hydroxide precipitate in aluminum nitrate substrate solutions was visible upon the addition of the KOH solution. However, the prepared solutions normally did not show any "visible" precipitation of the hydroxide after aging the solution for 30 minutes with agitation.

An MIR spectrum for $Al(OH)_3$ precipitate was obtained by spreading the aluminum nitrate solution containing visible $Al(OH)_3$ precipitate on the clean germanium plate. The $Al(OH)_3$ precipitate was prepared by adding a KOH solution to an aluminum nitrate solution ([OH]/[Al]=3). The obtained spectrum for the $Al(OH)_3$ precipitate shows the broad band near 3450 cm^{-1} like the broad band near 3500 cm^{-1} for the multilayer samples, as shown in Fig. 14 (the bottom spectrum).

5. THE EFFECT OF ADSORPTION OF ALUMINUM HYDROXIDE

An aluminum resinate multilayer sample showing no broad band near 3500 cm^{-1} was purposely contaminated by immersing it into an aluminum nitrate solution with the [Al] = 3.16×10^{-4} M for 3 hours. The pH of the solution was raised by adding

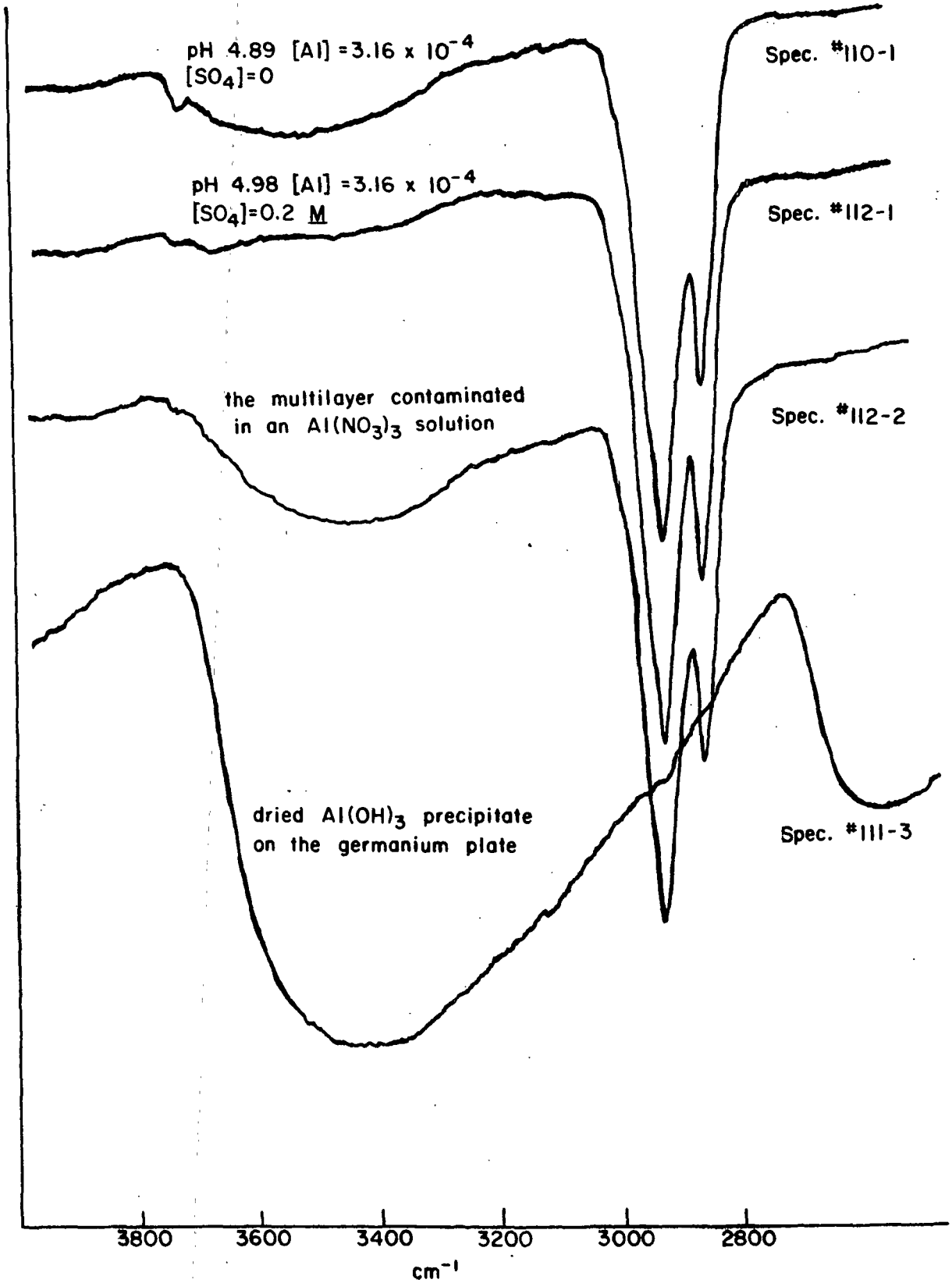

Figure 14. Changes in MIR-IR Spectra of the TABSH Monolayer Sample by the Addition of Sulfate and by the Contamination of Aluminum Hydroxide. The Spectrum of the $Al(OH)_3$ Precipitate Dried on the Ge Plate is Included

OH ions ([OH]/[Al] = 2.2). (The solution did not show any visible precipitation of aluminum hydroxide.)

Figure 14 illustrates the effect of $Al(OH)_3$ contamination on the MIR spectrum for the multilayer samples on the germanium plate. The top spectrum shows the broad band for the monolayer reacted in the absence of sulfate at pH 4.9. The second spectrum from the top shows no broad band for the monolayer reacted in the presence of excess sulfate (0.2M). This cast multilayer sample was then contaminated in the aluminum nitrate solution and its spectrum is shown in the figure (the third spectrum). After being contaminated the spectrum shows again the broad band near 3450 cm^{-1} which looks like the broad band for the first sample (the top spectrum).

Although the maximum peak (3450 cm^{-1}) of the contaminated sample appears to be a little off from the peak (3500 cm^{-1}) of the original multilayer sample, these results strongly suggest that the broad absorption band is caused by the adsorption of aluminum hydroxide by the spread monolayers from the substrate solution during the multilayer deposition. The small deviation in the maximum peak for the contaminated sample may be due to a difference in the intermolecular structure of the adsorbed hydroxides between the artificially adsorbed hydroxide on the surface of the multilayer and the actually adsorbed hydroxide between the monolayers during the multilayer deposition.

Furthermore, the diminishing effect of sulfate ions on the broad absorption band is not due to the penetration of sulfate ions into aluminum resinate complexes by replacing coordinated OH groups (10,60). No sulfate absorption band appears near 1100 cm^{-1} for the monolayers reacted in the presence of excess sulfate.

In summary, the results of these experiments leads to the conclusion that the broad absorption band in the 3700-3300 cm^{-1} may be attributed to the adsorption of aluminum hydroxide (precipitate) during the multilayer deposition on the Ge plate. However, it does not rule out the possibility that other hydroxylated Al ions (monomeric or polymeric ions) are also involved in the adsorption on the spread monolayers (80-85). The broad band sometimes appeared for the monolayers reacted on the aluminum nitrate substrate solutions which apparently did not show any visible precipitation upon preparation.

The diminishing of the bonded OH absorption band by the sulfate addition without affecting the salt bands (ionized COOH) also suggests that polymeric Al ions [e.g., $Al_8(OH)_{20}^{+4}$ (72) or $Al_{18}(OH)_{32}^{+7}$ (62,66,74,77)] if they form in the solutions, are not responsible for the formation of basic aluminum resinate complexes. The basic salt complexes should reveal the bonded OH band in their IR spectra because the OH groups in the hydroxylated complexes are likely to be intramolecularly bonded to each other through the olation (8,60,68,69).

DISCUSSION

PROPOSED REACTION PRODUCTS BETWEEN TABSH MONOLAYERS AND ALUMINUM IONS AT pH 4.0-5.0

Before proceeding to the discussion about the effects of sulfate on the reaction between TABSH monolayers and aluminum ions, it is felt that it is necessary to gain an insight into the nature of the reaction products, i.e., aluminum resinates.

From the results obtained with MIR spectroscopy, π-A isotherm measurements and contact-angle measurements, the aluminum resinate formed at pH 4.0 appears to be different in its structure from the salt formed at a pH above 4.4. It is now proposed that aluminum resinates formed in the monolayer reaction at a pH range of 4.0 to 5.0 is a mixture of two kinds of aluminum resinate; aluminum triresinate (trisoap) and monobasic aluminum diresinate (disoap). The triresinate is believed to be a major reaction product at pH 4.0, while the diresinate is the major one possibly at a pH above 4.4.

Experimental evidence for the formations of the triresinate and the monobasic diresinate in the monolayer reaction can be summarized as follows:

1. No free OH absorption band at 2.69 μm (3710 cm^{-1}) was shown in the MIR spectrum for the triresinate formed at pH 4.0, while the spectrum for monobasic diresinate formed at the pH higher than 4.4 showed the free OH band and its intensity was increased as the pH of the salt formation was increased (see Fig. 11 and 12).
2. The π-A isotherm for the TABSH monolayer reacted at pH 4.0 was different from the isotherm at pH > 4.4. The aluminum resinate monolayer formed at pH 4.0 had a lower $\pi_{K,EX}$ value than the monolayer formed at pH > 4.4 (see Fig. 8 and 10).

3. The contact-angles of water on the aluminum resinate monolayer formed at pH 4.0 were lower than the contact-angles on the monolayer formed at pH > 4.4 (see Table V and Fig. 10).

The absence of a free OH absorption band at 2.69 μm (3710 cm^{-1}) is regarded as strong evidence for the existence of the triresinate because Leger, et al. (45) and Ellis and Pauley (46) also presented this spectroscopic evidence for the existence of aluminum trisoaps. The presence of a free OH band for the aluminum resinate formed at pH > 4.4 is, in turn, believed to be strong evidence for the formation of monobasic diresinate in the monolayer. The presence of a free OH absorption band at 2.7 μm (3700 cm^{-1}) in the IR spectrum for monobasic aluminum disoap was proved by previous investigators such as Harple, Scott, Bauer and their coworkers (42-44) using IR spectroscopy, chemical analysis, synthesis of a specific aluminum soap and x-ray spectroscopic techniques. The formation of monobasic diresinate in the size precipitate is supported by Davison (25) and Major (11) who used chemical analysis and IR spectroscopic techniques.

The observed changes in π-A isotherms for aluminum resinate monolayers with increasing pH appears to be consistent with the changes observed by Spink and Sanders (134) with stearic acid monolayers on aluminum sulfate substrate ([Al] = 2×10^{-3}M); they report that while solid condensed films are obtained at pH values between 3.4 and 4.2, solid-expanded brittle films are obtained when the pH is between 4.2 and 5.4.

In their report, abrupt changes in the A_o values (the molecular area at $\pi = 0$) appeared between pH 4.2 to 4.45 which are analogous to the changes in the X_{TABSH} values shown in Fig. 8.

Thomas and Schulman (135,136) also observed changes in the film properties at pH 4.4 when they determined π-A isotherms of sodium cetyl sulfate monolayers and of fatty acid monolayers on aluminum sulfate substrates with an increase in the pH. They speculated that the adsorption of aluminum hydroxide precipitate or hydroxylated aluminum ions by the monolayers might be related to the changes in the film properties (solidification).

MOLECULAR MODELS FOR ALUMINUM TRITETRAHYDROABIETATE AND ALUMINUM MONOBASIC DITETRAHYDROABIETATE

The Fisher-Taylor-Hirschfelder molecular models were built for the most probable structures of aluminum tritetrahydroabietate and of monobasic ditetrahydroabietate existing in the compressed monolayers and in the collapsed monolayers. Photographs of the models are illustrated in Fig. 15 (a,b,c,d,e, and f).

Figure 15(a) shows the side view of a model of tetrahydroabietic acid possibly oriented in the monolayer spread on aqueous solutions. The carboxylic acid molecule is oriented so that the polar carboxyl group is in the substrate, and the nonpolar hydrocarbon groups are on the top.

Figure 15(b) is the side view of a possible structure of the tritetrahydroabietate in the monolayer. It may be interesting to notice that the model of aluminum triresinate can be built without any bond strain and steric hindrance of bulky hydrocarbon chains as demonstrated in Fig. 15(b).

Figure 15(c) shows the top view of the triresinate model. The figure suggests the possibility that the complex structure in the monolayer can promote the intramolecular interaction between the adjacent hydrocarbon chains, so that the stability of the triresinate in the monolayer can be increased.

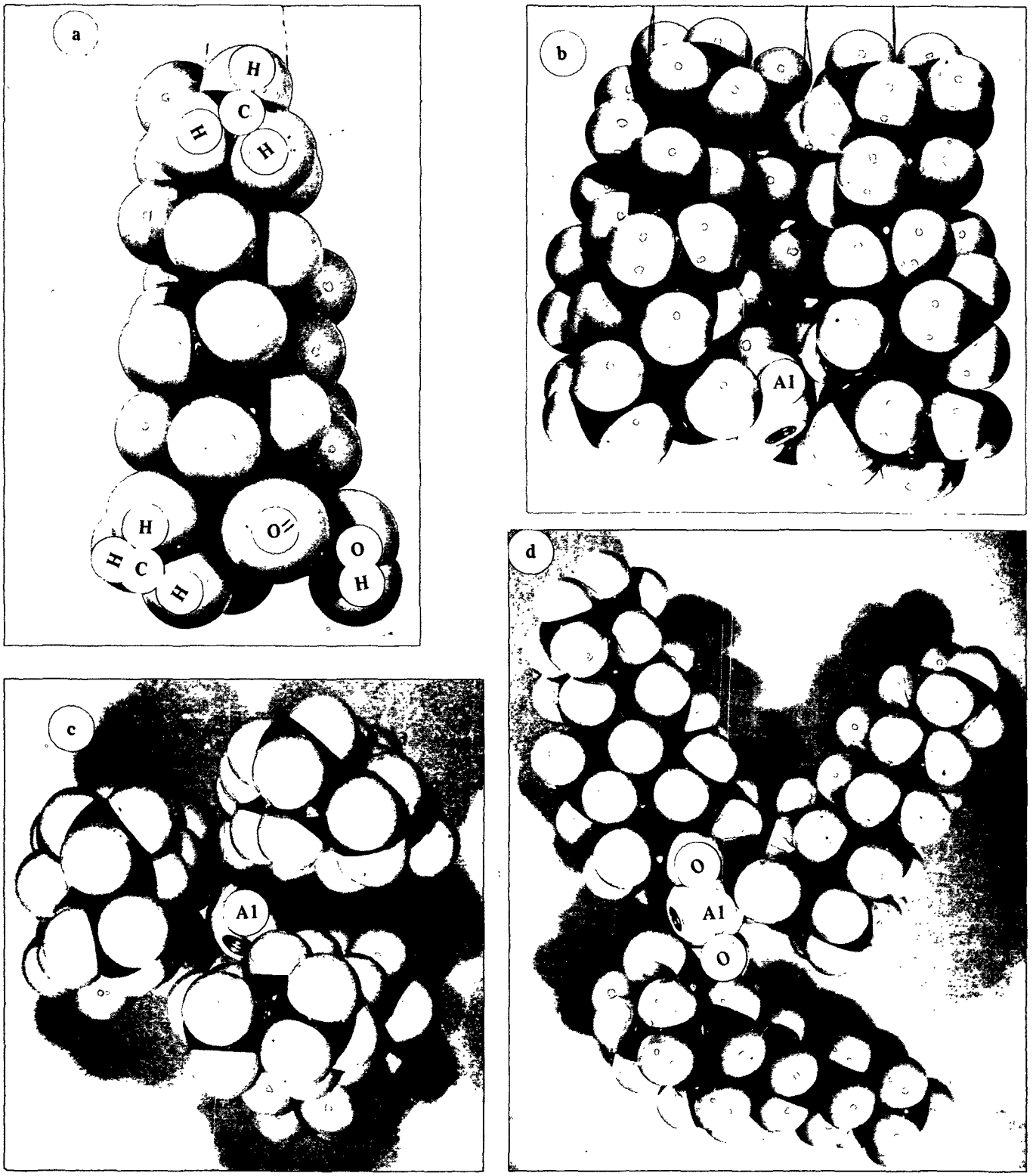

Figure 15. Photographs of Molecular Models of Tetrahydroabietic Acid, Aluminum Tritetrahydroabietate, and Aluminum Monobasic Ditetrahydroabietate. (a) Tetrahydroabietic Acid (Side View); (b) Aluminum Tritetrahydroabietate (Side View); (c) Top View of (b); (d) Aluminum Tritetrahydroabietate in the Collapsed Monolayer

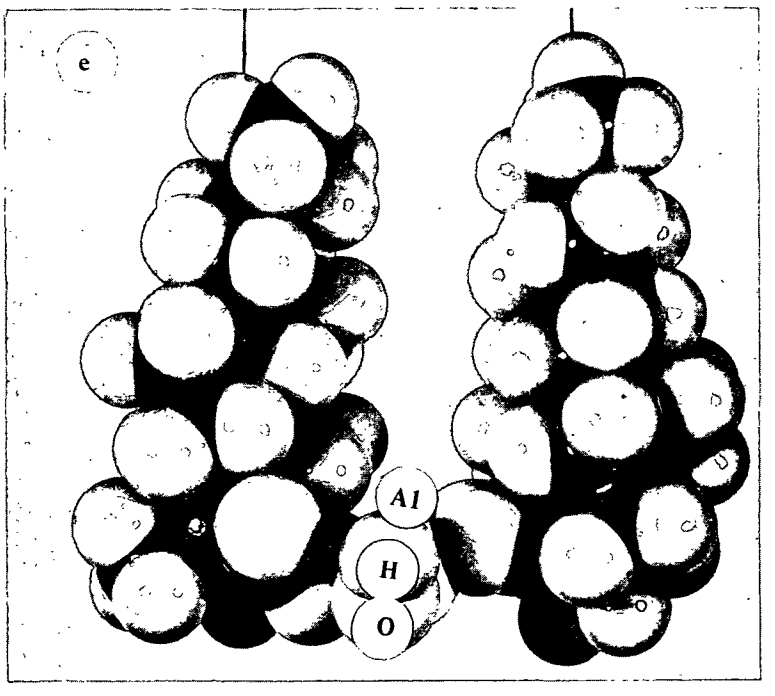

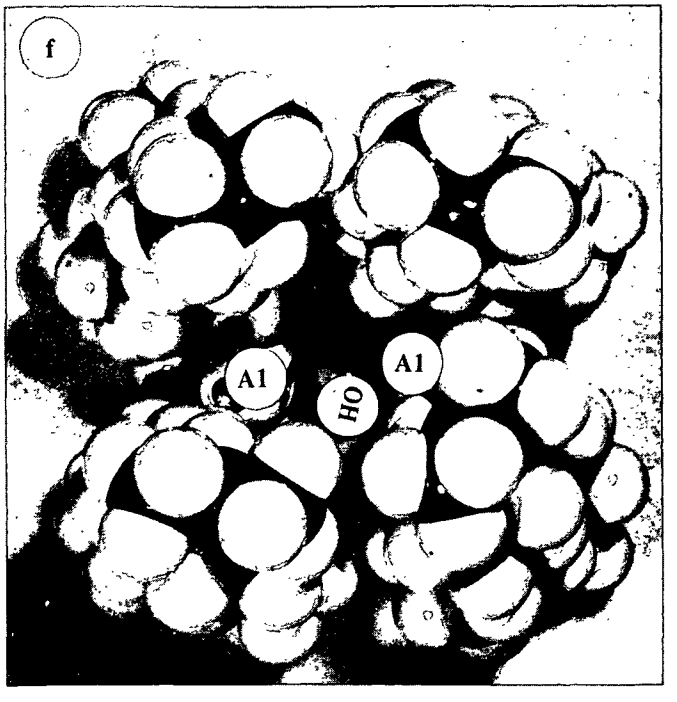

Figure 15 (Continued). Photographs of Molecular Models of Tetrahydroabietic Acid, Aluminum Tritetrahydroabietate, and Aluminum Monobasic Ditetrahydroabietate. (e) Aluminum Monobasic Ditetrahydroabietate (Side View); (f) Hypothetical Dimerized Aluminum Monobasic Tetrahydroabietates (Top View)

Figure 15(d) shows a possible structure of the triresinate in the collapsed monolayer. In contrast to the structure in the monolayer shown in Fig. 15(c), the intramolecular interaction between hydrocarbon chains appears to be impracticable. Thus, it is conceivable that when the triresinate has the collapsed structure as shown in Fig. 15(d), the complex structure is liable to a hydrolytic decomposition.

The side view of a model of monobasic ditetrahydroabietate in the monolayer is shown in Fig. 15(e) and the side view of a hypothetical model of the dimerized diresinate is also shown in Fig. 15(f). It can be seen in Fig. 15(f) that two aluminums of two diresinates appear to be linked through a hydroxyl bridge, which is termed "olation" (68). Unlike the collapsed structure of the triresinate, the diresinate can have the intramolecular interactions even in the collapsed monolayer, which may prevent a further hydrolytic decomposition.

STABILITY OF ALUMINUM TRIRESINATE

On the basis of the molecular models shown in Fig. 15(c,d), apparently the triresinate structure in the collapsed monolayers has weaker stability than the structure in the uncollapsed monolayer. This may account for the difference in the observed value of $\underline{X}_{TABSH}$ between Major's result (11) and the present work. The $\underline{X}_{TABSH}$ value obtained by Major was 0.52 for the monolayer reacted on the substrate with: $[Al] = 3.16 \times 10^{-3}\underline{M}$, $[SO_4] = 1.5 \times 3.16 \times 10^{-3}\underline{M}$ $[=Al_2(SO_4)_3]$, and pH 4.0, while the value obtained in this study is 0.12. This difference may be caused by hydrolytic decomposition of the collapsed triresinate monolayer samples (skimmed, crumpled ones) during the washing and drying stages which Major (11) employed for the composition analysis of the monolayer.

Leger, et al. (45) found by the IR spectroscopic technique that the aluminum trisoap formed initially in the bulk reaction was decomposed into monobasic diresinate and free acid in the presence of traces of water in the reaction medium.

The weak stability of the triresinate (trisoap) formed in the bulk reaction or in the collapsed monolayer may be able to account for the failure in detecting or isolating the triresinate by Major (11), Ekwall and Bruun (37), and Frieberg and Bruun (38) who analyzed the chemical composition of size precipitate formed at pH 4.0. However, most previous workers such as Davison (25), Price (32), Back and Steenberg (21), and Guide (8) analyzed the size precipitate formed at a pH above 4.3 (not at pH 4.0).

ARGUMENTS AGAINST FORMATION OF DIBASIC MONORESINATE AT pH 4-5

One might speculate the formation of dibasic monoresinate in the reaction of TABSH monolayer instead of tri- and diresinates (37,38,109,110). On the contrary, the formation is not likely because of the obtained experimental evidence and some theoretical reasons.

All the MIR spectra obtained for the TABSH monolayers reacted with aluminum ions at the pH range of 4.0 to 5.0 did not show bonded OH absorption near 3 μm (3340 cm^{-1}), as Harple, et al. (42) found with their aluminum monosoap. The absence of the absorption band of the bonded hydroxyl group is believed to be sufficient evidence for ruling out the existence of the dibasic monoresinate in the monolayers reacted at the pH range under investigation. From a theoretical point of view, the formation of monoresinate by the reaction of TABSH monolayers with aluminum ions is not likely to occur because of lack of sufficient $Al(OH)_2^{+1}$ ions in aqueous aluminum salt solutions with pH 4.0-5.0 (61-85). Most predominant aluminum ions in the pH range of 4.0 to 5.0 are trivalently charged Al ions (Al^{+3}) and divalently charged Al ions [$Al(OH)_1^{+2}$).

In the presence of sulfate ions in the substrate solutions, the $AlSO_4^+$ ion is a predominant species as will be discussed later. However, this monovalent ion did not appear to be capable of reacting with the resin acid monolayer forming a sulfato aluminum resinate complex (i.e., $RCOO-AlSO_4$) because none of the obtained spectra of the reacted monolayers showed any S-O absorption band of the sulfato ligand.

Considering the cation-exchange reaction mechanism (115), the most probable reaction products in the reaction between TABSH monolayers and aluminum ions would be aluminum triresinate and diresinate. Nazarov and his coworkers (57) studied the mechanism of the sorption of metal ions on carboxylic acid cation-exchange resins. They established by many studies (53-57) that the number of carboxyl groups reacting with a metal ion is equal to the charge of the metal ion in the formation of a metal complex at the interface of the exchange resins.

In the literature review, Ekwall and Bruun (37) and Frieberg and Bruun (38) in Scandinavia appear to be the only group who maintain that the dibasic monoresinate is the major salt formed at pH 4.0-5.0. The evidence for the existence of the monoresinate presented by them is the ratio of the Al to the carbon content, indicating the existence of dibasic monoresinate in their collapsed monolayer samples.

However, their collected monolayer samples used for the chemical analysis are not believed to be composed of all of the salt molecules, which they believed from their π-A isotherm measurements. The IR spectra for their monolayer samples revealed the presence of a considerable fraction of free acid molecules in the reacted monolayer, as shown in one of their papers (38). Nevertheless, they claim that the observed absorption band at 1700 cm^{-1} is not due to the presence of free acid, but to ionized carboxyl groups with a disturbed electron symmetry.

This interpretation of the spectrum implies that the absorption band at 1700 cm^{-1} cannot disappear even when all the free acid molecules in the monolayer react with aluminum ions. On the contrary, it is found in this study that, when the monolayer completes the reaction with aluminum ions, the absorption band at 1700 cm^{-1} disappears in the MIR spectrum as shown in Fig. 2, 7, and 11.

The MIR spectrum obtained in this experiment for the monolayer sample reacted under the conditions similar to Ekwall and coworkers ([Al] = 1.0×10^{-3}M, pH 4.0, as shown in Appendix VI) revealed the presence of a considerable fraction of free acid in the reacted monolayer, i.e., approximately 30%.

Therefore, the reported values of the [Al]/[C] ratio may be meaningless for the evidence of the formation of monodiresinate unless a correction is made for the fraction of free acid in their (37,38) aluminum resinate monolayer samples formed at pH 4.0-5.0.

The possibility of the formation of monoresinate at a pH above 5.0, however, cannot be ruled out because at a pH above 5.0 the monovalent Al ion [$Al(OH)_2^{+1}$] may become the predominant ion species instead of $Al(OH)^{+2}$ ion (8,64,67). Nazarenko and Nevskaya (67) determined spectrophotometrically the formation constant of $Al(OH)_2^{+1}$ ions and suggested that the $Al(OH)_2^{+1}$ ion becomes a more predominant species than $Al(OH)_1^{+2}$ ions as the pH is increased above 5.5.

INTERPRETATION OF THE INHIBITING ACTION OF SULFATE ON THE MONOLAYER REACTION AT pH 4.0

It is now a well-established fact (75-78) that the unhydrolyzed aluminum ion, i.e., $Al^{+3}(6H_2O)$, forms the sulfato complex with the sulfate ion, $AlSO_4^{+}(4H_2O)$, in acidic solutions containing both aluminum and sulfate ions. It is also known (61-67) that about 10% of uncomplexed Al ions (but hydrated) exist in the form of

hydrolyzed ions, i.e., $Al(OH)^{+2}(5H_2O)$ in the aluminum salt solution free of sulfate ions at pH 4.0. Therefore, in the evaluation of the sulfate effect on the reaction between TABSH monolayers and aluminum ions, at least four Al ion species will have to be considered, i.e., Al^{+3}, $AlSO_4^{+1}$, $Al(OH)^{+2}$, the dimer of $Al(OH)^{+2}$ (62,71). The water of hydration is neglected in this discussion.

According to the mechanism of cation-exchange reactions (57), it is reasonable to assume that the unhydrolyzed, Al^{+3} ions will react with TABSH monolayers and form aluminum triresinate at pH 4.0.

The observed inhibiting action of excess sulfate in the formation of the aluminum resinate should be due to the removal of the Al^{+3} ion by sulfate ions from the interface reaction. The Al^{+3} ion should complex with sulfate forming $AlSO_4^+$ in the substrate solution in preference to the formation of aluminum triresinate at the interface.

To prove this assumption, it is necessary to know the concentrations of all ionic species for the substrate conditions of the monolayer reaction experiments, in which the sulfate concentration was varied at pH 4.0. In the freshly prepared acidic solution containing aluminum and sulfate ions, the following coupled equilibria of complex formations are believed to occur (75):

$$\begin{array}{ccccc} & & HSO_4 & & \\ & & \downarrow\uparrow\ K_3 & & \\ H_2O & & H^+ & & \\ + & & + & & \\ Al^{+3} & + & SO_4^{-2} & \overset{K_2}{\rightleftharpoons} & AlSO_4^{+1} \\ \downarrow\uparrow\ K_1 & & & & \\ Al(OH)^{+2} & & \overset{K_4}{\rightleftharpoons} & & Al_2(OH)_2^{+4} \end{array}$$

The computations were carried out using the following set of equations according to Stryker and Matijevic (76)

$$A\,[AlSO_4^+]^3 + B\,[AlSO_4^+]^2 + C\,[AlSO_4^+] + D = 0 \qquad (36)$$

in which

$$A = -K_2^2 \qquad (37)$$

$$B = ([Al] + 2[SO_4])K_2^2 + (1+K_1/[H])(1+K_3[H])K_2 - (1+K_3[H])(K_1^2K_4/[H]^2) \qquad (38)$$

$$C = (-2[SO_4][Al]\,K_2^2) - (1+K_1/[H])(1+K_3[H])[SO_4]\,K_2 \qquad (39)$$

$$D = [Al][SO_4]^2 \cdot K_2^2 \qquad (40)$$

$[SO_4]$, $[Al]$ and $[H^+]$ designate the total content of the system in sulfate, aluminum, and hydrogen ions, respectively, expressed in moles per liter

$$K_1 = [Al(OH)^{+2}][H]/[Al] = 10^{-5.02} \quad (64)$$

$$K_2 = [AlSO_4^+]/[Al][SO_4] = 370 \quad (76)$$

$$K_3 = [HSO_4^+]/[SO_4][H] = 97 \quad (76)$$

$$K_4 = [Al_2(OH)_2^{+4}]/[Al(OH)^{+2}]^2 \div 6000 \quad (71).$$

A computer program (see Appendix VII) was written to solve the above coupled equilibrium equations simultaneously for the equilibrium concentrations and the percentage of each Al ion species in the aluminum nitrate plus potassium sulfate solutions under investigation. The results of this calculation are given in Table VII which shows changes in the concentration of $AlSO_4^+$, Al^{+3}, $Al(OH)^{+2}$, and $Al_2(OH)_2^{+4}$ ion as the sulfate concentration is increased from 4.73×10^{-3}M to 0.45M at pH 4.0. In Fig. 16 the changes in the fraction of individual ion species, i.e., Al^{+3}, $Al(OH)^{+2}$, and $Al(SO_4)^{+1}$, with an increase in the $[SO_4]$ are illustrated with changes in the free acid mole fraction in the monolayer.

TABLE VII

CHANGES IN EQUILIBRUIM CONCENTRATION OF ALUMINUM COMPLEX IONS AS $[SO_4]$ IS INCREASED IN ALUMINUM NITRATE PLUS POTASSIUM SULFATE SOLUTION WITH pH 4.0

$[SO_{4\ tot}]$	pH	$[AlSO_4^{+1}]$	$[Al^{+3}]$	$[Al(OH)^{+2}]$	$[Al_2(OH)_2^{+4}]$	X_{TABSH}
4.73×10^{-3}M [= $Al_2(SO_4)_3$]	4.005	1.614×10^{-3} (51.09%)	1.409×10^{-3} (44.06%)	1.362×10^{-4} (4.309%)	1.309×10^{-9} (0.000%)	0.04
1.25×10^{-2}M	4.001	2.436×10^{-3} (77.09%)	6.606×10^{-4} (20.905%)	6.323×10^{-5} (2.001%)	2.694×10^{-9} (0.000%)	0.15
2.50×10^{-2}M	3.990	2.786×10^{-3} (88.16%)	3.423×10^{-4} (10.832%)	3.194×10^{-5} (1.011%)	2.692×10^{-9} (0.000%)	0.23
5.0×10^{-2}M	4.001	2.971×10^{-3} (94.022%)	1.724×10^{-4} (5.456%)	1.650×10^{-5} (0.522%)	4.613×10^{-9} (0.000%)	0.34
1.0×10^{-1}M	4.010	3.065×10^{-3} (97.003%)	8.628×10^{-5} (2.730%)	8.431×10^{-6} (0.267%)	1.219×10^{-9} (0.000%)	0.71
2.0×10^{-1}M	4.005	3.113×10^{-3} (98.503%)	4.313×10^{-5} (1.365%)	4.167×10^{-6} (0.132%)	1.411×10^{-9} (0.000%)	0.85
3.0×10^{-1}M	4.001	3.128×10^{-3} (99.003%)	2.876×10^{-5} (0.910%)	2.753×10^{-6} (0.087%)	1.75×10^{-9} (0.000%)	0.88
4.0×10^{-1}M	4.015	3.136×10^{-3} (99.25%)	2.156×10^{-5} (0.682%)	2.131×10^{-6} (0.067%)	1.511×10^{-9} (0.000%)	0.91
4.5×10^{-1}M	3.955	3.139×10^{-3} (99.34%)	1.919×10^{-5} (0.607%)	1.652×10^{-6} (0.052%)	1.265×10^{-9} (0.000%)	0.97

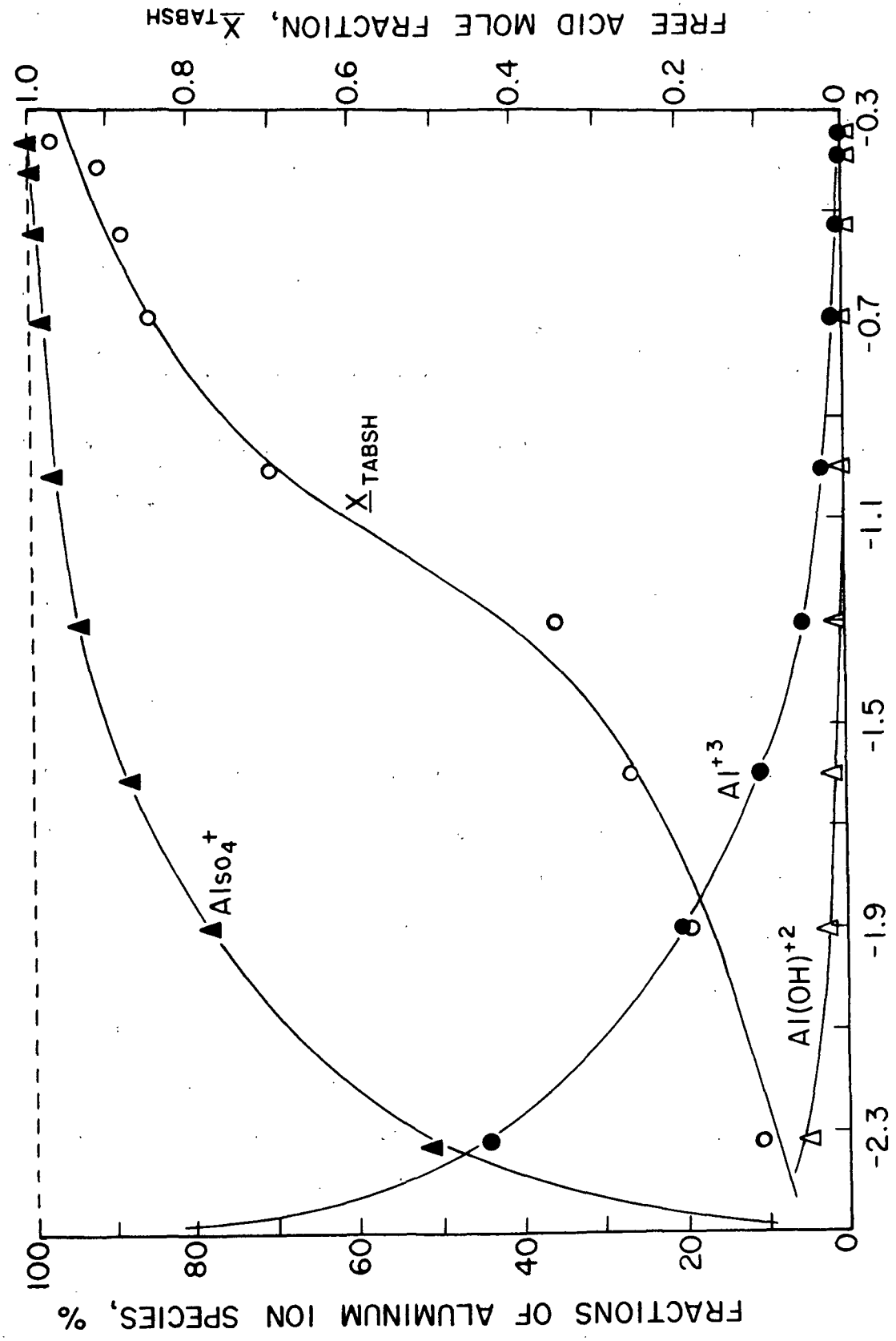

Figure 16. Changes in Concentrations (% Fraction) of Aluminum Ion Species in Aluminum Nitrate plus Potassium Sulfate Substrate Solutions as a Function of Sulfate Concentration at pH 4.0. Also Included are the Changes in $\underline{X}_{TABSH}$ of the Monolayers Spread on These Substrates

If the formation of $AlSO_4^+$ is responsible for the decrease in the concentration of unhydrolyzed Al^{+3} ion reacting with the monolayer in the substrate, the concentration of Al^{+3} ion should be decreased with increasing free acid fraction in the monolayer spread on the substrate as the addition of K_2SO_4 is increased. As shown in Table VII and Fig. 16, the amount of Al^{+3} ion is decreased corresponding to the increase in the $[AlSO_4]$ upon raising the $[SO_4]$ at pH 4.0. The result shows rather convincingly that at pH 4.0 the unhydrolyzed Al ion acts as the major reactive cation species in the formation of the triresinate salt in the monolayer.

The decrease in the resin acid salt formation by the addition of excess sulfate in the substrate is due to the complexing of the Al^{+3} ion to form $AlSO_4^+$ in preference to the salt formation. Therefore, the role of sulfate ion in the reaction between TABSH monolayers and aluminum ions at pH 4.0 is the removal of reactive ionic species such as Al^{+3} ion from the interface by forming the sulfato-complex.

It is also noteworthy that the concentration of $AlSO_4^+$ appears to be high ($\sim$ 50%) at the lowest addition of sulfate (equivalent to the $[SO_4]$ in alum). The amount of $AlSO_4^+$ increases rapidly corresponding to the rapid decrease in the Al^{+3} concentration when the $[SO_4]$ is increased up to 0.1M. At high concentrations of sulfate above 0.1M, the increase in the $[AlSO_4^+]$ becomes gradual corresponding to the slow decrease in the residual amount of Al ion. It should be noted that essentially all of the Al ions initially existing in the substrate convert to the sulfato-complex at the $[SO_4]$ = 0.45M. At this substrate condition, apparently, the salt formation in the monolayer is completely prevented. This may indicate that the value of the formation constant of $AlSO_4^+$ (K_2 = 370) used in this calculation is a reasonably well-approximated constant for the substrate conditions under investigation.

INTERPRETATION OF THE DECREASE IN THE SULFATE INFLUENCE ON THE MONOLAYER REACTION AT pH ABOVE 4.0

As shown in Fig. 7 and 8 and Table IV, the inhibiting action of sulfate decreases rapidly as the pH of the substrate is increased from 4.0 to 4.5. To understand this behavior of sulfate, the concentrations of all the Al ion species existing in the aluminum nitrate plus potassium sulfate (0.2M) substrate solution with varied pH were calculated in the same manner as described before. Table VIII represents the result of the calculation for the pH change at $[SO_4] = 0.2M$.

At the high concentration of sulfate most of the Al ions exist as the sulfato-complex, but upon raising the solution pH, the concentration of the hydrolyzed Al ion, i.e., $Al(OH)^{+2}$, increases. Although the increased concentration of the $Al(OH)^{+2}$ is not higher than the residual concentration of Al^{+3} ion, the increase in the salt formation in the presence of excess sulfate with an increase in the pH may be attributed primarily to the increase in the reaction of the monolayer with $Al(OH)^{+2}$ ions, instead of the reaction with Al^{+3} ions. The continuous salt formation in the presence of excess sulfate indicates that the reaction between TABSH monolayers and $Al(OH)^{+2}$ ions is not influenced by sulfate, unlike the monolayer reaction with Al^{+3} ions. This is partly due to the possibility that $Al(OH)^{+2}$ ions cannot form a stable $Al(OH)SO_4$ complex with sulfate in preference to the formation of monobasic diresinate, as compared to the formation of $AlSO_4^{+1}$ at pH 4.0.

The formation of monobasic diresinate without being influenced by sulfate ion suggests that the stability constant of the diresinate complex is higher than that of the triresinate. Thus, the abrupt diminishing of the sulfate effect in the somewhat narrow pH range can be attributed partly to the high stability of the monobasic diresinate in the presence of sulfate.

TABLE VIII

CHANGES IN EQUILIBRIUM CONCENTRATION OF ALUMINUM COMPLEX IONS AS pH IS INCREASED IN ALUMINUM NITRATE SOLUTIONS[a] CONTAINING 0.2M POTASSIUM SULFATE

pH	$[AlSO_4^{+1}]$	$[Al^{+3}]$	$[AlOH^{+2}]$	$[Al_2(OH)_2^{+4}]$	X_{TABSH}	X_{TAB-AL}
3.685	3.114×10^{-3}M (98.56%)	4.361×10^{-5} (1.38%)	2.016×10^{-6} (0.064%)	1.709×10^{-10} (0.000%)	0.93	0.07
3.985	3.113×10^{-3}M (98.503%)	4.316×10^{-5} (1.366%)	3.982×10^{-6} (0.126%)	1.454×10^{-9} (0.000%)	0.88	0.12
4.005	3.113×10^{-3}M (98.503%)	4.314×10^{-5} (1.365%)	4.168×10^{-6} (0.132%)	-- (0.000%)	0.85	0.15
4.108	3.112×10^{-3}M (98.471%)	4.304×10^{-5} (1.362%)	5.271×10^{-6} (0.167%)	8.149×10^{-10} (0.000%)	0.68	0.32
4.214	3.110×10^{-3}M (98.428%)	4.295×10^{-5} (1.359%)	6.714×10^{-6} (0.212%)	1.409×10^{-10} (0.000%)	0.37	0.63
4.325	3.108×10^{-3}M (98.370%)	4.287×10^{-5} (1.357%)	8.652×10^{-6} (0.274%)	1.164×10^{-10} (0.000%)	0.16	0.84
4.510	3.104×10^{-3}M (98.230%)	4.274×10^{-5} (1.352%)	1.321×10^{-5} (0.418%)	1.139×10^{-9} (0.000%)	0.044	0.956
4.630	3.099×10^{-3}M (98.101%)	4.265×10^{-5} (1.350%)	1.737×10^{-5} (0.550%)	1.012×10^{-10} (0.000%)	0	1.0

[a] $[Al^{+3}] = 3.16 \times 10^{-3}$M.

POSSIBLE EFFECT OF ADSORPTION HYDROLYZED Al IONS ON THE MONOLAYER REACTION

When the excess sulfate (0.2M) is added to the aluminum nitrate solution at pH > 4.0, most of Al^{+3} ions are removed in the form of $AlSO_4^+$, but $Al(OH)^{+2}$ ions remain without complexing with sulfate and increase in concentration with increasing pH, as shown in the calculation of the coupled equilibria which is assumed to be valid (see Table VIII). However, as given in the table, there is little change in the Al^{+3} concentration and the increase in the concentration of $Al(OH)^{+2}$ ion upon increasing the pH from 4.0 to 4.5 appears to be small compared to the large increase of the resinate salt fraction in the monolayer. Accordingly, it is difficult to believe that this small increase can account for the abrupt increase in the salt formation at the interface even though the stability constant of the monobasic diresinate is high compared to that of the triresinate. Besides the salt formation equilibria it is possible that there is an adsorption equilibrium of hydrolyzed Al ions from the bulk solution onto the spread monolayer.

For monolayer reactions at liquid interfaces, it is generally believed (58, 59,119) that the concentration of a reacting ion species at the interface is higher than its bulk concentration, even at equilibrium, when the species is preferentially adsorbed by the monolayer and the adsorbed ion forms an insoluble complex with the monolayer molecules like aluminum resinate complex.

It will be shown below that in the monolayer reaction between TABSH monolayers and aluminum ions, hydrolyzed Al ions appear to be preferentially adsorbed by the monolayers during the progress of the salt formation in the monolayer. The surface concentration of unhydrolyzed Al ions may not be significantly different from its bulk concentration due to lower adsorbability of Al^{+3} ions onto the monolayers than that of $Al(OH)^{+2}$ ions (80-85). Consequently, the preferential

adsorption of $Al(OH)^{+2}$ ion at the interface may account for the rapid increase in the monobasic diresinate formation with rising pH even though the increase in the bulk concentration of $Al(OH)^{+2}$ ion appears to be somewhat small.

The high adsorbability of hydrolyzed Al ions on lyophobic surfaces is a well-known phenomenon in the colloid chemistry of coagulation of lyophobic colloidal particles by aluminum ions. Matijevic (80,81) and Stumm (82-85) and their co-workers have established without any doubt that replacing at least one coordinated water molecule of a hydrated metal, e.g., $Al^{+3}(6H_2O)$, by a hydroxyl ion dramatically enhances the adsorbability of this ion on lyophobic surfaces of various chemical compositions. Since the insoluble, nonionized TABSH monolayer spread on the aluminum nitrate substrate is a lyophobic surface, the adsorption of hydrolyzed Al ions by the monolayer becomes probable when the concentration of the hydrolyzed ion is increased by increasing the pH of the substrate solution.

In fact, direct evidence for the adsorption of hydrolyzed Al ions by the spread monolayer was found by determinations of the changes in the π-A isotherm caused by interfacial aging of the compressed monolayers. After the initial π-A isotherms of the spread monolayers were determined, the expanded monolayers were recompressed to π = 18 dynes/cm^{-1} and aged on the substrate solutions for approximately 18 minutes. The final π-A isotherms of the monolayers were determined from the compressing surface pressure, and the compressed monolayers were re-expanded to the zero surface pressure. Figure 17 shows five pairs of π-A isotherms of five sets of experiments. The top three pairs of isotherms in the figure are for the monolayers spread on aluminum nitrate substrates free of sulfate at pH 4.0, 4.4, and 4.95, respectively, (the [Al] = 3.16×10^{-3}M for pH < 4.5 and = 3.16×10^{-4}M for pH > 4.5). The bottom two pairs are for the monolayers spread on the substrates containing excess sulfate at pH 4.45 and 4.9, respectively. For each pair of π-A curved the right side isotherm is

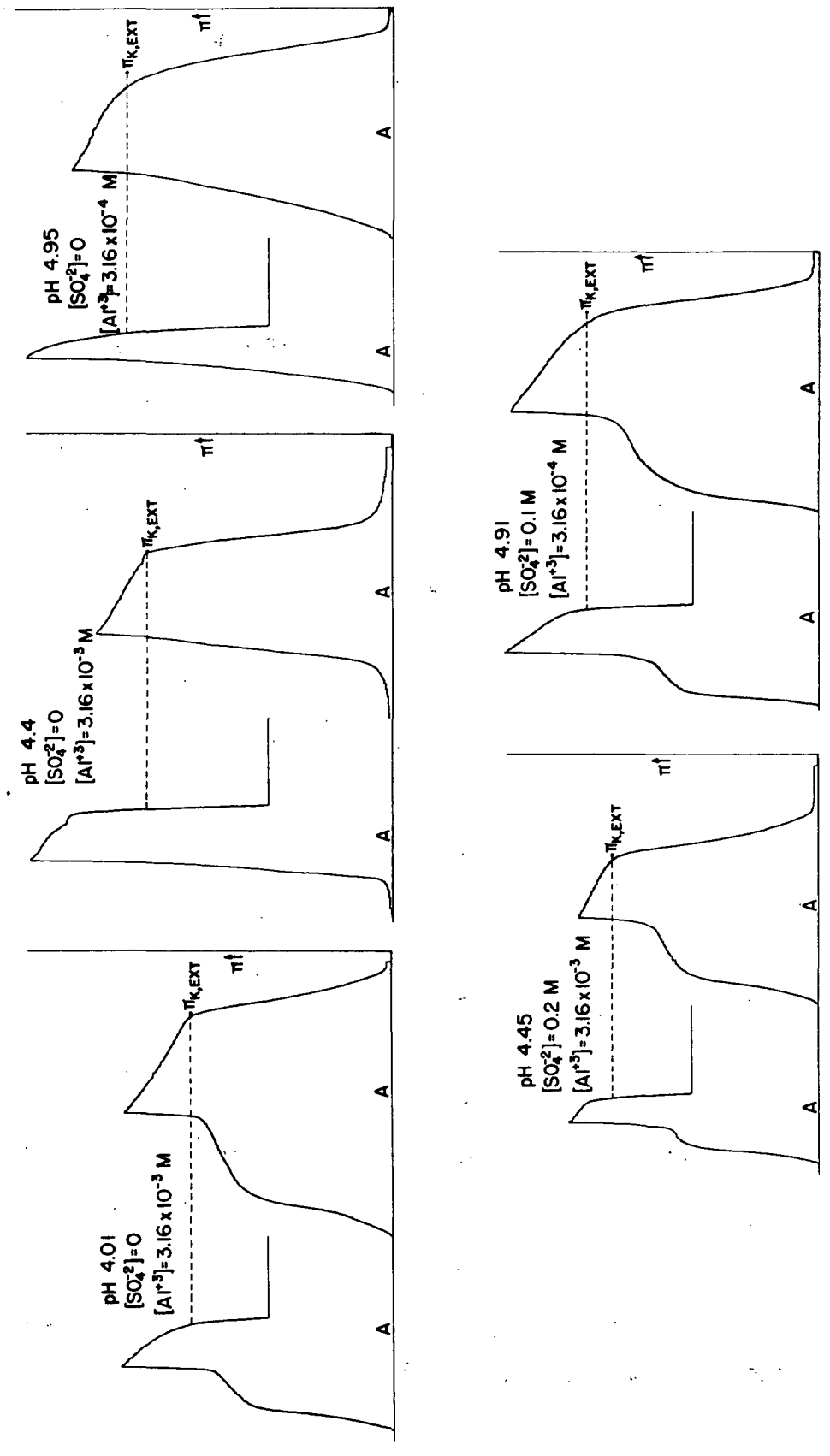

Figure 17. Changes in π-A Isotherms of TABSH Monolayers Spread on Aluminum Nitrate Substrates with Sulfate and Without Sulfate After Interfacial Aging at Different pH (the [OH]/[Al] = 0.03 for pH 4.01; 0.64 for pH 4.4; 2.2 for pH 4.95 when the $[SO_4]$ = 0, and [OH] = 0 when $[SO_4] \geq 1.0M$)

the initial π-A isotherm and the left isotherm is the final isotherm of the compressed monolayer after the aging.

For the monolayer on the substrate free of sulfate at pH 4.0, the $\pi_{K,EX}$ value does not appear to be increased significantly after the interfacial aging (the top left side isotherm). However, for the monolayers spread at pH 4.4 and 4.95 in the absence of sulfate, the $\pi_{K,EX}$ values are increased significantly after the aging as shown in the top middle and right side isotherms.

It should be noted that the π-A isotherms of the expanding stage for the monolayers at pH 4.4 and 4.95 are quite different from the expanding isotherm of the monolayer at pH 4.0. The monolayers at pH 4.4 and 4.95 appear to be solid-like films in which no molecular rearrangement occurs during the expanding stage.

The increase in the $\pi_{K,EX}$ value caused by the interfacial aging at the raised pH may be due to excess adsorption of hydrolyzed Al ions because the aluminum nitrate solutions free of sulfate contain higher concentrations of the hydrolyzed ion than required for salt formation in the monolayer. The hydrolyzed ions (monomeric or polymeric) appear to be preferentially adsorbed by the aluminum resinate monolayer when the monolayer is aged on the substrate containing large amounts of hydrolyzed Al ions (the [OH]/[Al] = 0.64 for pH 4.4; ca. 2.0 for pH 4.9).

The adsorption of hydrolyzed Al ions by the monolayer was also shown in the MIR spectra for the monolayer samples spread on the aluminum nitrate substrates. As shown in Fig. 11 and 12, the monolayer samples spread on the substrate containing hydrolyzed Al ion in the absence of sulfate, always showed the broad absorption band near 3500 cm^{-1} ranging from 3800 to 3300 cm^{-1} in their MIR spectra. This absorption band whose intensity appeared to be increased upon raising the pH may be due to hydrolyzed Al ions adsorbed beneath the monolayer which were spread on the substrate containing OH ions (the [OH]/[Al] < 1.0).

Therefore, the changes in π-A isotherms of aged monolayers and MIR spectra of the reacted monolayer samples indicate that hydrolyzed ions appear to be adsorbed by the spread monolayer during the progress of the interfacial reaction of the resinate formation.

However, it is not clear in these experiments which hydrolyzed ion species is predominantly adsorbed among $Al(OH)^{+2}$, $Al(OH)_3$ and other polymerized complex ions.

Since the freshly prepared aluminum nitrate solutions used in these experiments showed no visible precipitation, the most likely absorbed species which is responsible for the salt formation is believed to be the $Al(OH)^{+2}$ ion; this species is the most predominant hydrolyzed ion existing in the substrate solutions with pH 4.0-5.0 (67). However, there is no denying that supersaturated precipitated aluminum hydroxide can be adsorbed with $Al(OH)^{+2}$ ion as discussed previously in the result of identification of the broad absorption band for the multilayer cast on the Ge plate. The polymeric hydrolyzed Al ions are not believed to be responsible for the salt formation in the monolayer reaction at pH > 4.5, even if these polymeric ions are formed and absorbed on the spread monolayer, because no bonded OH absorption band appeared in the obtained MIR spectra for all the reacted monolayer samples as discussed before.

The possibility that the adsorption of hydrolyzed ions plays an important role in the rosin-alum sizing system was indicated in the results of previous workers. Guide (8) reported that nonstoichiometric results of his analysis of sodium aluminate-abietate size precipitate was partly due to the coprecipitation of $Al(OH)_3$. The coprecipitated $Al(OH)_3$ in the size precipitate may be the hydrolyzed Al ions adsorbed on the surfaces of size precipitate particles.

Ekwall and Bruun (37,110) found from the surface chemical study that the aluminum ion concentration required for the aluminum resinate monolayers decreased rapidly as the pH of the substrate was increased.

The adsorption of hydrolyzed Al ion may account for the decrease in the aluminum concentration. The positive charge of the size precipitate observed by Guide (8) and Thode (7,35) and many others (9,24,36) may be due to the preferential adsorption of positively charged hydrolyzed Al ions on the surface of the size precipitate.

THE EFFECT OF SULFATE ON THE ADSORPTION OF HYDROLYZED Al IONS

As shown with the two bottom isotherms in Fig. 17, addition of excess sulfate in the substrate solution with pH > 4.4 does not cause the significant increase in $\pi_{\underline{K},\underline{EX}}$ value after the aging. The expanding π-$\underline{A}$ isotherms of the monolayers do not lose the characteristics of the monolayer on which hydrolyzed Al ions are not adsorbed, as shown in the isotherms for the monolayer spread at 4.0 in the absence of sulfate. The $\pi_{\underline{K},\underline{EX}}$ values for the monolayers spread at pH > 4.4, however, are decreased by the addition of sulfate even though the compositions of the monolayers are not changed significantly.

The strong intensity of the broad absorption band near 3500 cm^{-1} in the MIR spectra was diminished by the addition of sulfate as shown in Fig. 13.

Those results indicate that the increase in sulfate concentration in the aluminum nitrate substrate appears to prevent the spread monolayer from adsorbing hydrolyzed Al ions excessively. It is possibly due to removal of part of hydrolyzed Al ions by converting them into $AlSO_4^+$ complexes through the reversion to unhydrolyzed Al ions according to the coupled equilibria occurring in the substrate solution which was discussed previously.

FORMATION CONSTANTS OF ALUMINUM TRIRESINATE AND MONOBASIC DIRESINATE

To support the evidence for the formation of aluminum triresinate and basic diresinate in the monolayer reaction, equilibrium formation constants of the diresinate and triresinate are calculated from the known values of the concentration of each complex aluminum ion in the substrate given in Tables VII and VIII and the value of $\underline{X}_{TABSH}$ in the monolayer spread on the substrate under investigation.

As discussed previously, at the interface between the spread TABSH monolayer and aluminum ions, two equilibrium reactions of the triresinate formation and of the diresinate formation are believed to occur simultaneously under the assumption that the reaction forming the complex aluminum ions in the substrate has already reached an equilibrium state before the monolayer is spread on the substrate:

$$3R\text{-}COOH + Al^{+3}(6H_2O) \xrightleftharpoons{K_T} \underset{\text{Triresinate}}{Al(OOCR)_3} + 3H^+$$

$$K_T = K_{AlR_3} = [Al(OOCR)_3][H^+]^3/[Al^{+3}][RCOOH]^3 \qquad (42)$$

$$2R\text{-}COOH + Al(OH)^{+2} \xrightleftharpoons{K_D} \underset{\text{Diresinate}}{Al(OH)(OOCR)_2} + 2H^+$$

$$K_D = K_{Al(OH)R_2} = [Al(OOCR)_2][H^+]^2/[AlOH^{+2}][RCOOH]^2 \qquad (43)$$

$$\underline{X}_{TABSH} + 2\underline{X}_{Al(OH)R_2} + 3\underline{X}_{AlR_3} = 1 \qquad (44)$$

where $\underline{K_T}$ and $\underline{K_D}$ are the formation constants of aluminum tritetrahydroabietate and monobasic ditetrahydroabietate, respectively, in the monolayer reaction.

By the process of iteration, with the known values of the $\underline{X}_{TABSH}$, $[Al^{+3}]$, $[Al(OH)_2{}^{+2}]$ and pH, the approximated constant values of $\underline{K_T}$ and $\underline{K_D}$ can be estimated at 1.2×10^{-9}; 1.5×10^{-4}, respectively, for the monolayer reaction at the $[SO_4]$ = 0.1-0.4M, pH 3.685-4.108.

From the estimated values of K_D and K_T, the mole fraction of triresinate and of diresinate can be calculated to examine the consistency of the K_T and K_D values for the reaction conditions of the $[SO_4]$ and pH. The results of the computation are summarized in Table IX.

TABLE IX

CALCULATION[a] OF MOLE FRACTIONS OF ALUMINUM TRIRESINATE AND DIRESINATE IN THE TABSH MONOLAYERS WHICH WERE REACTED WITH ALUMINUM IONS IN THE PRESENCE OF EXCESS SULFATE

			Calculated			Obtained
$[SO_4]$, M	pH	X_{TABSH}	X_{AlR_3}[b]	$X_{Al(OH)R_2}$[c]	$1 - X_{TABSH}$ $[=3X_{AlR_3}+2X_{Al(OH)R_2}]$	$1 - X_{TABSH}$ $(=X_{TABS^-})$[d]
0.2	4.005	0.85	0.0318	0.045	0.186	0.15
0.2	3.985	0.88	0.0318	0.044	0.183	0.12
0.2	3.685	0.93	0.0048	0.006	0.026	0.07
0.2	4.108	0.68	0.034	0.066	0.232	0.32
0.1	4.010	0.73	0.041	0.067	0.255	0.27
0.3	4.001	0.88	0.024	0.032	0.136	0.12
0.4	4.015	0.91	0.022	0.029	0.124	0.09
0.2	4.214	0.37	0.011	0.037	0.107	0.63
0.05	4.001	0.34	0.009	0.03	0.086	0.65

[a] Calculated the mole fraction of X_{AlR_3} and $X_{Al(OH)R_2}$ by solving three equations, (42), (43), (44), simultaneously using the estimated values of K_{AlR_3} and $K_{Al(OH)R_2}$, i.e., 1.2×10^{-9} and 1.5×10^{-4}, respectively.

[b] X_{AlR_3}, the mole fraction of aluminum triresinate.

[c] $X_{Al(OH)R_2}$, the mole fraction of aluminum monobasic diresinate.

[d] Calculated from Equations (33), (34), and (35).

At the $[SO_4]$ = 0.1M to 0.4M at pH 3.185 to 4.108, the calculated values of the salt fraction appeared to be close to the obtained values considering possible experimental error in determining the values of X_{TABSH}. However, at the

$[SO_4] < 0.1\underline{M}$, and pH > 4.108, the calculated values deviated to a great extent from the obtained values. The deviation with decreasing $[SO_4]$ may be due to the decrease in ionic strength, and deviation with increasing pH may be attributed to possible increase in the preferential adsorption of $Al(OH)^{+2}$ ion by the spread monolayer. The deviation appeared to increase when the fraction of hydrolyzed Al ions in the substrate solution was increased by raising pH (Table VIII) and lowering the $[SO_4]$ (Table VII). This suggests that the interfacial reaction between TABSH monolayers and unhydrolyzed and hydrolyzed Al ions may also involve an adsorption equilibrium of the ionic species from the solution to the spread monolayer in addition to the equilibria of the salt formations [Equations (42) and (43)]. The possible existence of the adsorption equilibrium was not taken into account in the above calculation, due to unavailability of its equilibrium constant.

It is interesting to note that the $\underline{K_D}$ value of diresinate is much higher than the value of triresinate when small amounts of Al^{+3} and $Al(OH)^{+2}$ ions are almost equally present in the substrates containing excess sulfate. The higher value of $\underline{K_D}$ may confirm the fact that the monobasic diresinate is a more stable complex than the triresinate and that the preferential adsorption of hydrolyzed $Al(OH)^{+2}$ may contribute a more favorable equilibrium condition to the diresinate formation as discussed before.

As shown in Table IX, the monolayers reacted at the high concentrations of sulfate appear to contain the diresinate molecules in an amount comparable to the triresinate. However, as the $[SO_4]$ increased further at pH 4.0, the mole fraction of diresinate appears to decrease with the residual fraction of triresinate. The decrease in the diresinate mole fraction may be attributed to the removal of $Al(OH)^{+2}$ ions existing in the substrate due to reversion of hydrolyzed ions to unhydrolyzed ions as discussed before.

CHANGES IN COMPONENTS OF FREE-SURFACE ENERGY FOR THE MONOLAYER

The measured contact angles of two pairs of liquids, water-methylene iodide, and methylene iodide-formamide, given in Tables III and VI were used to calculate total surface free energy and its components for the cast monolayers with the Owens-Wendt equation (24). The changes in surface energy components, i.e., dispersion force, and polar force component (fractional polarity), with increasing $[SO_4]$ in the substrate are illustrated in Tables X and XI. It is shown in Table X that as the $[SO_4]$ in the substrate with pH 4.0 is increased, the total free-surface energy, particularly its polar force component increases.

The increase in polar force component (fractional polarity) corresponds to the increase in the mole fraction of free acid in the monolayer. The origin of the polar force may be attributed to overturning of the free acid molecules when brought into contact with a polar liquid like water, as will be discussed later. In Table XI the changes in surface energy components by the addition of excess sulfate are compared at pHs of 4.0, 4.4 and 4.9. The addition of excess sulfate in the substrate does not increase polarity or the total free-surface energy for the monolayers reacted at pH > 4.4.

The observed increase in total free surface energy and its polarity of the monolayer gives a quantitative explanation for the possibility that in the actual papermaking process the sizing can be decreased upon building up sulfate ions in the white water when the pH of the white water is decreased to 4.0 or below as a result of continuous additions of alum or alum and sulfuric acid in the closed white water system.

The insensitivity of free-surface energy of the monolayer to the addition of sulfate at pH > 4.4 suggests that the excess sulfate in the white water will not

TABLE X

CHANGES IN COMPONENTS OF SURFACE FREE ENERGY FOR THE MONOLAYERS CAST ON CMC FILMS AS $[SO_4]$ IN ALUMINUM NITRATE SUBSTRATE SOLUTIONS[a] IS INCREASED

		Components of Surface Free Energy, ergs/cm^2[b]							
		Dispersion, r_s^d		Polar, r_s^p		Total, r_s		Fractional Polarity, p	
$[SO_4]$	pH	H_2O-CH_2I_2,	CH_2I_2-$HCONH_2$	H_2O-CH_2I_2,	CH_2I_2-$HCONH_2$	H_2O-CH_2I_2,	CH_2I_2-$HCONH_2$	H_2O-CH_2I_2,	CH_2I_2-$HCONH_2$
0	4.01	33.7	34.6	1.7	0.2	35.4	34.8	0.05	0.01
$3.16\times10^{-3}\times1.5$ ($=Al_2SO_4$)	4.025	33.2	33.4	1.7	1.1	34.9	34.5	0.05	0.03
1.25×10^{-2} M	4.010	33.2	32.5	2.7	5.3	35.9	37.8	0.08	0.14
5×10^{-2} M	4.001	33.3	32.4	2.4	5.9	35.7	38.3	0.07	0.15
1.0×10^{-1} M	4.017	31.4	32.8	14.1	5.4	45.5	38.2	0.31	0.14
2.0×10^{-1} M	3.970	31.1	32.8	18.3	6.5	49.3	39.2	0.37	0.16
3.0×10^{-1} M	3.965	(39.6	41.2)[c]	(24.7	12.9)	(64.3	54.0)	(0.38	0.24)
		30.4	31.1	23.2	16.6	53.6	47.7	0.43	0.35
4.5×10^{-1} M	3.970	(39.1	40.3)[c]	(27.2	16.7)	(66.3	57.0)	(0.41	0.29)
		30.9	31.6	31.6	24.8	62.5	56.3	0.51	0.44
Pure TABSH monolayer	4.0	38.3	39.2	23.7	16.7	62.0	55.9	0.38	0.30

[a] $[Al(NO_3)_3] = 3.16 \times 10^{-3}$.

[b] Calculated by Owens-Wendt solution with obtained contact angles of two pairs of liquids, water-methylene iodide, and methylene iodide-formamide.

[c] The cast monolayer was rinsed with triple-distilled water to remove contaminated potassium sulfate salt on the monolayer.

TABLE XI

COMPONENTS OF SURFACE FREE ENERGY FOR THE REACTED MONOLAYER TRANSFERRED FROM ALUMINUM NITRATE PLUS POTASSIUM SULFATE SUBSTRATES WITH DIFFERENT pH ONTO CMC FILMS

		Components of Surface Free Energy, ergs/cm^2							
		Dispersion, r_s^d		Polar, r_s^p		Total, r_s		Fractional Polarity, p	
$[SO_4]_T$	pH	H_2O-CH_2I_2,	CH_2I_2-$HCONH_2$	H_2O-CH_2I_2,	CH_2I_2-$HCONH_2$	H_2O-CH_2I_2,	CH_2I_2-$HCONH_2$	H_2O-CH_2I_2,	CH_2I_2-$HCONH_2$
0[a]	4.01	33.7	34.6	1.7	0.2	35.4	34.8	0.05	0.01
1.0×10^{-1}M	4.017	31.4	32.8	14.1	5.4	45.5	38.2	0.31	0.14
2.0×10^{-1}M	3.970	31.1	32.8	18.3	6.5	49.3	39.2	0.37	0.16
0[a]	4.4	32.4	32.9	1.3	0.4	33.6	33.2	0.04	0.01
0.2M	4.45	33.7	34.2	1.1	0.2	34.8	34.5	0.03	0.01
0[b]	4.95	33.0	33.7	0.7	0.0	33.7	33.7	0.02	0.00
0.1M	4.91	33.9	34.2	0.6	0.2	34.6	34.5	0.02	0.01

[a] $[Al(NO_3)_3] = 3.16 \times 10^{-3}$M.

[b] $[Al(NO_3)_3] = 3.16 \times 10^{-4}$M.

decrease the sizing as long as the pH of the white water is maintained above 4.4 in view of the surface chemistry of rosin sizing (12). However, if the excess sulfate in the white water adversely affects electrokinetic potentials of the size precipitate and fiber surfaces, as Guide (8) and Strazdins (9) pointed out, it could cause a decrease in the sizing due to poor retention of low free-surface energy materials such as aluminum resinate molecules on fiber surfaces. It may be also interesting to notice that the free-surface energy of aluminum resinate monolayer formed at pH 4.0 appears to be slightly higher than the surface energy of the aluminum resinate formed at pH > 4.4. This may indicate that aluminum monobasic diresinate is a more effective sizing species than the triresinate in the rosin-alum internal sizing process.

LOW CONTACT ANGLES ON PURE TABSH MONOLAYER

The observed contact angles of water on pure TABSH monolayers deposited on the CMC film appear to be lower than the reported contact angles on solid rosin surfaces. The low contact angles could be caused by three possible mechanisms:

(1) The overturning of a free acid molecule when brought into contact with water.

(2) The roughness effect. On rough surfaces each liquid will appear to wet the surface better. Thus, the observed contact angle on rough surfaces is lower than the true angle.

(3) The penetration of water into the molecular scale pores in the monolayer, or entrapment of water molecules when the monolayer is transferred onto the CMC film from the substrate surface.

To investigate why the contact angles of water on TABSH monolayers are so low, the same TABSH monolayer was deposited on different solid surfaces and the water

contact angles on the monolayers were measured and compared with the contact angles on solid rosin blocks. The results are summarized in Table XII.

TABLE XII

CONTACT ANGLES ON WOOD ROSIN SOLID BLOCK AND ON PURE TABSH MONOLAYER CAST ON VARIOUS SOLID SURFACES

Solid Surface	Initial Advancing Contact Angles	
	Water	CH_2I_2
WG rosin surface (smooth)	83.9 ± 0.9[a]	
WW rosin surface (uneven)	74.0 ± 3.9	
Monolayer on the untreated CMC film	41.5 ± 1.5	31.8 ± 1.3
Monolayer on the treated CMC film with $Al(NO_3)_3$ solution	85.5 ± 2.4	
Monolayer on a silver film	86.0 ± 3.0	33.0 ± 3.0
Monolayer on a glass slide	20.8 ± 4.2	47.3 ± 2.4

[a] 95% Confidence limit.

The contact angles on solid rosin blocks and on the monolayer deposited on the silver film, whose surfaces appear as smooth as the surface of a mirror, were higher than the angles on the monolayer on the CMC film. At first this result could suggest that the low contact angles may be due to roughness of the CMC film cast on the glass slide.

However, when the CMC film was immersed in a solution of aluminum nitrate prior to deposition of the monolayer, the contact angles on the monolayer became as high as the angles on the reacted monolayer. Apparently, high contact angles observed with the aluminum ion-treated CMC film cannot be accounted for with the roughness effect.

The lowest contact angles observed with unreactive solid surfaces such as a glass slide strongly suggests that the low contact angles are not due to roughness of the CMC film, but to the overturning of free acid molecules held on unreactive surfaces such as the CMC film and glass, when it is brought into contact with water.

The overturning mechanism can give a logical explanation for lowering the contact angles of water for pure TABSH monolayers on the CMC film. The roughness effect of the prepared CMC film is not believed to be solely responsible for lowering the contact angles of water, but it may decrease some of the observed contact angles to some degree which affects adversely the uniformity of the contact-angle measurement.

The surfaces of the CMC film used in this experiment did not appear as smooth as mirrorlike surfaces such as the surface of solid rosin melted against the glass surfaces, and as the surface of the silver-coated glass surface. The roughness of the CMC film may be caused by the presence of insoluble tiny bumps in the prepared solution of Na-CMC solutions as shown in Appendix V.

In addition to the overturning of free acid molecules and the surface roughness, the lowering of contact angles could be partly due to the contamination of the deposited TABSH monolayer with soluble CMC molecules if the cast CMC films were dissolved to some extent in water during the film casting and the monolayer deposition.

Another mechanism of lowering the contact angles, the penetration or entrapment of water molecules may not be responsible in this case. The penetration and entrapment of water molecules may be dependent upon the degree of packing of molecules in the cast monolayers. The same close-packed monolayer compressed at π = 18 dynes cm^{-1} was deposited on the different solid surfaces. However, the same monolayer was found to give different contact angles depending upon the solid surface on which the monolayer was deposited.

OVERTURNING OF FREE ACID MOLECULES

The observed low contact angles of water on pure TABSH monolayer cast on the CMC film and the increase in the polarity of free-surface energy for the monolayer of which the free acid mole fraction increases can be attributed chiefly to rapid overturning of free acid molecules when brought into contact with water, or polar liquids.

The observed high contact angles of water and no polarity of the surface energy for the aluminum resinate monolayer indicate that the aluminum resinate molecule was so strongly anchored on the CMC surface that probably the water drop does not "overturn" the carboxyl groups; rather, it only holds onto it longer when it does overturn.

The overturning of carboxylic acids such as stearic acid by the mechanism proposed by Langmuir (15) was first shown by Rideal and Tadayon (16,17) and later Gaines (18). They found that radioactive stearic acid molecules deposited on unreactive substrates can transfer to reactive substrates when brought into contact with reactive solid surfaces.

Yiannos (19) gave quantitative evidence for overturning of stearic acid molecules deposited on unreactive metal surfaces when in contact with water. Katz and Swanson (138) studied quantitatively the molecular reorientation of dehydroabietic acid by the method of Yiannos. They found that approximately 27% of the molecules in the top molecular layer were overturned when a wetting equilibrium was established.

To see if TABSH molecules deposited on the CMC film can overturn as readily as the stearic acid, the pure TABSH monolayer cast on CMC film was brought into contact with a very reactive metal surface such as copper oxide film (139). The copper oxide film was prepared on glass slides by the vacuum evaporation technique. The aluminum resinate monolayer cast on the CMC film was also brought into contact with

the copper film. The contact angles of water on the contacted copper surfaces and on the controlled copper surfaces were measured and compared after one hour, and two hours contact. The results are summarized in Table XIII.

TABLE XIII

CONTACT ANGLES OF WATER ON COPPER SURFACES WHICH WERE CONTACTED WITH THE MONOLAYER CAST ON CMC FILM

	Nature of Contacted[a] Copper Film Surface	Contact Time, hr	Initial Advancing Contact Angles of Water, degrees
Expt. 1	Contacted with pure TABSH monolayer	1	35.1, 44.9
	Contacted with the reacted monolayer[b]	1	19.6, 20.1
	Stored copper film[c]	1	17.1 ± 3.2
Expt. 2[d]	Contacted with pure TABSH monolayer	1	64.3 ± 6.7
		2	71.6 ± 9.9
	Contacted with the reacted monolayer	1	46.9 ±11.2
		2	71.0 ± 3.2
	Contacted with clean CMC film	1	45.7 ± 5.1
		2	66.1 ± 2.1
	Stored copper film[c]	2	66.9 ± 5.0

[a] Copper film slide was brought into contact with the monolayer cast on CMC film slide in a clean desiccator at 22.5°C room temperature.

[b] The TABSH monolayer reacted on the substrate containing aluminum nitrate ([Al] = 3.16×10^{-3}M) in the absence of sulfate ion with pH 4.0.

[c] Stored in aluminum desiccator over ignited aluminum powders.

[d] Experiment 2 was conducted with a different copper film slide from Experiment 1.

Apparently, the contact angles of water on the copper surface contacted with the pure TABSH monolayer for one hour are higher than the contact angles on the surface contacted with the aluminum resinate monolayer and on the stored copper

surface. However, after 2 hours contact, the difference in the contact angles become insignificant because of contamination on the copper surface from ambient air in addition to the transfer of free acid molecules. Nevertheless, the higher contact angles on the copper contacted with the pure TABSH appear to provide qualitative evidence that the TABSH molecules deposited on the CMC film can overturn readily when brought into contact with polar liquids such as water. This is in agreement with the hypothesis that Swanson originally proposed for lowering of water contact-angles on rosin acid monolayers (12).

CONCLUSIONS

The conclusions of this investigation can be stated as follows:

1. Excess sulfate ions in aluminum nitrate plus potassium sulfate substrate with pH 4 can prevent the TABSH monolayers from reacting with aluminum ions by depleting or sequestering reactive aluminum ions. The effect of sulfate diminishes rapidly as pH of the substrate is increased and at pH > 4.5 the sulfate has little or no effect on the reaction between TABSH monolayers and aluminum ions.

2. The reaction product in the interfacial reaction between the monolayers and aluminum ions at pH 4.0-5.0 appears to be a mixture of aluminum triresinate (trisoap) and monobasic diresinate (disoap). The triresinate is believed to be the major reaction product at pH 4, where the unhydrolyzed aluminum ion is the predominant Al ion species in the substrate without sulfate. The monobasic diresinate forms with the hydrolyzed aluminum ion and becomes a major salt with increasing pH of the substrate, due to the increase in the hydrolyzed ion concentration relative to the unhydrolyzed ion upon increasing the pH.

3. The formation of the trisoap in the monolayer at pH 4.0 appears to be completely inhibited by excess sulfate ($\sim$ 0.45M) when most of the unhydrolyzed aluminum ions are removed from the interface due to the formation of $AlSO_4^+$. This sulfato-complex ion is not involved in the formation of any salt with resin acid monolayers at pH 4.0-5.0.

4. The observed fact that excess sulfate has little or no effect on the monolayer reaction at pH > 4.5 can be accounted for by the incapability of sulfate to form a stable basic sulfato-complex with the hydrolyzed aluminum ion $[Al(OH)^{+2}5H_2O]$ and by the high adsorbability of the hydrolyzed Al ion on the

spread monolayer compared to the unhydrolyzed Al ion [$Al^{+3}(6H_2O)$]. Consequently, the sulfate ion appears to have no effect on the reaction between TABSH monolayers and hydrolyzed Al ions forming monobasic diresinates, which apparently have high stability constant compared to that of the triresinate.

5. The inhibiting action of sulfate on the monolayer reaction at pH 4.0 results in lowering of the contact angle of water on the monolayer cast on the CMC film. This corresponds to increasing the free acid mole fraction in the monolayer.

6. The increase in the polar force component of the total free-surface energy for the monolayer under investigation can account for the lowering of the contact angle of water on the monolayer reacted in the presence of excess sulfate at pH 4.0. The increase in the fractional polarity of the surface energy is due to the increase in the fraction of free acid molecules which can overturn readily when brought into contact with liquid water.

NOMENCLATURE

$\underline{A}$ = average cross-sectional area of monolayer molecules, A^2 molecule^{-1}

$\underline{A}_{10}$ = average cross-sectional area of monolayer molecules when π = 10 dynes cm^{-1}, A^2 molecule^{-1}

$\Delta\underline{A}$ = change in total solid surface area, cm^2

$\underline{A}_{CH}$ = absorbance of CH at 2930 cm^{-1} for the multilayer sample on Ge plate

$\underline{A}_{COO^-}$ = absorbance of $TABS^-$ at 1590 cm^{-1} for the multilayer sample on Ge plate

$\underline{A}_{COOH}$ = absorbance of TABSH at 1695 cm^{-1} for TABSH multilayer sample on Ge plate

$\underline{A}_{\underline{ij}}$ = attractive constant in Lennard-Jones potential function for interaction of phases $\underline{i}$ and $\underline{j}$, ergs cm^6

$\underline{A}^{d}_{\underline{ij}}$ = dispersion-force contribution to $\underline{A}_{\underline{ij}}$, ergs cm^6

$\underline{A}^{i}_{\underline{ij}}$ = induction-force contribution to $\underline{A}_{\underline{ij}}$, ergs cm^6

$\underline{A}^{o}_{\underline{ij}}$ = orientation-force contribution to $\underline{A}_{\underline{ij}}$, ergs cm^6

$\underline{A}_{\underline{K}}$ = average cross-sectional area of monolayer molecules when the monolayer collapses, A^2 molecule^{-1}

$\underline{A}_{\underline{K},\underline{EX}}$ = average cross-sectional area of monolayer molecules at the extrapolated collapse point of the monolayer, A^2 molecule^{-1}

$\underline{A}_{\underline{t}}$ = total area occupied by the monolayer molecules, cm^2

[Al] = total molar concentration of aluminum ion species in the system
= moles of aluminum added to system

$[Al^{+3}]$ = (equilibrium) molar concentration of unhydrolyzed trivalent aluminum ion species

$Al(6H_2O)^{+3} = Al^{+3}$ = unhydrolyzed aluminum ion

$[Al(OH)^{+2}]$ = (equilibrium) molar concentration of hydrolyzed divalent aluminum ion species

$[Al_2(OH)_2{}^{+4}]$ = (equilibrium) molar concentration of a dimer of hydrolyzed aluminum ion species

$Al(OH)_2 4H_2O = Al(OH)_2{}^{+1}$ = dihydroxo aluminum ion

$Al(OH)(5H_2O)^{+2} = Al(OH)^{+2}$ = hydrolyzed aluminum ion or monohydroxo aluminum ion

$Al(R)_3$ = aluminum triresinate = aluminum tritetrahydroabietate

$Al(R)_2(OH)$ = monobasic aluminum diresinate = monobasic aluminum ditetrahydroabietate

$[AlSO_4^+]$ = (equilibrium) molar concentration of aluminum sulfate complex ion species

$\underline{B}$ = barrier distance, cm

$\underline{b}$ = base of the droplet for contact angle

$\underline{C}$ = area occupied by the teflon end loops, cm^2

CMC = carboxymethylcellulose

$\underline{D}$ = diffusion coefficient

$d\underline{A}/d\underline{t}$ = rate of reduction of average area available to monolayer molecules, A^2 $molecule^{-1}$ $minute^{-1}$

$d\underline{L}/d\underline{t}$ = rate of penetration

$\Delta\underline{F}^{\underline{S}}$ = change in total surface free energy per unit area of solid surface, $ergs/cm^2$

$\underline{g}$ = gravitational constant

Ge = germanium

H^+ = hydrogen ion

$\underline{h}$ = height of the droplet for contact angle

$\underline{K}_{22}$ = formation constant of $Al_2(OH)_2^{+4}$ ion species from Al^{+3} ion species

$\underline{K}_{CH}$ = absorptivity of the multilayer sample on Ge plate at 2930 cm^{-1}, cm^{-1} $mole^{-1}$

$\underline{K}_{COO^-}$ = absorptivity of the multilayer sample on Ge plate at 1590 cm^{-1}, cm^{-1} $mole^{-1}$

$\underline{K}_{COOH}$ = absorptivity of TABSH multilayer sample on Ge plate at 1695 cm^{-1}, cm^{-1} $mole^{-1}$

$\underline{K}_{\underline{i}}$ = formation constant of complex $\underline{i}$

$\underline{L}$ = effective length of the float, cm
= depth of penetration

$\underline{\ell}_{\underline{c}}$ = lever arm for the calibration weights, cm

$\underline{\ell}_{\underline{f}}$ = lever arm for the float, cm

MIR = multiple internal reflectance

Na CMC = sodium carboxymethylcellulose

N_{CH} = number of moles of total monolayer sample on Ge plate

N_{COO^-} = number of moles of $TABS^-$

N_{COOH} = number of moles of TABSH

[OH]/[Al] = mole ratio of OH^- ion added to the system to the total aluminum ion in the system

p = fractional polarity

r = capillary radius

$[SO_4]$ = total molar concentration of sulfate species in system
= moles of sulfate added to system

t = time of penetration

$TABS^-$ = ionized tetrahydroabietic acid (the aluminum salt of the TABSH acid)

TABSH = sample of tetrahydroabietic acid used in this work

W = the width of the substrate solution surface in the Langmuir trough, cm

w = calibration weight, g

X_{TABS^-} = mole fraction of $TABS^-$

X_{TABSH} = mole fraction of TABSH

γ = surface free energy, ergs/cm^2

γ_{12} = interfacial free energy between Phases 1 and 2, ergs/cm^2

γ_c = Zisman's critical surface tension of wetting, dynes/cm

γ_i^d = dispersion-force component to the surface free energy of substance i, ergs/cm^2

γ_i^p = polar component to the surface free energy of substance i, ergs/cm^2

γ_ℓ = liquid surface free energy, ergs/cm^2

γ_{LV} = specific free-surface energy of the liquid-vapor interface

γ_s = solid surface free energy in vacuum, ergs/cm^2

γ_{SL} = specific free-surface energy of the solid-liquid interface

$\gamma_{s\ell}$ = solid liquid interfacial free energy, ergs/cm^2

$\gamma_{\underline{SV}}$ = specific free-surface energy of the solid-vapor interface

$\gamma_{\underline{sv}}$ = solid-vapor interfacial free energy, ergs/cm^2

η = coefficient of viscosity of the liquid

θ = contact angle between liquid and solid

$\theta_{\underline{A}}$ = advancing contact angle between liquid and solid

π = surface pressure of monolayer, dyne cm^{-1}

$\pi_{\underline{e}}$ = equilibrium film pressure of adsorbed vapor, ergs/cm^2

$\pi_{\underline{K}}$ = lateral force per unit width of the monolayer (surface pressure) when the monolayer collapses, dyne cm^{-1}

$\pi_{\underline{K},\underline{EX}}$ = surface pressure at extrapolated collapse point of the monolayer, dyne cm^{-1}

σ = standard deviation

ϕ_{12} = Girifalco-Good interaction parameter for Substances 1 and 2, dimensionless

$\phi_{\underline{A}}$ = component of ϕ dependent upon attractive force constants in potential energy function; independent of intermolecular distance terms, dimensionless

$\phi_{\underline{r}}$ = component of ϕ dependent upon terms involving intermolecular distance; independent of attractive constants, dimensionless

SUGGESTIONS FOR FUTURE RESEARCH

The results of this study suggest that rosin-alum sizing will not be deteriorated by excess sulfate build-up in the closed white water system as long as pH of the water is maintained above 4.5. This may be interesting to be verified further for the actual papermaking process. Previous reports of the detrimental effect of sulfate (1-5) on rosin sizing did not take account of the possible dependence of the sulfate effect on pH. If the rosin-alum sizing were indeed deteriorated even at pH > 4.5, this might be the case in which excess sulfate has an adverse effect on electrokinetic charges of the size precipitate or of cellulosic fiber surfaces in view of the retention mechanism as suggested by Strazdins (9) and others (6-8).

The adsorption of hydrolyzed Al ion and its role in the rosin-alum sizing system or in other retention mechanisms of fillers and wet-end additives in the papermaking process have been poorly understood or sometimes ignored. The adsorption of hydrolyzed Al ion appears to play an important role in the formation of basic aluminum resinate as shown in this study. Evidently it will also play a role in affecting or developing the electrokinetic charges of colloidal size precipitates and of cellulose fiber surface as Matijevic and his coworkers (61,72,80,81) have observed in the coagulation phenomena of various lyophobic colloids present in aqueous aluminum salt solution. Thus, it should be interesting to investigate quantitatively the role of hydrolyzed Al ions in affecting electrokinetic charges in the rosin-alum-fiber system with determining the adsorption isotherm and its kinetics on the surfaces under investigation.

The amount of the adsorption of the hydrolyzed Al ion can be determined by the MIR spectroscopic technique used in this study and internal reflection techniques recently suggested by Yang, et al. (140) for an infrared study of adsorption

in situ at the liquid-solid interface. However, an inevitable problem will be encountered in this investigation; the effect of monomeric hydrolyzed Al ion species should be distinguished from that of polymeric ion species by controlling the conditions of the preparation of aluminum solutions. To this author's knowledge, no good experimental technique appears to be available at present for isolating the monomeric species from the polymeric species. Some techniques such as a freezing technique of the aluminum solution should be developed in order to suppress the polymerization of monomeric hydrolyzed ions or to prepare a well-defined solution in terms of contents of specific ion species. The complication by the presence of aluminum hydroxide should be also avoided when a significant amount of OH^- ion ([OH]/[Al] > 2.0) has to be added to the solution.

This study also suggests that the dibasic monoresinate can be formed with $Al(OH)_2(4H_2O)^{+1}$ in the pH range 5.5-6.5 when the monovalent ion is a predominant species according to Nazarenko and Nevskaya (67). If the monovalent species forms [some workers such as Kubota (71) deny the formation] and reacts with the resin acid monolayer forming the dibasic salt, the MIR spectrum for the reacted monolayer sample should reveal the presence of bond OH groups near 3 μm. The possibility of the dibasic resinate formation should be investigated at pH > 5.0 with verifying the presence of the $Al(OH)_2(4H_2O)^{+1}$ in the solution.

ACKNOWLEDGMENTS

The author wishes to express his sincere gratitute to Professor J. W. Swanson whose guidance and assistance made this investigation possible. Special thanks are also given to other members of the thesis advisory committee: Dr. D. G. Williams, Dr. D. B. Easty, and Mr. C. V. Piper for serving on this committee with great interest, especially to Dr. Williams for his helpful advice.

The many helpful discussions with and suggestions from Dr. R. H. Atalla, Dr. D. C. Johnson, Professor E. E. Dickey, Dr. A. J. Miller, and Mr. J. O. Church are also acknowledged.

This author is deeply indebted to the following Institute Staff: Mr. M. C. Filz, Jr., and Paul F. Van Rossum for constructing much of the apparatus, Mr. K. W. Hardacker for building and maintaining the electrical system for the apparatus, Mr. L. G. Borchardt for the gas chromatographic analysis of the resin acid sample and for emission analysis of aluminum and sulfate ions, Mrs. H. M. Kaustinen for the electron micrographs, Mr. F. R. Sweeney and Mr. D. E. Beyer for the photographic work. The author would like to thank a fellow student, J. L. Ferris, for sharing the contact-angle apparatus which he built and his computer program.

Acknowledgments would not be complete without special reference to the encouragement and support of my wife, Soon Wha, who was also kind enough to type the manuscript.

LITERATURE CITED

1. Wilson, W. S., and Duston, H. E., Tech. Assoc. Papers 27:673-8(1944).

2. Dennet, F., and Libby, C. E., Tech. Assoc. Papers 25:617-23(1940).

3. Dohne, W. P., and Libby, C. E., Tech. Assoc. Papers 25:663-9(1942).

4. Churchill, R. K., and Martin, L. L., Paper Trade J. 140(15):20-2(April 9, 1956).

5. Aldrich, L. C., and Janes, R., Tappi 56(3):92-6(March, 1973).

6. Collins, T. T., Jr., Davis, H. L., and Rowland, B. W., Tech. Assoc. Papers 25:606-11(1942).

7. Gorham, T. F., and Thode, E. F., Tappi 36:315-19(1953); Thode, E. F., Gorham, J. F., and Atwood, R. H., Tappi 36(7):310-14(1953).

8. Guide, R. G. A study of the sodium aluminate-abietate size precipitates. Doctoral Dissertation. Appleton, Wis., The Institute of Paper Chemistry, 1959. 102 p.

9. Strazdins, E., Tappi 48(3):157-64(1965).

10. Cobb, R. M. K., and Lowe, D. V., Tappi 38(2):49-65(1955).

11. Major, E. H., Jr. The reaction between tetrahydroabietic acid monolayers and aluminum ions. I. The influence of oxalate. Doctoral Dissertation. Appleton, Wis., The Institute of Paper Chemistry, 1969. 108 p.

12. Swanson, J. W., Tappi 44(1):142A-81A(1961).

13. Washburn, E. W., Phys. Rev. 17:273-83(1921).

14. Dupre, A. Theorie Mechanique de la Chaleur. Paris, 1869. 368 p.; Cited in Adamson, A. W. Physical chemistry of surfaces. New York, Interscience, 1960. 629 p.

15. Langmuir, I. Overturning and anchoring of monolayers. In Moulten's Recent advances in surface chemistry and chemical physics. Publication No. 7 of the American Association for Advancement of Science, 1939. p. 9-18.

16. Rideal, E. K., and Tadayon, J., Proc. Royal Soc. (London) A225:346-56(1954).

17. Rideal, E. K., and Tadayon, J., Proc. Royal Soc. (London) A225:357-61(1954).

18. Gaines, G. L., Nature 186:384-5(1960).

19. Yiannos, P. N. Molecular reorientation of some fatty acids when in contact with water. Doctoral Dissertation. Appleton, Wis., The Institute of Paper Chemistry, 1960. 115 p.

20. Swanson, J. W., Kumler, R. W., and Mispley, R. G. The process of sizing. In Internal sizing of paper and paperboard. TAPPI Monograph Series No. 33. Edited by J. W. Swanson. New York, TAPPI, 1971.

21. Back, E., and Steenberg, B., Svensk Papperstid. 54(15):510-15(Aug. 15, 1951).

22. Ekwall, P., and Bruun, H., Paper and Timber (Finland) 32(7):194-202(1950).

23. Watkins, S. H., Tappi 45(5):216A-20A(May, 1962).

24. Vandenberg, E. J., and Spurlin, H. M., Tappi 50(5):209-24(May, 1967).

25. Davison, R. W., Tappi 47(10):609-16(Oct., 1964).

26. Watkins, S. H. Rosin and rosin size. Preparation and properties. In Internal Sizing of paper and Paperboard. TAPPI Monograph Series No. 33. Edited by J. W. Swanson. New York, TAPPI, 1971.

27. Buchanan, M. A. Extraneous components of wood. In Browning's The chemistry of wood. p. 313-67. New York, Interscience, 1963.

28. Lawrence, R. V., Tappi 42(10):867-9(Oct., 1959).

29. Genge, C. A., Anal. Chem. 31:1750-3(1959).

30. Engel, E. M. The internal sizing of paper. In Libby's Pulp and paper-science and technology. Vol. II: Paper. p. 40-59. New York, McGraw-Hill, 1962.

31. Davies, J. T., and Rideal, E. K. Electrostatic phenomena. Chapter 2. In Interfacial phenomena. p. 108-51. New York, Academic Press, 1961.

32. Price, D., Paper Trade J. 126(15):61-6(TS 191-6)(April 8, 1948); Price, D., Ind. Eng. Chem. 39(9):1143-7(Sept., 1947).

33. Jayme, G., and Seidel, W., Wochbl. Papierfabrik. 83:947(1955).

34. Jayme, G., and Seidel, W., Papier 11:500(1957).

35. Thode, E. F., Gorham, J. F., and Atwood, R. H., Tappi 36(7):310-14(July, 1953).

36. Strazdins, E., Tappi 46(7):432-7(July, 1963).

37. Ekwall, P., and Bruun, H. H., Acta Chem. Scand. 9:412-23(1955); Ekwall, P., and Bruun, H. H., Acta Chem. Scand. 9:424-9(1955); Tappi 37(7):303-6(1954).

38. Frieberg, S., and Bruun, H. H., Arkiv. Kemi. 25(45):491-8(1966); Frieberg, S., and Bruun, H. H., Arkiv. Kemi. 25(45):533-41(1966).

39. McBain, J. N., and McClatchie, W. L., J. Am. Chem. Soc. 54:3267(1932).

40. McGee, C. G., and McBain, J. N., J. Am. Chem. Soc. 71:278-82(1949).

41. Gray, V. R., and Alexander, A. E., Proc. Royal Soc. (London) 200:162-8(1950).

42. Harple, W. W., Wiberley, S. E., and Bauer, W. H., Anal. Chem. 24:635-8(1952).

43. Scott, F. A., Goldensen, J., Wiberley, S. E., and Bauer, W. H., J. Phys. Chem. 58:61-4(1954).

44. Bauer, N. H., Fisher, J., Scott, F. A., and Wiberly, S. E., J. Phys. Chem. 59(1):30-2(Jan., 1955).

45. Leger, A. E., Haines, R. L., Hubley, C. E., Hyde, J. C., and Sheffer, H., Can. J. Chem. 35:799-816(1957).

46. Ellis, J. W., and Pauley, J. L., J. Colloid Sci. 19:755-64(1964).

47. Mehrotra, R. C., Nature 172:74(1953).

48. Glazer, J., McRoberts, T. S., and Schulman, J. H., J. Chem. Soc. 1950:2082-3.

49. Gilmour, A., Jobling, A., and Nelson, S. M., J. Chem. Soc. 1956:172-6.

50. Shiba, S., Bull. J. Chem. Soc. Japan 34:804-9(June, 1961).

51. Ninck Block, C. J. J., Pulp Paper Mag. Can. 57(3):208-15(1956).

52. Nyren, V., and Back, E., Acta Chem. Scand. 12:1516-20(1958).

53. Wall, F. T., and Drenan, J. W., J. Polymer Sci. 7:83-8(1951).

54. Wall, F. T., and Gill, S. J., J. Phys. Chem. 58:1128-30(1954).

55. Mandel, M., and Leyte, J. C., J. Polymer Sci. Part A, 2:1883-99(1964).

56. Gustafson, R. L., and Lirio, J. A., J. Phys. Chem. 69(9):2849-56(1965).

57. Nazarov, P. P., Chuveleva, E. A., and Chmutov, K. V., Russian J. Phys. Chem. 43(9):1288-90(1969).

58. Langmuir, L., and Schaefer, V. J., J. Am. Chem. Soc. 59:2400-14(1937).

59. Davies, J. T., and Rideal, E. K. Reactions at liquid surface. Chap. 6. In Interfacial phenomena. p. 282-99. New York, Academic Press, 1961.

60. Thomas, A. W., Tech. Assoc. Papers 18:242-5(1935).

61. Matijevic, E., and Stryker, L. J., J. Colloid Sci. 22:68-77(1966).

62. Akitt, J. W., Greenwood, N. N., and Khandelwal, B. L., J. Chem. Soc., Dalton, 1972:604-10.

63. Akitt, J. W., Greenwood, N. N., and Lester, G. D., J. Chem. Soc. A, 1969:803-7.

64. Frink, C. R., and Peech, M., Inorg. Chem. 2(3):473-8(1963).

65. Holmes, L. P., Cole, L., and Eyring, E. M., J. Phys. Chem. 73(1):301-4(1968).

66. Patterson, J. H., and Tyree, S. Y., Jr., J. Colloid Interface Sci. 43(2):389-98(May, 1973).

67. Nazarenko, V. A., and Nevskaya, E. M., Russian J. Inorg. Chem. 14(1):1696-9 (1969).

68. Thomas, A. W. Colloid chemistry. p. 161-4. New York, McGraw-Hill, 1934.

69. Pokras, L., J. Chem. Educ. 33:152-61(1956).

70. Grunwald, E., and Fong, D. W., J. Phys. Chem. 73:650-3(1969).

71. Kubota, H. Properties and volumetric determination of aluminum ion. Doctoral Dissertation. Madison, Wis., The University of Wisconsin, 1956. 121 p.

72. Matijevic, E., Mathai, K. G., Ottewill, R. H., and Kerker, M., J. Phys. Chem. 65:826-30(1961).

73. Beidermann, G., Svensk. Kem. Tidskr. 76:362-84(1964).

74. Aveston, J., J. Chem. Soc. 1965:4438-41.

75. Miceli, J., and Steuhr, J., J. Am. Chem. Soc. 90(25):6967-72(1968).

76. Stryker, L. J., and Matijevic, E., J. Phys. Chem. 73(5):1484-7(May, 1969).

76a. Behr, B., and Wendt, H., Z. Elektrochem. 66:223(1962); cited in Ref. (76).

76b. Nanda, R. K., and Aditya, S., Z. Phys. Chem. (Frankfurt am Main) 35:139(1962); cited in Ref. (76).

76c. Nichide, T., and Tsuchiya, R., Bull. Chem. Soc. Jap. 38:1398(1964); cited in Ref. (76).

77. Brosset, C., Biedermann, G., and Sillen, L. C., Acta Chem. Scand. 8(10): 1917-26(1954).

78. Akitt, J. W., Greenwood, N. N., and Khandelwal, B. L., J. Chem. Soc., Dalton 1972:1226-9.

79. Thomas, A. W., and Vartanian, R. D., J. Am. Chem. Soc. 57(1):4-7(1935).

80. Matijevic, E., Janauer, G. E., and Kerker, M., J. Colloid Sci. 19:333-46(1964).

81. Matijevic, E., J. Colloid Interface Sci. 43(2):217-45(May, 1973).

82. Hahn, H. H., and Stumm, W. Coagulation by Al(III). In Weber and Matijevic's Adsorption from aqueous solution. Adv. in Chem. Series No. 79. Washington, D.C., American Chemical Society, 1968.

83. Hahn, H. H., and Stumm, W., J. Colloid Interface Sci. 28:134-44(1968).

84. O'Melia, C. R., and Stumm, W., J. Colloid Interface Sci. 23:437-47(1967).

85. Stumm, W., and Morgan, J. J. Metal ions in aqueous solution: aspects of coordination chemistry. p. 238-99. In Aquatic chemistry. New York, Wiley-Interscience, 1970.

86. Young, T., Phil. Trans. Roy. Soc. (London) 95:65(1805); cited in Ref. (87).

87. Adamson, A. W. The nature and thermodynamics of liquid-gas interface. In Physical chemistry of surfaces. p. 53-108. New York, Interscience, 1967.

88. Zisman, W. A. Relation of the equilibrium contact angle to liquid and solid constitution. In Fowkes' Contact angle, wettability, and adhesion. Adv. in Chem. Ser. No. 43. Washington, D.C., American Chemical Society, 1964.

89. Dupre, A. Theorie mecanique de la chaleur. p. 368-9. Paris, 1869.

90. Bangham, D. H., and Razouk, R. I., Trans. Faraday Soc. 33:145-72, 805-11(1937).

91. Fowkes, F. M. In Marchessault and Skaar's Surfaces and coatings related to paper and wood. Chap. 5. p. 507. Syracuse, N.Y., Syracuse University Press, 1967.

92. Wenzel, R. N., Ind. Eng. Chem. 28(8):988-94(Aug., 1936).

93. Tamai, Y., and Aratani, K., J. Phys. Chem. 76(22):3267-71(1972).

94. Sharpe, L. H., and Schonhorn, H., Ref. (88). p. 189-201.

95. Girifalco, L. A., and Good, R. J., J. Phys. Chem. 61(7):904-9(July, 1957).

96. Chan, R. K. S., J. Colloid Interface Sci. 32(3):492-504(March, 1970).

97. Dann, J. R., J. Colloid Interface Sci. 32(2):302-31(Feb., 1970).

98. Fowkes, F. M., Ind. Eng. Chem. 56(12):40-52(Dec., 1964).

99. Owens, D. K., and Wendt, R. D., J. Appl. Polymer Sci. 13(8):1741-7(Aug., 1969).

100. Good, W., J. Colloid Interface Sci. 44(1):63-71(1973).

101. Good, R. J. Theory for the estimation of surface and interfacial energies. In Fowkes' Contact angle, wettability, and adhesion. Adv. in Chem. Ser. No. 43. p. 74-87. Washington, D.C., American Chemical Society, 1964.

102. Good, R. J., J. Phys. Chem. 61(6):810-13(June, 1957).

103. Good, R. J., and Elbing, E., Ind. Eng. Chem. 62(3):54-78(March, 1970).

104. Fowkes, F. M. Reference (88), p. 99.

105. Fowkes, F. M., J. Phys. Chem. 67(12):2538-41(Dec., 1963).

106. Fowkes, F. M., J. Colloid Interface Sci. 28(3/4):493-505(Nov.-Dec., 1968).

107. Wu, S., J. Phys. Chem. 74(3):632-8(Feb. 5, 1970).

108. Ekwall, P., Svensk Kem. Tid. 63:277-307(1951).

109. Bruun, H. H., Acta Chem. Scand. 9:1721-3(1955).

110. Bruun, H. H. Surface balance studies of rosin acid monolayers. Doctoral Dissertation. Abo, Finland, Abo Akademi, 1954. 111 p.

111. Adamson, A. W. The nature and thermodynamics of liquid-gas interfaces. In Physical chemistry of surfaces. p. 51-102. New York, Interscience, 1960.

112. Harrick, N. J. Internal reflection spectroscopy. p. 327. New York, Interscience, 1967.

113. Muller, H., and Friberg, S., Acta Chem. Scand. 23:515-21(1969).

114. Sharpe, L. H., Proc. Chem. Soc. Dec., 1961:461-3.

115. Loeb, G. I., J. Colloid Interface Sci. 26(2):236-8(Feb., 1968).

116. Loeb, G. I., J. Polymer Sci. Part C, (34):63-71(1971).

117. Takenaka, T., NoGami, K., and Gotoh, H., J. Colloid Interface Sci. 35(3):395-407(March, 1971); 40(3):409-16(Sept., 1972).

118. Neuman, R. D. The properties, structure, and multilayer deposition of stearic acid-calcium stearate monolayers. Doctoral Dissertation. Appleton, Wis., The Institute of Paper Chemistry, 1973. 205 p.

119. Gaines, G. L., Jr. Insoluble monolayers at liquid-gas interfaces. New York, Interscience, 1966. 386 p.

120. Wilks, P. A., Jr., Appl. Spectroscopy 23(1):63-6(1969).

121. Gilby, A. C., Cassell, J., and Wilks, P. A., Jr., Appl. Spectroscopy 24(5): 530-43(1970).

122. White, M. L. The detection and control of organic contaminants on surfaces. In Goldfinger's Clean surfaces. p. 361-73. New York, Marcel Dekker, Inc., 1970.

123. Harkins, W. D., and Jordan, H. F., J. Am. Chem. Soc. 52(5):1751-72(May, 1930).

124. Brown, P. F. The role of surface chemistry in the bonding of a cellulose substrate treated in a corona discharge. Doctoral Dissertation. Appleton, Wisconsin, The Institute of Paper Chemistry, 1971. 120 p.

125. Ferris, J. The wettability of cellulose film as affected by vapor phase adsorption of amphipathic molecules. Doctoral Dissertation. Appleton, Wisconsin, The Institute of Paper Chemistry. To be published.

126. Silverstein, R., and Bassler, G. C. Spectroscopic identification of organic compounds. New York, John Wiley and Sons, 1958. 423 p.

127. Bellamy, L. J. The infrared spectra of complex molecules. New York, John Wiley and Sons, 1958. 423 p.

128. Gamo, L., Bull. Chem. Soc. Japan 35(7):1055-77(1962).

129. Nakamoto, K., Fujita, J., Tanaka, S., and Kobayashi, M., J. Am. Chem. Soc. 79:4904(1957).

130. Potts, W. J., Jr. Chemical infrared spectroscopy. Vol. 1. Techniques. New York, John Wiley and Sons, 1963. 322 p.

131. Bagg, J., Abramson, M. B., Fichman, M., Haber, J. D., and Gregor, H. P., J. Am. Chem. Soc. 86:2759-63(1964); Bagg, J., Haber, M. D., and Gregor, H. P., J. Colloid Interface Sci. 22:138-43(1966).

132. Schulman, J. H., and Rideal, E. K., Proc. Roy. Soc. (London) A130:284(1931).

133. Eisenberg, D., and Kauzmann, W. The structure and properties of water. New York, Oxford Univ. Press, 1969. 296 p.

134. Spink, J. A., and Sanders, J. V., Trans. Faraday Soc. 51:1154-65(1955).

135. Thomas, J. G. N., and Schulman, J. H., Trans. Faraday Soc. 51:1131-9(1954).

136. Wolstenholme, G. A., and Schulman, J. H., Trans. Faraday Soc. 47:788-94(1951).

137. Max Nestler, F. H., and Zinkel, D. F., Anal. Chem. 39(10):1118-24(Aug., 1967).

138. Katz, G., and Swanson, J. W. Molecular reorientation of dehydroabietic acid when in contact with water. Unpublished work, 1961.

139. Ow, S. K., and Swanson, J. W. Determination of reactivity between metal surfaces and fatty acid monolayers. Unpublished work, 1971.

140. Yang, R. T., Low, M. T. D., Haller, G. L., and Fenn, J., J. Colloid Interface Sci. 44(2):249-58(Aug., 1973).

APPENDIX I

MATERIALS

TETRAHYDROABIETIC ACID

The sample of tetrahydroabietic acids (TABSH) was obtained from Hercules Incorporated in November, 1971. The sample was further purified by recrystallization from methanol to remove a small fraction of n-hexane-insoluble materials.

The recrystallized sample was analyzed by gas chromatography in the same manner described in the thesis of Major (11) in order to determine its isomeric composition, and the amount of impurity. The column used was an EGSS-X rather than the DEGS column employed in the previous study. The new column is basically the same except that it contained methyl silicone chemically bonded to the ethylene succinate to improve stability. The greater stability makes it possible to use higher temperatures which are required to elute the resin acids. The two columns were compared in their ability to separate three components, whereas the old DEGS column indicated two components.

The identification is based on retention values reported by Max Nestler and Zinkel (137). The relative retention values of methyl esters of the three known tetrahydroabietic acids (pimarate = 1.00) are given in Table XV. In this analysis all of the observed peaks were assumed to represent isomers of tetrahydroabietic acid because the gas chromatographic analysis did not reveal the presence of other resin or fatty acid in the sample.

The results indicate that the sample of TABSH is composed of approximately equal quantities of 8β, 9α, 13α-H, and 8α, 9α, 13α-H tetrahydroabietic acid and a trace amount of 8β, 9α, 13β-H isomers (6%), as shown in Table XVI.

TABLE XV

RELATIVE RETENTION VALUES (PIMARATE = 1.00) FOR METHYL ESTERS OF KNOWN TETRAHYDROABIETIC ACIDS ON DEGS (137)

Tetrahydroabietate	Relative Retention Value (Pimarate = 1.00) on DEGS Obtained by Max Nestler and Zinkel (137)
8β, 9α, 13α-H	0.92
8β, 9α, 13β-H	1.01
8α, 9α, 13α-H	1.12

TABLE XVI

RELATIVE RETENTION VALUES (PIMARATE = 1.00) AND PERCENTAGES OF TOTAL PEAK AREA FOR METHYL ESTERS OF TABSH SAMPLE ON EGSS-X

Ester Peak	Isomers	Relative Retention Value (Pimarate = 1.00) on EGSS-X	Total Peak Area, %
No. 1	8β, 9α, 13α-H	0.91	48
No. 2	8β, 9α, 13β-H	1.00	6
No. 3	8α, 9α, 13α-H	1.09	46

This isomeric composition of tetrahydroabietic acid is essentially the same as the composition of the sample used by Major (11).

n-HEXANE

Matheson Coleman and Bell reagent grade n-hexane was used in this thesis work. This hexane solution was further purified to remove traces of surface-active impurities, by the methods used by Neuman (118): double distillation in a grease-free glass system and percolation through an adsorption column (activated alumina plus silica gel). The purified n-hexane was evaluated with respect to its completeness of evaporation at the liquid-air interface. The amount of n-hexane normally used

to spread a TABSH monolayer was deposited on the liquid-air interface of the surface balance and allowed to evaporate. The cleanliness of the water surface was then checked by the surface film balance technique (119). No surface pressure was detected on the water surface.

ALUMINUM NITRATE

Matheson Coleman and Bell reagent-grade aluminum nitrate, $Al(NO_3)_3 \cdot 9H_2O$ (crystals), was used as received. This material was checked for metal salt contamination. Analysis of the aqueous aluminum nitrate solution by emission spectroscopy showed no significant levels of contamination.

POTASSIUM SULFATE

B and A (Allied Chemical) reagent-grade potassium sulfate, K_2SO_4 (crystal) was also used as received. The maximum limit of foreign metal ions impurities was 0.007% according to manufacturer's specifications. To remove possible insoluble impurities the dissolved solution of potassium sulfate was filtered through Millipore (pore size 0.22 μm).

PARAFFIN

Sun oil paraffin wax number 5512 (melting range 63-69°C) was obtained for this investigation. The paraffin was purified to remove possible surface-active impurities. Portions of the paraffin were melted and passed through a 500-mm Liebig condenser packed with activated silica gel. The condenser jacket was heated with steam, and the silica gel was renewed after 1200 ml of molten paraffin were processed. The first 300-ml portion was discarded, and the remainder of the paraffin was collected.

The purified paraffin was tested for surface-active impurities by dropping small pieces of it on the surface of distilled water sprinkled with ignited talc. No spreading was observed.

METHYLENE IODIDE

Eastman Kodak white label diiodomethane (d. 3.3/20°), CH_2I_2, was received and purified before it was used in the contact-angle measurement. The methyl iodide was passed through a column of alternating layers of silica gel and activated alumina until colorless. The purified methylene iodide was kept in a dark bottle which was wrapped with aluminum foil to exclude light. The surface tension of purified CH_2I_2 was 50.53 dynes cm^{-1} at 22.5°C.

FORMAMIDE

Eastman Kodak white label formamide (< 0.01% water), $HCONH_2$, was received. The formamide was purified further by the same method for the methylene iodide. The surface tension was 57.4 dynes cm^{-1} at 22.5°C.

APPENDIX II

$\pi_{\underline{K},\underline{EX}}$, $\underline{A}_{\underline{K},\underline{EX}}$, $\underline{A}_{10}$ AND $\underline{A}_{18}$ VALUES FOR THE TABSH MONOLAYERS ON HYDROCHLORIC ACID SUBSTRATES AT pH 4.0[a]

Substrate Condition						
SO_4	Al	pH	$\pi_{\underline{K},\underline{EX}}$	$\underline{A}^2_{\underline{K},\underline{EX}}$	$\underline{A}^2_{18}$	$\underline{A}^2_{10}$
0	0	3.90	19.4	43.1	43.5	45.5
(pure TABSH)		3.950	19.5	43.2	43.6	45.6
		3.910	19.9	43.6	44.0	46.0
		4.01	19.6	44.0	44.3	46.5
		4.01	19.7	43.7	44.0	46.5
		3.95	19.4	43.0	43.3	45.3
		3.95	19.6±0.2[b]	43.4±0.28[b]	43.8±0.39[b]	45.9±0.52[b]

[a] Substrates were at 22°C, reaction time = 10 minutes, and $d\underline{A}^2/d\underline{t} = 2.521$ A^2 molecule^{-1} minute.

[b] 95% Confidence limit.

APPENDIX III

THE AGING OF THE SUBSTRATE SOLUTION AND THE COMPOSITION OF THE TABSH MONOLAYERS REACTED ON THE SUBSTRATE AT pH 4.0[a]

Sample No.	Aging Time[b]	X_{TABSH}	pH	Spectrum No.
TAB-Al-S-1-7	80 min	0.703	4.015	85
TAB-Al-S-1-8	90 min	0.708	4.010	86
TAB-Al-S-1-9	25 hr	0.706	4.005	87

[a] TABSH monolayers were spread on the substrates with the [Al] = 3.16×10^{-3}M and [SO_4] = 0.1M.

[b] Aging at temp. of 22.5°C.

APPENDIX IV

ABSORBANCE RATIO FOR PURE TABSH SAMPLES[a]

Sample No.	$\underline{A}_{COOH}/\underline{A}_{CH}$	Spectrum No.
TABSH-Spread 3	0.318/0.236 = 1.21	61-1
TABSH-Spread 4	0.464/0.394 = 1.18	62-1
TABSH-Spread 5	0.321/0.267 = 1.20	64
TABSH-1-21M[b]	0.319/0.268 = 1.19	65
TABSH-22M[c]	0.568/0.454 = 1.25	66-1
TABSH-23M[b]	0.482/0.402 = 1.20	67
TABSH-Spread 10	0.581/0.472 = 1.23	68
TABSH-Spread 11	0.474/0.391 = 1.21	78

Average value = $1.209 \pm \sigma$

= 1.209 ± 0.020

---

[a] Pure TABSH samples were prepared on the Ge plate by two methods: multilayer deposition (designated as TABSH-M) for hydrochloric acid substrates and spreading of the TABSH-hexane spreading solution directly on the Ge plate (designated as TABSH-Spread).

[b] 45 Layers.

[c] 57 Layers.

APPENDIX V

ELECTRON MICROSCOPY[a]

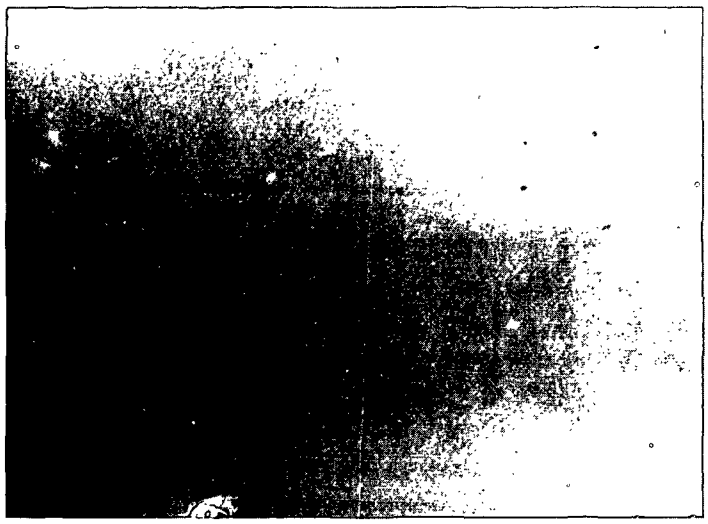

Figure 18(a). Electron Micrograph of Pure CMC Film Cast on Glass Slide (Smooth)

Figure 18(b). Electron Micrograph of Pure CMC Film Cast on Glass Slide (Rough)

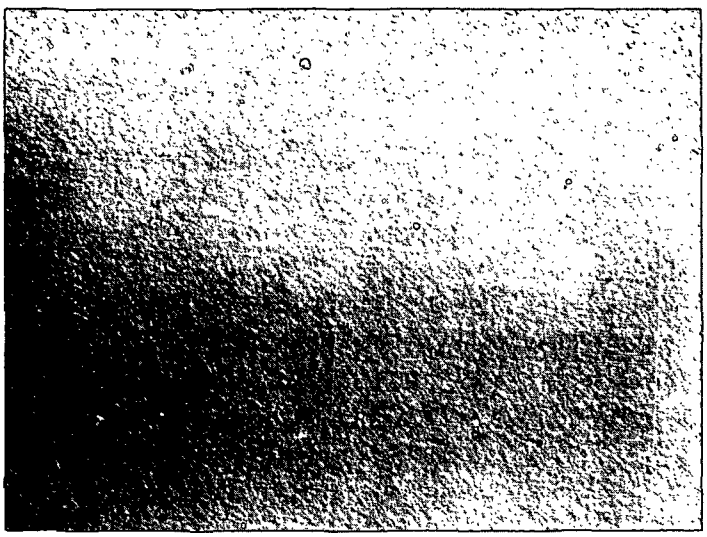

Figure 18(c). Electron Micrograph of Reacted TABSH Monolayer [with $Al(NO_3)_3$ at pH 4.0]. Deposited on the CMC Film

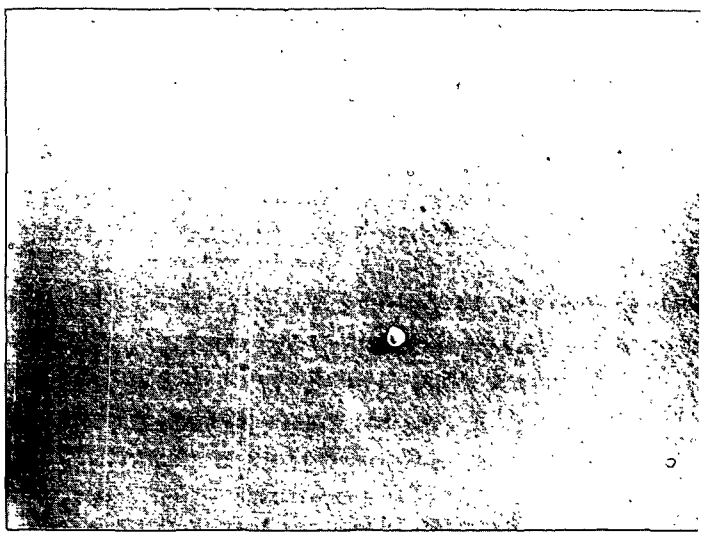

Figure 18(d). Electron Micrograph of Free TABSH Monolayer Deposited on the CMC Film

[a]Magnification: 22,400X.

APPENDIX VI

$\underline{A}_{COOH}/\underline{A}_{CH}$ VALUES AND $\underline{X}_{TABSH}$ FOR THE REACTED TABSH MONOLAYERS[a]

Sample No.	pH[b]	$\underline{A}_{COOH}/\underline{A}_{CH}$	$\underline{X}_{TABSH}$[c]	Spectrum No.
TAB-Al-C2-5	4.013	0.160/0.397 = 0.404	0.334	72
TAB-Al-C2-6	4.015	0.151/0.399 = 0.391	0.323	73
TAB-Al-C2-7	3.995	0.161/0.389 = 0.415	0.343	74
TAB-Al-C2-8	4.008	0.164/0.402 = 0.408	0.337	75
TAB-Al-C2-9	4.005	0.153/0.388 = 0.395	0.326	76
		Average value =	0.333 ± σ	
		=	0.333 ± 0.008	

[a] The TABSH monolayers were spread on the aluminum sulfate substrate with [Al] = 1.0×10^{-3} M, [SO_4] = 1.5×10^{-3} M [$Al_2(SO_4)_3$] at 22.5°C, reaction time = 30 min.

[b] pH of the substrate was adjusted with 0.1N HCl.

[c] $\underline{X}_{TABSH}$ was calculated based on $\underline{K}_{CH}/\underline{K}_{COOH}$ for pure TABSH = 1/1.21 on a Ge plate according to Equation (33).

APPENDIX VII

COMPUTER PROGRAM FOR THE CALCULATION OF EQUILIBRIUM CONCENTRATIONS OF ALUMINUM COMPLEX ION SPECIES IN ALUMINUM NITRATE PLUS POTASSIUM SULFATE SOLUTIONS

```
C. CALCULATION OF  CONC. OF  ALSO4  IN THE  CUBIC EQUATION BY MULLER  METHOD
      DIMENSION COEFR(20),COEFI(20),ROOTR(20),ROOTI(20)
C     DOUBLE PRECISION COEFR,COEFI,ROOTR,ROOTI
      REAL K1,K2,K3,K4
      K1=0.00000955
      K2=370
      K3=97
      K4=6000
1     READ(5,9001) ST,AT,PH
      WRITE(6,9008) ST,AT,PH
9008  FORMAT(1H ,'ST=',1E10.4,'AT=',1E10.4,'PH=',F5.3)
      H=EXP(-PH*ALOG(10.))
      E=1+K3*H
      C=K1*K1*K4/H*H
      D=1+(K1/H)
      COEFR(1)=-K2*K2
      COEFR(2)=AT*K2*K2 -E*C+D*E*K2+2*ST*K2*K2
      COEFR(3)=-2*ST*AT*K2*K2-D*E*K2*ST-K2*K2*ST*ST
      COEFR(4)=AT*K2*K2*ST*ST
      WRITE(6,9003)(COEFR(I),I=1,4)
C     DO 100 I = 2,4
C 100 COEFR(I) = COEFR(I)/COEFR(1)
C     COEFR(1) = 1.
C     WRITE(6,9003)(COEFR(I),I=1,4)
9003  FORMAT(1H ,4E14.6)
      N = 3
      M  = 0
      CALL ROOTS(COEFR,COEFI,N,M,ROOTR,ROOTI)
      WRITE(6,9002) ST,AT,H,(ROOTR(I),ROOTI(I),I=1,3)
      DO 9 I =1,3
      IF(ROOTR(I))9, 9,10
10    IF(ROOTR(I)-AT)11,9,9
11    AS=ROOTR(I)
      SO4=(ST-AS)/E
      AL=AS/(K2*SO4)
      ALOH=(K1*AL)/H
      DALOH=AT-AL-AS-ALOH
      PAL  =(AL/AT)*100.
      PAS=(AS/AT)*100.
      PALOH=(ALOH/AT)*100.
      PDALOH=(DALOH/AT)*100.
      WRITE(6,9006) AS,AL,ALOH,DALOH
9006  FORMAT(1H ,'AS=',1E14.6,'AL=',1E14.6,'ALOH=',1E14.6,'DALOH=',
     1 1E14.6)
      WRITE(6,9009) PAS,PAL,PALOH,PDALOH
9009  FORMAT(1H ,'PAS=',1F8.3,'PAL=',1F8.3,'PALOH=',1F8.3,'PDALOH=',
     2 1F8.3)
9     CONTINUE
      GO TO 1
9001  FORMAT(3E10.4)
9002  FORMAT(1H ,3E10.4,/,1H ,6E14.6)
```